uOttawa

L'Université canadienne
Canada's university

FACULTÉ DES ÉTUDES SUPÉRIEURES ET POSTDOCTORALES

uOttawa

L'Université canadienne
Canada's university

FACULTY OF GRADUATE AND POSTDOCTORAL STUDIES

Khalid Omari

AUTEUR DE LA THÈSE / AUTHOR OF THESIS

Ph.D. (Earth Sciences)

GRADE / DEGREE

Department of Earth Sciences

FACULTÉ, ÉCOLE, DÉPARTEMENT / FACULTY, SCHOOL, DEPARTMENT

A New Multiple Scattering Scheme for the FLAIR Forest Radiative Transfer Model – Application to Biochemical and Biophysical Parameter Retrieval Using Hyperspectral Data

TITRE DE LA THÈSE / TITLE OF THESIS

K. Staenz

DIRECTEUR (DIRECTRICE) DE LA THÈSE / THESIS SUPERVISOR

CO-DIRECTEUR (CO-DIRECTRICE) DE LA THÈSE / THESIS CO-SUPERVISOR

EXAMINATEURS (EXAMINATRICES) DE LA THÈSE / THESIS EXAMINERS

E. Cloutis

B. Daneshfar

D. King

S. Mitchell

Gary W. Slater

Le Doyen de la Faculté des études supérieures et postdoctorales / Dean of the Faculty of Graduate and Postdoctoral Studies

A New Multiple Scattering Scheme for the FLAIR Forest Radiative Transfer Model

Application to Biochemical and Biophysical Parameter Retrieval Using Hyperspectral Data

Khalid Omari

Thesis submitted to the
Faculty of Graduate & Postdoctoral Studies
University of Ottawa
In partial fulfillment of the requirements for the
PhD degree in Earth Sciences
Ottawa-Carleton Geoscience Centre
and
University of Ottawa
Ottawa, Canada

Thèse soumise à
Faculté des Études Supérieures et Postdoctorales
Université d'Ottawa
En vue de l'obtention du
Doctorat en Sciences de la Terre
Centre Geoscientifique d'Ottawa-Carleton
et
Université d'Ottawa
Ottawa, Canada

Your file Votre référence
ISBN: 978-0-494-59510-7
Our file Notre référence
ISBN: 978-0-494-59510-7

Summary

This thesis investigated the development and assessment of a simple parameterization of the multiple scattering within canopies assuming the single scattering field is known and the background beneath the canopy is completely absorbing. The parameterization is based on the concept of spectral invariants related to recollision and escape probabilities from vegetation canopies. The simplified approach is evaluated against a detailed 3-D ray tracing model, PARCINOPY, as well as reference datasets from the Radiation Modelling Intercomparison Experiment On-Line Checker. Comparison with homogenous canopies simulated with PARCINOPY showed that the model's performance is best in both the solar principal and perpendicular planes at low and mid LAI levels for all solar zenith angles. The comparison to the On-line Checker datasets shows also that the model is a suitable approach to describe the multiple scattering components of physically based models.

This simple parameterization is then incorporated into the Four Scale Linear Model for Anisotropic Reflectance (FLAIR) canopy radiative transfer model to enhance the description of the spectrally dependant multiple scattered radiation field of a forest canopy. The contribution of the multiply scattered radiation between the canopy and the background is also added to the parameterization of the multiple scattering component. The validation of the new version of the FLAIR model was performed using the multi-angular data sets obtained by the airborne sensor POLarization and Directionality of the Earth's Reflectances (POLDER) during the BOReal Ecosystem-Atmosphere Study (BOREAS) campaign of 1994. The results indicate that this approach is well suited to the FLAIR model. It is also demonstrated that the multiple scattering problem can be parameterized by a limited number of architectural parameters and the leaf scattering coefficient.

Finally, the combined canopy-leaf PROFLAIR (PROSPECT + FLAIR) model is used to investigate the potential of simulating broadleaf forest canopy spectral reflectance. The comparison between simulated data and Hyperion reflectance data showed the ability of the PROFLAIR model to realistically simulate canopy spectral reflectance. The model was then inverted with hyperspectral Hyperion data using a look-up-table (LUT) approach to

retrieve canopy leaf area index (LAI), leaf chlorophyll content (C_{a+b}) and canopy integrated chlorophyll content (LAI x C_{a+b}). The LUT was populated by simulating the model in forward mode using a space of realization generated based on the specific distribution of the input parameters and based on a priori information from the field. The estimated variables were then compared to ground measurements collected in the field. The results showed a reasonable performance of the PROFLAIR model to the order of performances of other well-known models. When compared to ground measurements, the model showed its ability to retrieve canopy LAI from closed forest canopy with an RMSE of 0.47 and leaf chlorophyll content with an RMSE of 4.46 $\mu g/cm^2$.

Résumé

La contribution de la diffusion multiple peut excéder 50% de la luminance totale réfléchie par un couvert végétal dans le domaine du proche infrarouge. Ce domaine spectral n'est pas affecté par la diffusion atmosphérique et par conséquent il est très utile pour l'extraction des paramètres biophysiques des couverts végétaux à partir des images de télédétection. Cette étude a enquêté en premier lieu, le développement et l'évaluation d'un simple paramétrage de la diffusion multiple dans les couverts végétaux en supposant que la diffusion du premier ordre est connue et que la contribution du sol sou jacent est nulle (sol complètement absorbant). Le paramétrage est basé sur le concept d'invariance spectrale liée aux probabilités de ré-collision et d'échappement des couverts végétaux. L'approche simplifiée est évaluée en comparaison à un modèle tridimensionnel détaillé basé sur la technique du lancer de rayon appelé PARCINOPY. Également, cet approche est évalué conte des données références établies par l'expérience d'inter-comparaison des modélisations de la radiation RAMI *(Radiation Modelling Intercomparison Experiment)* disponible on ligne sur internet. La comparaison à des couverts homogènes simulés par le modèle PARCINIPY a montré que la performante de notre approche est meilleure à la fois lorsque les plans principal et azimutal sont parallèles ou perpendiculaires à des indices foliaires (LAIs) faibles et moyennes et cela quelque soit l'angle zénithal solaire. La comparaison à des références on ligne établies par l'exercice RAMI a montré que notre approche est adéquate pour modéliser la composante de diffusion multiple des modèles physiques des couverts végétaux.

Ce paramétrage est alors intégré dans le modèle FLAIR, un modèle de transfert radiative des couverts végétaux, pour améliorer la façon dont il décrit la composante de diffusion multiple dans les couverts forestiers. Une autre approche qui traite la contribution de la diffusion multiple entre le couvert et son sol sou jacent est également ajoutée à celle qui traite la diffusion multiple dans le couvert supposant un sol sou jacent complètement absorbant comme il est décrit auparavant. La validation de la nouvelle version du modèle FLAIR est réalisée en utilisant des données reflectances multi angulaires obtenues par le

capteur aéroporté POLDER (POLarization and Directionality of the Earth's Reflectances) durant la compagne de mesures de terrain de BOREAS (BOReal Ecosystem-Atmosphere Study). Les résultats de cette comparison ont indiqué que la modélisation de la diffusion multiple que nous avons proposé est convenable au modèle FLAIR. Ces résultats ont également démontré que le problème de diffusion multiple peut être paramètrer par un nombre limité des paramètres de structure du couvert forestier et des propriétés optiques du feuillage.

Finalement, nous avons combiné le modèle FLAIR avec le modèle des propriétés optiques de la feuille PROSPECT. Nous avons exploré le potentiel de ce modèle combiné (PROFLAIR) à simuler la reflectance spectrale d'un couvert forestier. La comparaison entre la réflectance mesurée par le capteur Hyperion et la réflectance simulée par le modèle a montré la capacité de ce dernier à simuler effectivement la réflectance spectrale d'un couvert forestier. Le modèle a été ensuite utilisé en mode inverse pour estimer l'indice foliaire du couvert (LAI), la concentration de la chlorophylle (C_{a+b}) et la chlorophylle intégrée au niveau du couvert (LAI x C_{a+b}) à partir des données hyperspectrales de Hyperion en utilisant la technique des tables de correspondance (LUT). Le LUT a été peuplé en simulant le modèle PROFLAIR en mode direct en utilisant des jeux de données d'entrée du modèle. L'échantionnage de chaque paramètre d'entrée est défini sur la base de l'information recueillie à priori sur le terrain. Les variables estimés ont été ensuite comparés à des mesures de terrain en utilisant une fonction de coût. Les résultats ont montré que la capacité du modèle à estimer ces paramètres est raisonnable à l'ordre des performances des autres modèles déjà connus. La comparaison entre les paramètres estimées et mesurées a montré la capacité du modèle PROFLAIR à estimer le LAI du couvert avec un RMSE de 0.47 et la concentration de la chlorophylle avec un RMSE de 4.46 $\mu g/cm^2$.

Acknowledgements

Firstly, I would like to express my sincere appreciation and recognition to Professor Karl Staenz, my thesis supervisor. I am humbled by the guidance, inspiration, moral support and wonderful advices I got from him. I thank him for the enthusiasm, patience, availability that he has always shown to me.

My stay at the Canada Centre for Remote Sensing (CCRS) was facilitated by a dynamic support of its members. My deep recognition goes especially to H. Peter White and Richard Fernandes. I thank them for the numerous discussions, ideas, suggestions and for their critical reviews of the publications during the course of this work. I also thank them for the financial support they provided during the past four years.

I would also like to thank other members of CCRS who helped me in one way or the other. My special thanks go to Lixin Sun, Ray Soffer, John Schwarz and Shahid Khurshid. Thanks also go to Nadia Rochdi from the Alberta Terrestrial Imaging Centre (ATIC), Marie Weiss from the INRA, France, and Abdou Bannari from the University of Ottawa for the fruitful discussions.

During the course of this work, I had the chance and pleasure to benefit from scientific advices, fruitful suggestions and guidance from Professors Douglas King (Carleton University) and André Desrochers from the University of Ottawa. All my gratitude goes to them. I also want to thank Dr. Bahram Daneshfar (Agriculture and Agri-Food Canada), Dr. Scott Mitchell (Carleton University) and Dr. Edward A. Cloutis (University of Winnipeg) for agreeing to participate in the jury of this thesis.

Finally, I am indebted more than I can ever say to my parents for their constant support and for showing me, by example, how to be a better person. It wouldn't have been possible without the devout support from my wife Hasna. You have always provided me with the courage and enthusiasm to strive for higher achievements.

This thesis was conducted at the Ottawa-Carleton Geoscience Center, Department of Earth Sciences at the University of Ottawa. I want to thank the faculty, staff and my fellow graduate students. This research was completed with financial support from the Admission Scholarship Program of the University of Ottawa. I am also gratefully acknowledging the support of the Canada Centre for Remote Sensing / Natural Resources Canada for the financial support and the infrastructure access.

To my parents
To my wife Hasna
To my beloved son Ziyad

Tables of Contents

List of Tables

List of Figures

Chapter 1

General introduction

1.1. Introduction

1.1.1. Remote Sensing of vegetation biochemistry and biophysics

In recent decades, a growing effort has been devoted in developing algorithms to retrieve canopy vegetation variables such as Leaf Area Index (LAI), fraction of Photosynthetically Active Radiation (fPAR), plant water status and canopy integrated chlorophyll content. These variables are a prerequisite to many climate and ecological models (Sellers, 1986). Indeed, estimates of foliage biochemistry such as chlorophyll concentration, nitrogen content and leaf water content are the best indicators of vegetation strain (Zarco-Tejada et al., 2004 and 2001; Curran, 1989). Furthermore, biophysical variables such as LAI and biomass are widely used in eco-physiological models to quantify the primary production of the carbon cycle of terrestrial ecosystems (Bonan, 1993). Analysis of these variables in the laboratory is expensive and time consuming. Their evaluation can require covering large areas which are generally difficult to sample. Remote sensing has been acknowledged to be a valuable alternative tool in this case, since it provides spatially comprehensive and temporally repeatable information at a low cost.

In vegetation applications, data acquired with conventional broadband remote sensing sensors, such as NOAA's Advanced Very High Resolution Radiometer (AVHRR) and NASA's Landsat Thematic Mapper (TM), were mostly used for quantifying canopy biophysical and biochemical parameters. Most studies have focused on modeling the

relationship between the biophysical properties of vegetation canopies and the canopy reflectance using in most cases only three to six spectral bands. On the other hand, the availability of large amounts of spectral information provided by hyperspectral imaging systems helps to discriminate among biochemical features that have specific absorption and reflection characteristics over narrow wavelength intervals. These features cannot be observed with with the same precision with conventional broadband sensors.

While airborne hyperspectral sensors have demonstrated their potential to assess the forest condition for many years at limited scales (Zarco-Tejda et al., 2001; Samson et al., 2000), the new generation of spaceborne sensors such as NASA's EO-1 Hyperion, the German hyperspectral satellite EnMAP have the potential to derive these vegetation canopy parameters at regional scales. The incorporation of these parameters into process models, as input constraints, will improve predictive capability and enable assessments of vegetation growth (Smith and Curran, 1995). A review of the remote sensing literature reveals different modelling approaches to extract this information from hyperspectral data.

1.1.2. Estimation methods of canopy biophysical and biochemical variables

The algorithms for estimating biophysical and biochemical variables from a canopy can be classified into three categories: empirical methods, physical methods and hybrid approaches. Empirical methods are based mainly on relating and adjusting the remote sensing signal,

usually the reflectance, and the biophysical or biochemical variable in question. These relationships, commonly known as vegetation indices, are based on linear or nonlinear relationships between the reflectance signal at different wavelengths to a vegetation variable such as LAI, fPAR and chlorophyll content (Smith et al., 2003; Curran et al., 1997; Martin and Aber, 1997, Coops et al., 2003; Gong et al., 2003). Different vegetation indices have been proposed and widely used in various applications including the common Normalized Difference Vegetation Index (NDVI) developed by Rouse et al. (1973) by taking advantage of the contrast between the reflectance in red and near-infrared spectral regions. Other well known vegetation indices include PVI (Perpendicular Vegetation Index; Richardson and Wiegand, 1977), SAVI (Soil Adjusted Vegetation Index; Huete, 1988), TSAVI (Transformed Soil Adjusted Vegetation Index; Baret and Guyot, 1991) and GEMI (Global Environmental Monitoring Index; Pinty and Verstraete, 1992). These algebraic combinations are determined in a fashion that they provide information about vegetation structure and the state of the vegetation cover, such as leaf density and distribution, leaf water content, and leaf chlorophyll content (Liang, 2004). This quantitative information is not achievable using the qualitative approach of traditional photographic interpretation techniques.

On the other hand, physically based methods rely on the description of the physical process of interaction between the radiation signal and the matter in a given wavelength. This process is governed by Maxwell's equations. By combining this method with the empirical one, a third category can be defined which is referred to in the literature as the hybrid approach (Gastellu-Etchegorry et al., 1996).

1.1.3. Physically-based models

Although, empirical relationships have been widely used in estimating biophysical and biochemical features predictive estimation may be hindered in areas beyond the study region due to variance in certain factors, such as the contribution of the understorey-background, the atmospheric effects and the solar-viewing geometry that were not represented in the empirical model. To explicitly improve the retrieval of the estimated biophysical and biochemical parameters while taking into account those influencing factors, it is preferable to use physically-based models of the radiative transfer within a forest canopy. The advantage of using these types of models is to understand which driving factors determine the canopy stand reflectance. In the literature, there are various models which have been applied to characterize the anisotropy of vegetation canopy reflectances (Chen and Leblanc, 1997; Li and Strahler, 1995; Myneni et al., 1992). However, each of these models has its own advantages and limits depending on specific conditions for which they were developed. The complexity and the differences in vegetation canopies, particularly forest environments, make simulations of the amount of solar energy absorbed, transmitted or reflected by the canopy dissimilar from one model to another. These quantities are determined by the optical properties of elements composing the canopy, their spatial organization and the reflectance of the underlying background such as soil and understorey vegetation. As an example, the Four-Scale Model (Chen and Leblanc, 2001 and 1997) can simulate the bidirectional reflectance distribution function (BRDF) by considering four architectural levels of the canopy: (1) tree grouping, (2) crown geometry, (3) branches and (4) crown foliage. This model has the advantage of using non-random tree distribution compared to most optic-geometrical models.

The Four-Scale Linear Model for Anisotropic Reflectance (FLAIR; White et al., 2001) is a linear kernel model developed based on the Four-Scale model radiative transfer theory proposed by Chen and Leblanc (1997). The idea behind the development of the FLAIR model is to make it flexible and simple for use in inversion mode (White et al., 2001). To achieve this goal, the authors reformulated the Four-Scale model by minimizing, as much as possible, the number of parameters depending on canopy architecture. This was done by keeping and simplifying those parameters which have a direct relationship between canopy architectural properties and model coefficients. The principal modifications in the FLAIR model are related to the theory of the probabilities of viewing illuminated background, directly illuminated crown foliage, shaded canopy and shaded background proportions. The main weakness of the FLAIR model is how the multiple scattering component is handled. The authors used constant multiple scattering factors to approximate the contribution of the shaded components to the observed reflectance. Nevertheless, Liang and Strahler (1993) demonstrated that this component is spectrally and angularly variant. In addition, the contribution of the multiple scattering component is very important, particularly in the near-infrared spectral region where the scattering from leaves is high. It can exceed 50% of the total scattering (Liang, 2004). Therefore, incorporating a more physically-based description of the multiple scattering contribution is essential, not only to simulate adequately the canopy reflectance, but also to link remote sensing data to biophysical and biochemical quantities of vegetation.

Model inversion techniques are a very important step in order to estimate these parameters. These models can also be coupled with radiative transfer models at the leaf level such as

PROSPECT (Jacquemoud and Baret, 1990) and LIBERTY (Dawson et al., 1998) in order to estimate certain biochemical or biophysical parameters specific to vegetation studied. However, there are some issues when retrieving canopy biophysical and biochemical variables by inverting radiative transfer models from hyperspectral remote sensing data.

1.1.4.Inversion techniques

The issues of retrieving canopy biophysical and biochemical variables from hyperspectral data using radiative transfer modelling can be summarized as follows:

- Well-calibrated data: The quality of hyperspectral data is a common problem for the majority of airborne and satellite hyperspectral sensors (Khurshid et al., 2006). Correcting sensor artefacts such as stripes, smile and noise, improper calibration, atmospheric and geometric effects are required to optimize the data quality. However, the advancement in hyperspectral technologies will certainly enhance the performance of future hyperspectral sensors as well as their calibration.

- Robust radiative transfer models: A precise model must describe all the mechanisms of interactions between electromagnetic radiation and all components of the scene as discussed earlier. This requires knowledge of the nature of the radiation and a detailed description of the canopy structure and optical properties of its constituents, and the different processes of extinction, diffusion and reflection for a incident light beam.

Unfortunately, precise models are always complex and their inversion is difficult to achieve.

- The inversion process: Inverting a physically based model is not always a straightforward process. In the simplest case, it can be achieved analytically for linear models. However, in most cases non-linear models require the use of optimization inversion approaches. Theses methods rely on minimizing the cost function expressing the distance between observed and modeled reflectance values. The definition of suitable cost functions is critical to the success of the inversion process. These functions account for the uncertainties associated with both the model and the measurements. Model uncertainties contain, in part, the assumptions made on the structure of the canopy and the way the electromagnetic radiation interacts with the canopy elements (Combal et al., 2002). The uncertainties associated with the measurements include the errors associated with the processing of remote sensing data (radiometric correction, atmospheric correction, etc). In practice, the use of the cost function is an iterative process based on searching the combination of model inputs that can lead to the closest match between estimated and measured values. However, this process is often time consuming and sensitive to the initial guesses of the solution (Pinty and Verstraete, 1991).

Common procedures of nonlinear model inversion are based on optimization approaches such as simplex (White et al., 2002) or quasi-Newton methods. They are widely used for their simplicity and minimum constraint demands on the input parameters. However, these

iterative approaches can converge to local minima rather than the desired solution. To avoid becoming trapped inside local minima, the initial guess of input parameters should be close the real solution. Other techniques based on pre-computed values stored in databases such as look-up-tables (LUTs) and Neural Networks (NN) are the most popular optimisation inversion approaches used for retrieval of canopy biophysical variables. The NN approach is based on training Artificial Neural Networks (ANNs) according to databases previously generated (Bacour et al., 2006; Weiss and Baret, 1999). These relationships (networks) between reflectance values and canopy biophysical and biochemical variables are then adapted to the actual situations. The NN method was previously applied to biophysical parameter retrieval from optical and microwave remote sensing data (Baret et al., 1995; Weiss and Baret, 1999). The LUT approach, on the other hand, consists of running a radiative transfer model in forward mode to simulate canopy BRFs from a wide range of canopy biophysical and biochemical variables. The resulting reflectance values are stored in a LUT. The measured reflectance values are then compared to the generated LUT using a minimizing function (Combal et al., 2002; Kimes et al., 2000; Weiss et al., 2000; Knyazikhin et al., 1998). The major advantage of the LUT approach is that it is not restricted to a given type of target cover (Roberts, 2001). Because of the ill-posed nature of the inverse problem (Combal et al., 2002), a unique inversion solution is not always achievable. For example, several canopy biophysical variables may yield similar spectral signatures (Weiss et al., 2000). Combal et al. (2002) proposed the use of *a priori* information as an approach to solve such ill-posed problems. Ancillary information such as soil type, land-cover type, and canopy density can be used to constrain the model inversion for the estimation of canopy characteristics.

1.2. Research objectives and hypothesis

The main goal of this research is to develop a method for quantitative retrieval of biophysical and biochemical variables of forest canopies from hyperspectral (Hyperion) data based on physical principles. The FLAIR and PROSPECT models will be linked, named as the PROFLAIR model, and inverted to estimate those parameters. The FLAIR model was designed first to model the angular influences to canopy reflectance. This model has been validated successfully with multi-angular data sets obtained by various sensors for the boreal forest area including airborne POLarization and Directionality of the Earth's Reflectances (*POLDER*) data, compact airborne spectrogarphic imager (*casi)* data, and ground-based Portable Apparatus for Rapid Acquisition of Bidirectional Observations of Land and (*PARABOLA*) data in the red and near-infrared wavelength regions (White et al., 2001 and 2002a). However, its use in hyperspectral applications is constrained due to the lack of a multiple scattering scheme that can be used in any wavelength particularly in the near-infrared spectral region.

It is important to note that the methodology of this research study is based on four hypotheses which can be summarized as follows:

1) Can a simple parameterization of the multiple scattered contribution to the bidirectional reflectance factors (BRF) of vegetation canopies based on canopy spectral invariance match the more complex 3D ray tracing models for a given vegetation canopy type assuming a black soil?

2) Will the implementation of this parameterization into the FLAIR model enhance its ability to simulate canopy BRF in comparison to the previous version in which the multiple scattering contribution was based on constant factors?
3) Can the combined PROSPECT+FLAIR (PROFLAIR) model with the incorporation of the proposed multiple scattering parameterization realistically simulate canopy reflectance compared to Hyperion reflectance data?
4) Can the retrieval of canopy LAI and chlorophyll content by inverting the PROFLAIR model using the LUT approach be successful on the order of field estimate uncertainties if a priori information based on commonly available ancillary data is used in the inversion process?

The objectives can be summarized as follows:

i) Developing a new multiple scattering scheme suitable for hyperspectral modeling of vegetation canopies based on the optical properties of the crown foliage and the background and the structural properties of the canopy.

ii) Incorporating the newly developed multiple scattering scheme into the FLAIR model and evaluating these enhancements by comparing the FLAIR model to the airborne POLDER data acquired during the BOReal Ecosystem-Atmosphere Study (BOREAS) campaign of 1994.

iii) Linking both the FLAIR model and the leaf optical properties model PROSPECT to simulate canopy bidirectional spectral reflectance of vegetation canopies.

iv) The coupled model will be applied to a forested area near Kamkotia, Ontario to quantify the effect of acid mine drainage on the surrounding forest area using Hyperion data.

1.3. Thesis outline

This thesis is organized into seven chapters. After this introduction in which the context of the conducted research is reviewed, the second chapter will entirely focus on the development of the new parameterization of the angular distribution of the multiple scattering radiation field which is based on radiative transfer theory. The new approach will be evaluated against a detailed 3-D ray tracing model, PARCINOPY, as well as reference datasets from the Radiation Modelling Intercomparison Experiment On-Line Checker (Pinty et al., 2004; Widlowski et al., 2007).

In the third chapter, the multiple scattering parameterization approach presented in the second chapter will be implemented into the FLAIR model to enhance its ability to describe both spectral and angular dependency of the multiple scattered radiation component. The modified model is tested using the multi-angular data sets obtained by the airborne sensor POLDER during the BOReal Ecosystem-Atmosphere Study (BOREAS) campaign of 1994.

In the fourth chapter, the dataset used in testing the PROFLAIR model in both forward and inverse modes is introduced. A description of the study site, plot design, methodology of field data acquisition and the procedure of processing the hyperspectral data is presented in this chapter.

In the fifth chapter, the potential for the retrieval of canopy leaf area index (LAI), leaf chlorophyll content (C_{a+b}) and canopy integrated chlorophyll content (LAI x C_{a+b}) is investigated by inverting the PROFLAIR model. Firstly, a direct comparison between spectral reflectances simulated with the PROFLAIR model is presented using a set of data collected in the field and Hyperion data acquired over the study site. Secondly, the inversion method used for the retrieval is outlined and finally, the results of the parameter retrieval process are discussed.

Chapter six includes the conclusion summarizing the principal results achieved in this work and the limitations of both methodology and datasets. The literature used for this work is listed in chapter seven.

Chapter 2

Simple parameterization of the angular distribution of multiple scattered radiation

This chapter is based on

Omari, K., Fernandes, R., Staenz, K., Rochdi, N., Chelle, M. (2009) "A simple parameterization of the angular distribution of the multiple scattered radiation", Remote Sensing of Environment (in review).

Abstract:

This study focused on the development and assessment of a simple parameterization of the multiple scattering within canopies assuming the single scattering field is known. The parameterization is based on the concept of spectral invariants related to recollision and escape probabilities from vegetation canopies. The simplified approach is evaluated against a detailed 3-D ray tracing model, PARCINOPY, as well as reference datasets from the Radiation Modelling Intercomparison Experiment On-Line Checker. Comparison to homogenous canopies simulated with PARCINOPY showed that the model's performance is best in both the principal and perpendicular planes at low and middle LAI levels for all solar zenith angles. The comparison to the On-line Checker datasets shows also that the model is a suitable approach to describe the multiple scattering components of physically based models.

2.1. Introduction

Satellite remote sensing of land surface parameters often involves the inversion of directional reflectance derived from measurements in optical wavelengths (Asrar, 1989). Numerical models of photon vegetation interactions offer a rigorous basis for inversion and provide additional constraints such as energy conservation (Myneni and Ross, 1991). There are two general approaches for modelling radiative transfer in vegetation. Monte-Carlo (MC) photon tracing approaches track statistics of photon fates over one or more canopy realizations (Ross and Marshak, 1991). Alternatively, classical radiative transfer (RT) models solve the

classical radiative transfer equation over volumes with defined optical properties (Myneni and Ross, 1991).

MC models are sufficiently accurate and precise that they now form the basis of reference standards for model intercomparison (Widlowski et al., 2007). However, MC models are not currently used for large area mapping since they would require building a large library of canopy realizations. Furthermore, Rochdi et al. (2006) suggested that these realizations may need details down to the single needle to avoid substantial biases in resolved canopy bidirectional reflectance factors (BRFs).

RT models have been widely used to describe BRFs of some canopies given that sufficiently detailed sets of input parameters are provided (Ross, 1981; Nilson, 1971; Li and Strahler, 1992; Verhoef, 1984; Chen and Chilar, 1996; Huang et al., 2007). However, even detailed RT models still deviate substantially from reference ensembles derived from MC models (Widlowski et al., 2007). Nevertheless, RT models are still widely used for parameter estimation for a number of reasons (Knyazikhin et al., 1998, Bacour et al., 2006, Chen et al., 2002; Gobron et al., 1997). Firstly, RT models can use statistical parameterizations of canopy structure that allow them to both describe landscapes of large areas typical of remote sensor measurements and to incorporate fine structural details such as needles. Secondly, inversion schemes using RT models usually require some specification of a priori parameter distributions that can in some cases compensate for approximations used in RT theory (Combal et al., 2002). Thirdly, RT models are currently much more computationally efficient that MC models when applied to complex natural landscapes.

Multiple scattering (MS) is one aspect in RT models that has often been treated in a simplified manner (Li and Strahler, 1995; Chen and Leblanc, 1997; White et al., 2001). This is primarily because, in wavelengths with high foliage absorptance, uncollided and single scattered fluxes are dominant while in wavelengths with low foliage absorptance multiple scattered fluxes tend to be somehow isotropic within the canopy (Ross, 1981). Approximations of MS contribution to the BRFs include the use of view factors (Chen and Leblanc, 2001), two-stream (Ross, 1981; Sellers, 1985) and four-stream (Verhoef et al., 1984; Liang and Strahler, 1993) RT models. These approaches do not typically require additional parameters besides single scattering modeling, and they do not seem to add complexity. However, it must be recognized that model inversion is often performed over a range of bands simultaneously. In this sense, it would be advantageous if the spectrally invariant aspects of multiple scattering could be modeled separately from those aspects that are sensitive to the optical properties of canopy elements, since this would provide additional constraints during model inversion.

Over the last decade the concept of canopy spectral invariants has been promoted as a means of concisely describing the relationship between canopy structure and optical properties and hemispherical fluxes. Knyazikhin et al. (1998) developed a Leaf Area Index (LAI) and fraction of Absorbed Photosynthetically Active Radiation (fAPAR) retrieval approach using inversion based on only the eigenvector corresponding to the dominant positive eigenvalue, p, of a three dimensional (3-D) RT problem with uniform upper and lower boundary conditions. In this paper, p corresponds to the expected value, taken over all collision orders

of the probability that a photon will recollide within vegetation in the presence of an absorbing lower boundary (Panferov et al., 2001). In general, the recollision probability, p, will vary with scattering order (Disney et al., 2005) and corresponds to a weighting of successive eigenvalues of the RT problem (Wang et al., 2003). However, Disney et al. (2005) demonstrated that a single effective p can model multiple scattered bi-hemispherical fluxes almost as well as using different p-factors per scattering order. Theoretical analyses (Knyazikhin et al., 1998) and Monte Carlo simulations (Smolander and Stenberg, 2005) suggest that, ignoring the first scattering order, p is minimally sensitive to the variation of the incident beam. The recollision probability is related to the density of canopy elements that can be approximated for shoots (Smolander and Stenberg, 2005) and for homogenous canopies (Smolander and Stenberg, 2005; Disney et al., 2005).

While the theoretical advances and empirical results reviewed in the previous paragraphs give confidence in the suitability of canopy spectral invariants for developing simple models of hemispherical fluxes, modifications are required to allow their use in modelling BRFs since some existing and proposed remote sensing platforms are designed to observe directional non-nadir reflected radiance such as acquired with the Multi-angle Imaging SpectroRadiometer (MISR) and the Compact High Resolution Imaging Spectrometer onboard the Project for On-Board Autonomy (CHRIS/PROBA). The goal of this paper is to develop and test a parameterization for resolving the multiply scattered contribution to the BRF for vegetation canopies making use of canopy spectral invariants (Huang et al., 2007). The scope is limited to relatively uniform canopies (i.e., described using only LAI and a single clumping factor) with an absorbing lower boundary condition. The former limitation

matches the level of complexity of many RT models used for inversion (Knyazikhin et al., 1998), while the latter can be extended to arbitrary boundary conditions following Knyazikhin et al. (1998). Keeping in mind these limitations, the specific research question is to determine how well the multiple scattered contribution to BRFs can be characterized using the same parameters (LAI, leaf single scattering albedo, and leaf extinction coefficient) as utilized in previous studies that have modeled bi-hemispherical fluxes, but with a spectrally invariant parameterization for structural properties. The null hypothesis when addressing this question is that there will be no substantial improvement in matching reference values of multiple scattering contributions to BRFs using the proposed new approach compared to assuming isotropic bi-hemispherical fluxes. In disproving this null hypothesis, the use of directional measurements will be facilitated for the retrieval of canopy parameters.

In section 2.2; the necessary additions to the current spectral invariant theory are described for our multiple scattering parameterization. Section 2.3 describes the datasets, derived from MC Ray Tracing simulations used to evaluate the theory. The suitability of the parameterization with respect to these datasets and for further applications is discussed in section 2.4.

2.2. Theory and Models:

2.2.1. Multiple Scattered Contribution to Bi-hemispherical Reflectance

The 1-Dimensional RT equation for a canopy with an absorbing lower boundary is given as:

$$t(\lambda)+r(\lambda)+a(\lambda)=1, \tag{2.1}$$

where $t(\lambda)$, $r(\lambda)$ and $a(\lambda)$ are the canopy bi-hemispherical transmittance, bi-hemispherical reflectance and absorptance, respectively and λ is the wavelength. The leaf scattering coefficient $\omega(\lambda)$ is defined as the sum of leaf reflectance $\rho(\lambda)$ and transmittance $\tau(\lambda)$. If $\omega(\lambda)$ is null the canopy interaction coefficient, i_o, defined as the probability that a photon from the incident radiation will hit a phytoelement, is the canopy interceptance as illustrated in Figure 2.1 (Smolander and Stenberg, 2005). The portion of intercepted photons that escape the canopy in both upward and downward directions is the canopy scattering coefficient and can be written as follows:

$$s(\lambda)/i_o = 1 - a(\lambda)/i_o \quad , \tag{2.2}$$

where $s(\lambda)$ is the sum of $t(\lambda)$ and $r(\lambda)$.

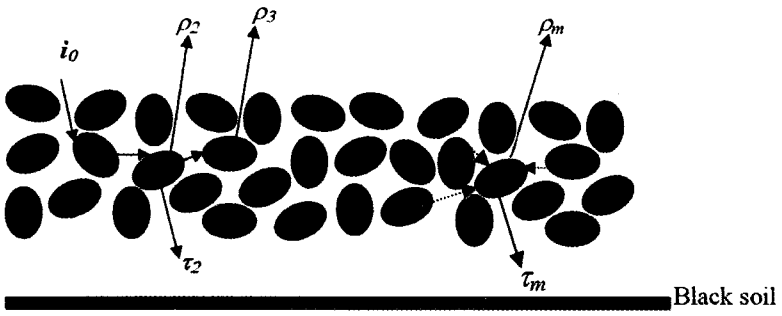

Figure 2.1: A schematic presentation of the distribution and orientation of canopy elements. The arrows illustrate the photon multiple interactions before exiting the canopy. i_o represents the incident photons, ρ_i the upward escape probability relative to the total scattering for photons that have completed *i-1* interactions and τ_i is the downward escape probability relative to the total scattering for photons that have completed *i-1* interactions.

Let p_i correspond to the photon recollision probability after the ith interaction. Following Smolander and Stenberg (2005), the multiple scattered contribution to the canopy scattering coefficient, $S_M(\lambda)$, is given by:

$$s_M(\lambda)/i_0 = \left[\omega^2(\lambda)p_1(1-p_2)+\omega^3(\lambda)p_1p_2(1-p_3)+\omega^4(\lambda)p_1p_2p_3(1-p_4)+\ldots + \omega^m(\lambda)p_1p_2p_3\ldots p_{m-1}(1-p_m)\right] . \quad (2.3)$$

The corresponding upward multiple scattered top of canopy flux, $r_M(\lambda)$, is then (Huang et al., 2007):

$$r_M(\lambda) = i_0\left[\omega^2(\lambda)p_1(1-p_2)\rho_2+\omega^3(\lambda)p_1p_2(1-p_3)\rho_3+\omega^4(\lambda)p_1p_2p_3(1-p_4)\rho_4+\ldots + \omega^m(\lambda)p_1p_2p_3\ldots p_{m-1}(1-p_m)\rho_m\right] , \quad (2.4)$$

where ρ_i is the upward escape probability relative to the total scattering for photons that have completed *i-1* interactions.

Assuming that both relative escape and recollision probabilities can be replaced by some constant effective values for all scattering orders (i.e., $\rho_i = \rho_m$ and $p_i = p_r$) as in Huang et al. (2007) and Disney et al. (2005), $r_M(\lambda)$ can then be written as follows:

$$r_M(\lambda) = \frac{i_0 \omega(\lambda)^2 p_r (1 - p_r) \rho_m}{1 - p_r \omega(\lambda)} \quad . \tag{2.5}$$

Disney et al. (2005) approximated $r_M(\lambda)$ in a similar fashion as:

$$r_M(\lambda) = \frac{\omega(\lambda)^2 R_2}{1 - p_r \omega} \quad . \tag{2.6}$$

Comparison between Eq. (2.5) and Eq. (2.6) suggests:

$$R_2 = \rho_m i_0 (1 - p_r) p_r . \tag{2.7}$$

Disney et al. (2005) verified that Eq. (2.6) is an adequate approximation when both p_r and R_2 were fitted to data from MC simulations. While their finding verifies the functional form of Eq. (2.6), an effort has to be made to relate both re-collision and relative escape probabilities to canopy parameters if inversion is to be performed.

The p factor can be approximated as a function of LAI using either analytical methods or by fitting to MC simulations (Mõttus and Stenberg, 2008; Stenberg, 2007; Mõttus, 2007; Smolander and Stenberg, 2005; Disney et al., 2005). In our study, the approximation of Mõttus (2007) with $p_r = a(1-\exp(-bL_e))$ was used although it corresponds to the effective recollision probability for all scattering orders and may have some bias for cases where single scattering dominates. The parameters a and b are parameters obtained via fitting to data from MC simulations and L_e is the effective LAI. The relative upward escape probability has previously been fixed at a constant value (e.g., Rautiainen and Stenberg, 2005). This assumption has not been extensively tested. More recently, Mõttus and Stenberg (2008) presented a simple semi-empirical parameterization of the ratio of canopy reflectance to the total scattering (Q-ratio) as a function of leaf albedo based on modeling results. This approximation has not been investigated in the multiple scattering parameterization case. In this study, ρ_m was related to the effective LAI and leaf angle distribution using a 1-dimensional discrete ordinate RT model (Myneni et al., 1991).

2.2.2. Bi-directional Reflectance Factor of Multiple Scattering

The BRF for multiple scattering, $r_M(\lambda,\Omega_s,\Omega_v)$, is defined as the portion of incoming photons along the direction Ω_s that are multiple scattered within the canopy and exit along the direction Ω_v. Ω_s and Ω_v refer to the illumination and exitant directions. The canopy phase function, $P_M(\Omega_s,\Omega_v)$, for this multiple scattered field can be defined as the fraction of scattered radiation that escapes the canopy in a given direction per unit steradian:

$$r_M(\lambda,\Omega_s,\Omega_v)=r_M(\lambda)P_M(\Omega_s,\Omega_v)\ . \tag{2.8}$$

Ross (1981) proposed a phase function relating leaf transmittance and albedo to the scattering phase angle. Liang and Strahler (1993) proposed the use of the Henyey-Greenstein phase function as an approximation to the real phase function and later, the anisotropy parameter is approximated as a polynomial function of leaf transmittance to canopy albedo ratio (Liang, 2004). Nevertheless, when dealing with the BRF of multiple scattering, the directional escape function should be azimuthally invariant (Knyazikhin et al., 1998; Liang, 2004; Gobron et al., 1997). In addition, it is known that for snow-free vegetated terrestrial surfaces, the reflectance factor of multiple scattering usually has a bowl shape (Pinty et al., 2001). Given that and assuming that the incident beam has a small effect on the multiple scattering, $P_M(\Omega_s,\Omega_v,\varphi)$ can be simplified to a mono-directional phase function $P_M(\Omega_v)$ (Huang et al., 2007).

Mõttus (2007) presented a straightforward approach in estimating the first-order canopy reflectance and transmittance. In this paper, the same logic is applied to approximate the directional reflectance factor of multiple scattering as follows:

$$r_M(\lambda,L,\theta_v)=r_M(\lambda)\frac{\int_0^L\sum_{j=2}^{\infty}I_{j-1}(l,\Omega_s)K_vT(l,K_v)dl}{\int_0^{2\pi}\left[\int_0^L\sum_{j=2}^{\infty}I_{j-1}(l,\Omega_s)K_vT(l,K_v)dl\right]\sin(\theta_v)d\theta_v}, \tag{2.9}$$

where $T_v(l,K_v)=e^{-K_v l}$ is the fraction of multiple scattered radiation escaping the canopy in the view direction without having further interaction and $K_v=\frac{G(\theta_v)\Omega(\theta_v)}{\cos(\theta_v)}$ is the extinction coefficient in the view direction. $G(\theta_v)$ expresses the projection of unit leaf area on a plane perpendicular to the view angle θ_v and $\Omega(\theta_v)$ represents the canopy clumping index introduced to take account for foliage grouping within the canopy (Kucharik et al., 1997; Chen, 1996; Nilson, 1971). $I_{j-1}(l, \Omega_s)$ expresses the radiation flux at the depth l (l is the downward cumulative leaf area index) in the direction of Ω_s that has been scattered $j-1$ times within the canopy before exiting the canopy. L is the canopy leaf area index. Under the assumption, that for the multiple scattering, the flux I_{j-1} is uniform within the canopy, it can be expressed as: $I_{j-1}(l,\Omega_s)\approx\overline{I_{j-1}}(\Omega_s)$. Thus, Eq. (2.9) becomes:

$$r_M(\lambda,L,\theta_v)=r_M(\lambda)\frac{\sum_{j=2}^{\infty}I_{j-1}(l,\Omega_s)\int_0^L K_v T(l,K_v)dl}{\sum_{j=2}^{\infty}I_{j-1}(l,\Omega_s)\int_0^{2\pi}\left[\int_0^L K_v T(l,K_v)dl\right]\sin(\theta_v)d\theta_v} \tag{2.10}$$

$$=r_M(\lambda)\frac{\int_0^L K_v T(l,K_v)dl}{\int_0^{2\pi}\left[\int_0^L K_v T(l,K_v)dl\right]\sin(\theta_v)d\theta_v}.$$

Comparison of Eq. (2.8) and Eq. (2.10) gives:

$$P_M(\Omega_v, L) = \frac{\int_0^L K_v T(l, K_v) dl}{\int_0^{\pi/2} \left(\int_0^L T(l, K_v) dl \right) \sin(\theta_v) d\theta_v}$$
$$= \frac{\int_0^L K_v e^{-K_v l} dl}{\int_0^{\pi/2} \left(\int_0^L e^{-K_v l} dl \right) \sin(\theta_v) d\theta_v} \qquad (2.11)$$
$$= \frac{\left(1 - e^{-K_v L}\right)}{\int_0^{\pi/2} \left(1 - e^{-K_v L}\right) \sin(\theta_v) d\theta_v}.$$

For horizontal leaves is:

$$\int_0^{\pi/2} \left(1 - e^{-K_v L}\right) \sin(\theta_v) d\theta_v = \left(1 - e^{-L}\right). \qquad (2.12)$$

Substituting Eq. (2.12) into Eq. (2.11), the phase function for multiple scattering becomes:

$$P_M(\Omega_v, L) = \frac{\left(1 - e^{-K_v L}\right)}{\left(1 - e^{-L}\right)}. \qquad (2.13)$$

Eq. (2.13) is used to approximate the phase function for other leaf angle distributions. Thus, the BRF of multiple scattering can be written as follows:

$$r_M(\lambda, \theta_v) = \rho_m \frac{i_0 \omega(\lambda)^2 p(1-p)}{1 - p\omega(\lambda)} \frac{\left(1 - e^{-K_v L}\right)}{\left(1 - e^{-L}\right)}. \qquad (2.14)$$

To test the proposed model, Eq. (2.14) is compared to results from a MC model as well as to the RAMI On-line Checker (ROMC) datasets.

2.3. Data sets

2.3.1. PARCINOPY

Several reference data sets generated using the PARCINOPY (PARticle traCINg in the canOPY) ray-tracing model were used (Chelle and Andrieu, 1996). This model has been previously used by Kuusk et al. (1997) to assess their Markov chain canopy reflectance model (MCRM) over barley and beet computer simulated crops. It was also used as a reference in Weiss et al. (2000) to investigate model inversion techniques to estimate canopy biophysical variables. More recently, Rochdi et al. (2006) used the same model to assess the effect of a simple parameterization of needle clumping within shoots on radiative transfer within canopies. PARCINOPY allows the separation of BRDF fields after any desired number of interactions. For the purpose of this study, the total scattering field was separated into the first and multiple scattering fields. The simulations were performed using computer designed canopies where leaves are randomly located and oriented using a spherical leaf angle distribution. Canopies with LAI values equal to 0.5, 1.9 and 5.9 were considered, and illumination angles (θ_s) were set to 0, 20 and 45 degrees. The outputs were sampled in both principal and perpendicular planes with 5° intervals starting from -75° to 75° view angle in the red and near infrared spectral (NIR) bands.

2.3.2. RAMI

The RAMI (RAdiation transfer Model Inter-comparison) exercise is a benchmarking attempt to evaluate the accuracy of radiative transfer models used in terrestrial surface characterization (Pinty et al., 2004; Widlowski et al., 2007). In the RAMI third phase, a standard reference "surrogate truth" has been developed as a result of a mutual agreement based on six 3-D Monte Carlo models laying within 1% of each other (Widlowski et al., 2007). At present, model developers can easily and autonomously assess the performance of their models using the On-line Model Checker (ROMC) available at http://romc.jrc.ec.europa.eu (Widlowski et al., 2007). The ROMC allows the comparison of RT models against already published RAMI results using the so-called debug mode.

In this study, the angular variability of the MS reflectances was selected from the ROMC datasets simulated using a turbid uniform media in the red and NIR bands in both principal and perpendicular planes with an LAI set to 3. The illumination angle (θ_s) is set to 20° and leaf reflectance (ρ) and transmittance (τ) are set to 0.0546 and 0.0149 in the red band and 0.4957 and 0.4409 in the NIR band. The ground reflectance is set to 0.127 and 0.159 in the red and NIR bands, respectively.

2.4. Results Discussion

Figure 2.2 shows an example of PARCINOPY outputs using the NIR band and sampled in the solar principal plane. This Figure shows the angular changes as well as the contribution

of the multiple scattering field to the total upward scattering field as a function of the geometry of the sampling and the structure of the canopy. The considered ground is not reflecting (black soil). Thus, the reflected radiation is purely a result of the canopy scattering. In this case, MS from the NIR band is considerably larger than MS from the red band suggesting that it is more important to have good relative agreement between PARCINOPY MS fields and the proposed simplified models' MS field for NIR.

Figure 2.3 illustrates the variation of ρ_m as a function of LAI and leaf angle distribution in the near infrared based on a 1-D discrete ordinates RT model (Myneni et al., 1991). As can be seen, the fraction of the upwelling multiple scattering component increases with LAI from 0.51 to 0.76 for a planophile canopy, from 0.51 to 0.69 for an erectophile canopy and from 0.51 to 0.70 for a uniform canopy for an LAI ranging from 0.5 to 7.0. Recently, Mottus and Stenberg (2007) have shown that while ρ_m can be related to LAI relatively consistently for homogenous canopies, there may be a need for more complex relationships when dealing with heterogeneous canopies.

Figure 2.4 shows the variation of the phase function for multiple scattering $P_M(\Omega_v, LAI)$ as defined in Eq. 13. The phase function transition from a flat (isotropic) shape to a bowl shape with decreasing LAI was also reported by Pinty et al. (2002). As it can be seen, all of the PARCINOPY and ROMC simulations also generate similarly bowl-shaped phase functions.

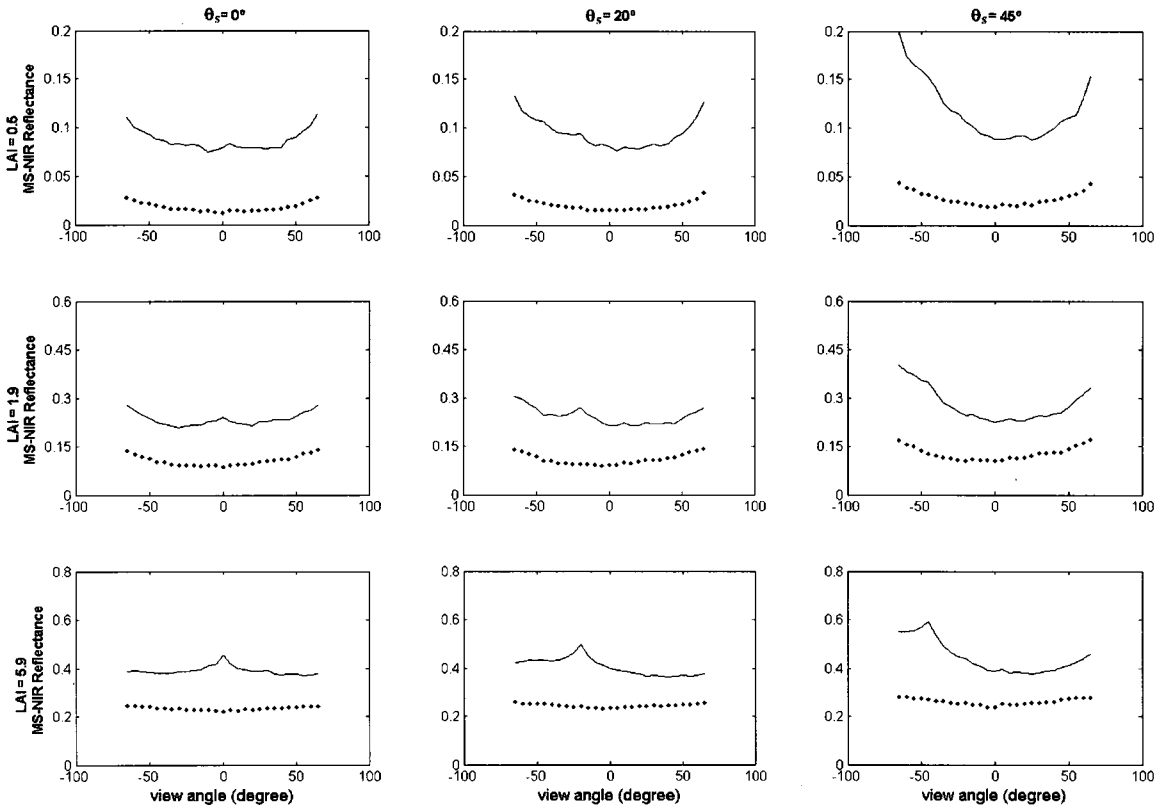

Figure 2.2: PARCINOPY total scattering (solid line) versus PARCINOPY multiple scattering (dots) in the principal solar plane for different LAI values.

Figures 2.5, 2.6, 2.7 and 2.8 illustrate the comparison between the PARCINOPY simulations and the proposed approximation (Eq. 2.14) in both principal and perpendicular planes for the red and NIR bands. Theses Figures show a good agreement in both magnitude and shape of the canopy multiple scattering reflectances in low and mid LAI values. In the NIR (Figures 2.5 and 2.6), the BRDF of multiple scattering calculated based on Eq. (2.14) reproduces reasonably the PARCINOPY equivalent in low and mid LAI. However, in high LAI canopy stands, Eq. (2.14) overestimates the BRDF of multiple scattering particularly at nadir view angle.

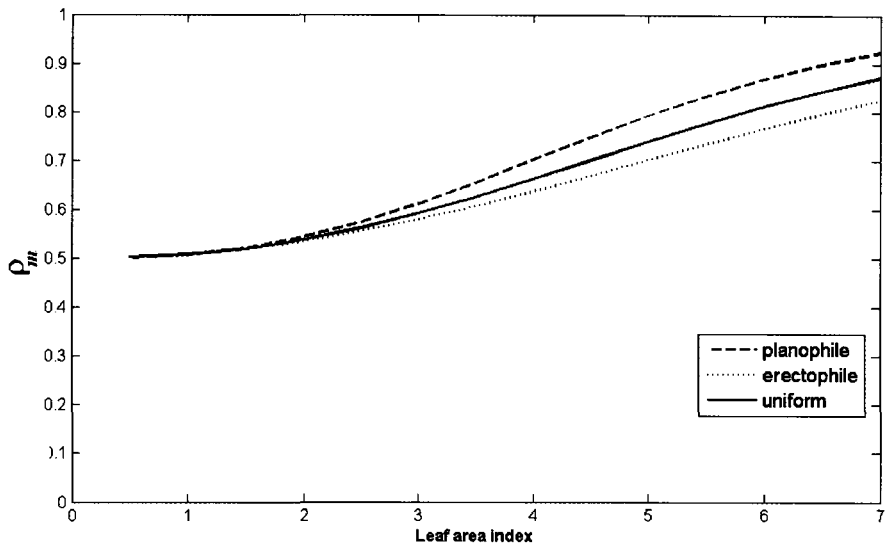

Figure 2.3: Variation of the constant ratio ρ_m as a function of LAI and leaf angle distribution based on the discrete ordinate model in the NIR region ($\rho(\lambda)= \tau(\lambda)$ =0.45) for a planophile, erectophile, and uniform canopy.

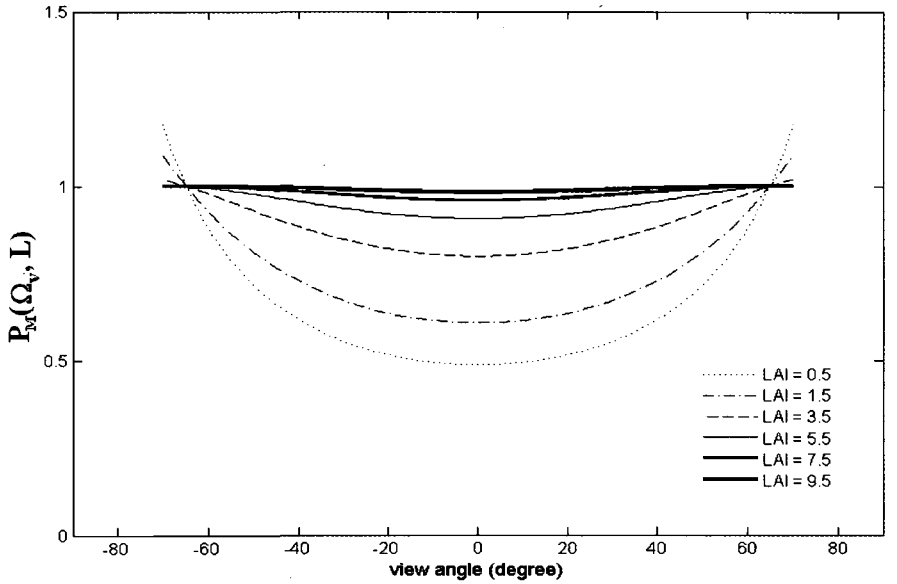

Figure 2.4: The approximated upward phase function for multiple scattering $P_M(\Omega_v, L)$ for different view angles and LAI.

This may be attributed to our assumption that the parameterization of mean re-collision probability p and multiple scattering re-collision probability (p_r) is the same. More investigations are needed to determine the most appropriate parameterization of p_r. In the red band (Figures 2.7 and 2.8), the reflectance factor of multiple scattering calculated based on Eq. (2.14) and the PARCINOPY equivalent are close for low and mid-LAI stands. However, when the LAI is high, the directional variability of multiple scattering reflectance factor generated with the PARCINOPY model is relatively large compared to the corresponding one calculated with Eq. (2.14). This may be due to the fact that the PARCINOPY simulation uses finite leaf sizes that implicitly induce clumping and reduces the effective LAI. In addition, the photons contributing to the reflectance factor of multiple scattering at the vertical downward depth l in the PARCINOPY case, are mostly coming from the upper side of the thickness dl due to the strong absorption of leaves in this wavelength and to the total absorbing background. However, the model based on Eq. (2.14) considers photons coming from all directions to the dl and contributing to the reflectance factor of multiple scattering. Neither of these will significantly impact the modeling of the total scattering since the contribution of multiple scattering to the total scattering is low (around 5%) in the red band. Overall, the model presented in this paper has demonstrated a potential for approximating the anisotropy of the reflectance factor of multiple scattering when compared with the PARCINOPY synthetic data.

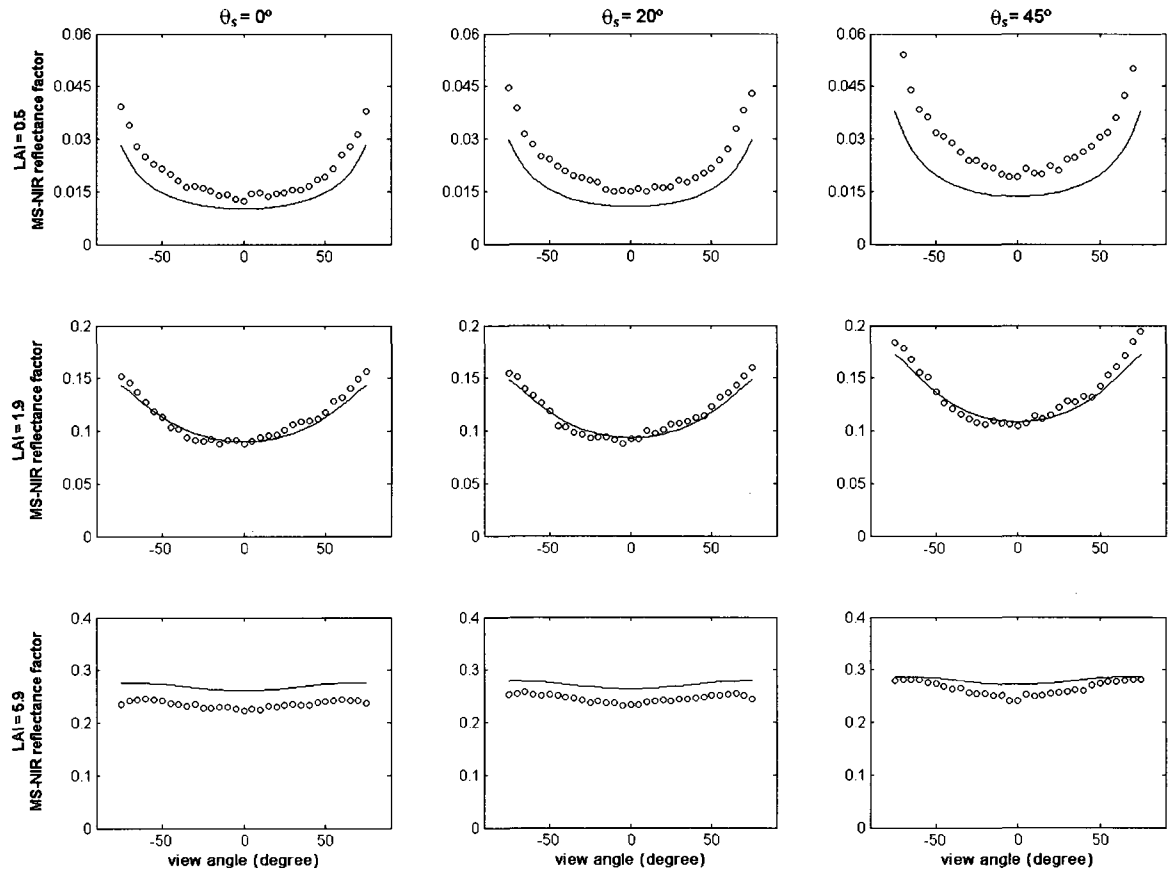

Figure 2.5: BRDF of multiple scattering (MS) based on the approximate model (solid line) versus PARCINOPY (circles) in the solar principal plane in the Near Infra-red (NIR) band.

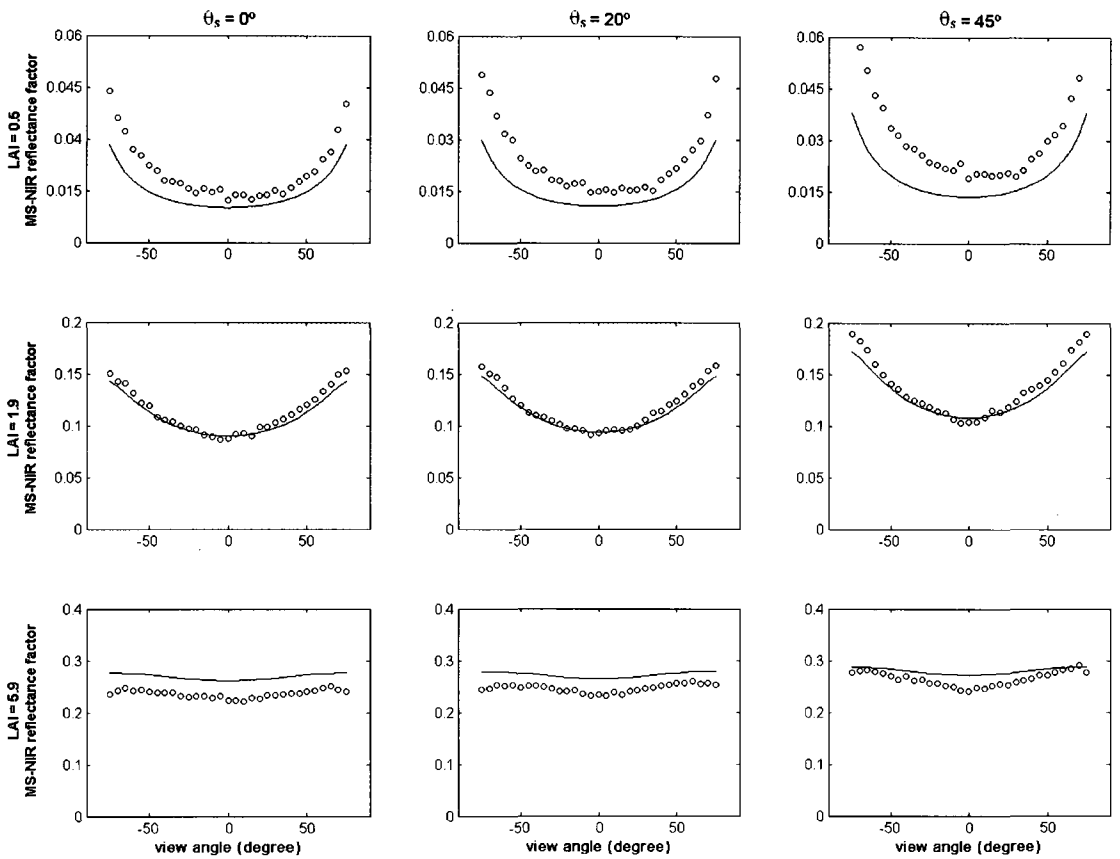

Figure 2.6: BRDF of multiple scattering (MS) based on the approximate model (solid line) versus PARCINOPY multiple scattering (circles) in the solar perpendicular plane in the Near Infra-red (NIR) band.

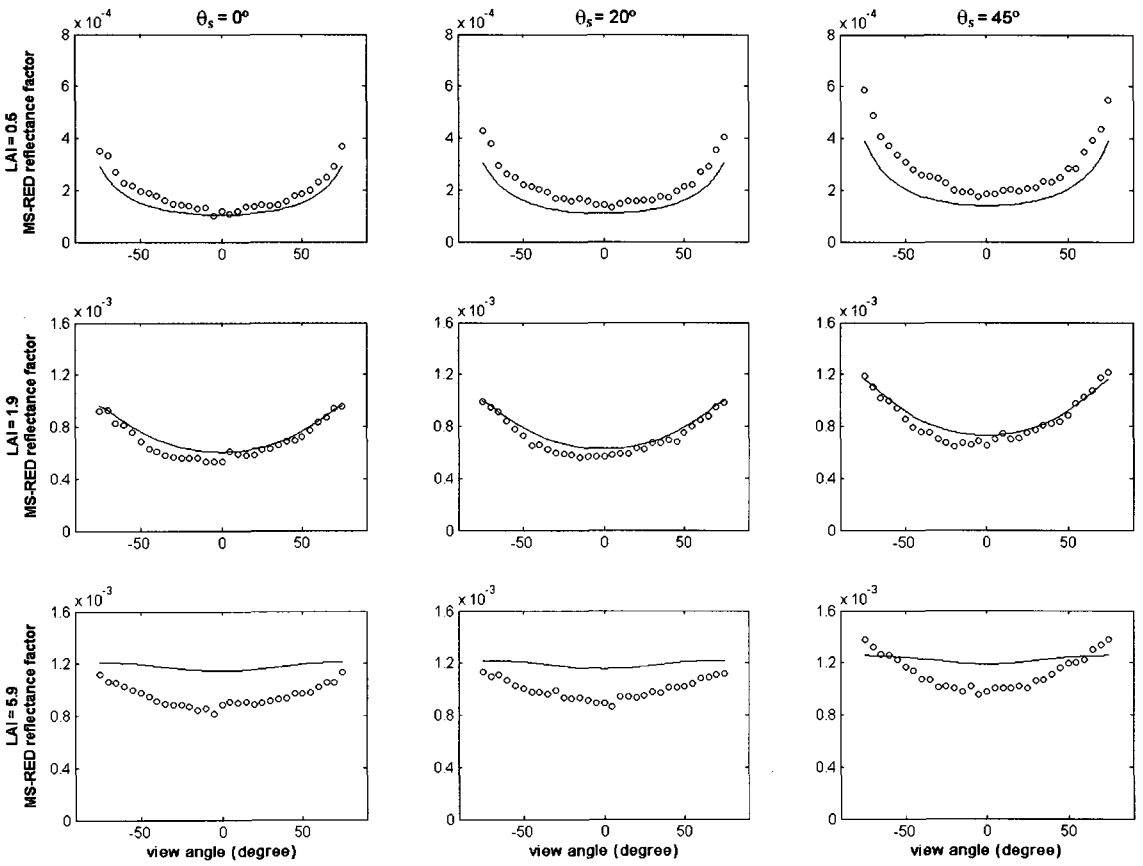

Figure 2.7: BRDF of multiple scattering (MS) based on the approximate model (solid line) versus PARCINOPY multiple scattering (circles) in the solar principal plane in the red band.

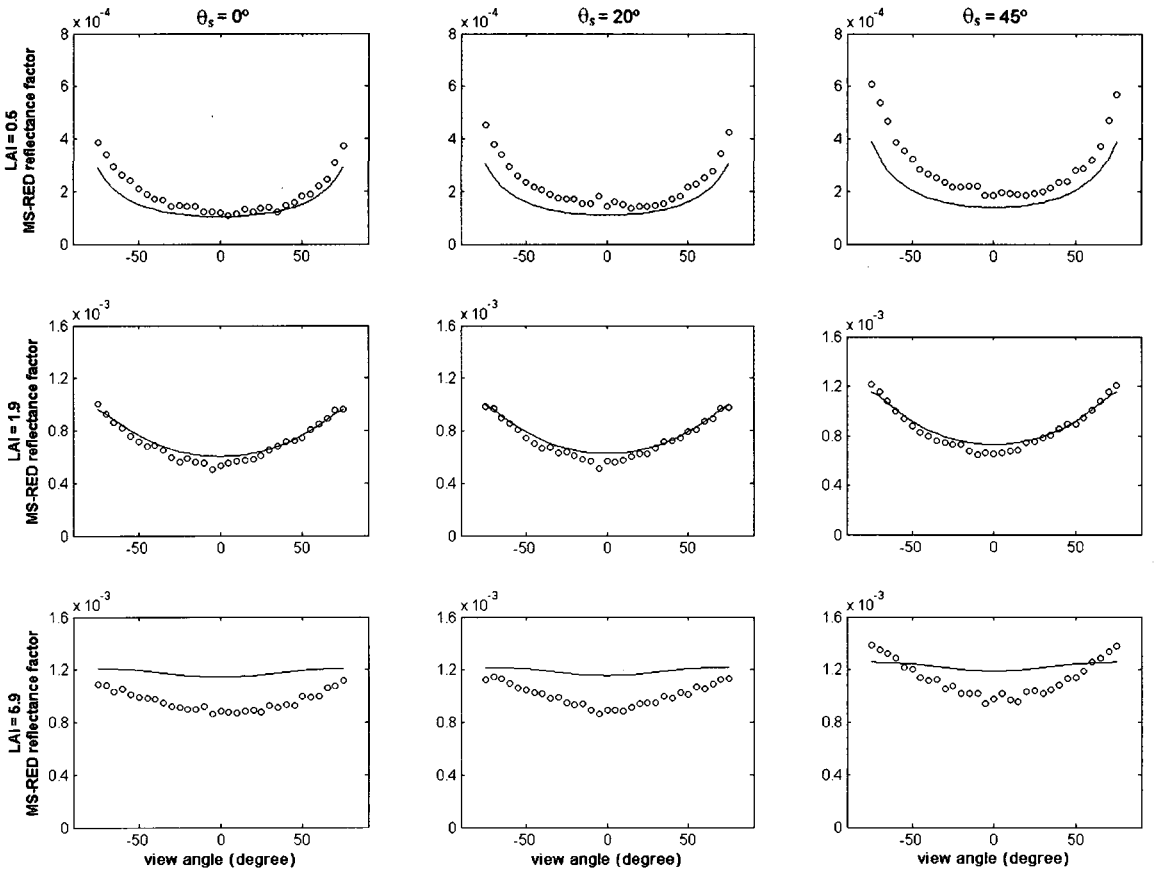

Figure 2.8: BRDF of multiple scattering (MS) based on the approximate model (solid line) versus PARCINOPY multiple scattering (circles) in the solar perpendicular plane in the red band.

Figure 2.9 shows the proposed model performance against the ROMC results. The angular variability of the MS field using the proposed approach was simulated with the assumption of black background (the ground reflectance is set to zero), while the clumping index Ω is set to 1 and $G(\theta_v)$ is set to 0.5.

In the red band, there is a good agreement between our model and the ROMC datasets for large view angles in both the solar principal and perpendicular planes. However, when the view angle is approaching nadir view, there is a significant underestimation of multiple scattering reflectances by the model presented in this paper. This is expected as the ROMC considers a relatively bright ground underneath the canopy compared to the completely absorbing ground considered in the proposed model. The effect of this discrepancy is negligible as the contribution of the multiple scattering in this spectral region has a very slight effect on the total radiometric response, typically 5%. Moreover, real terrestrial vegetation surfaces may have darker backgrounds (mostly composed of vegetation layers) in red and green than specified in ROMC trials. In contrast, the multiple scattering is highly significant for the NIR band, with a contribution of over 50% to the total radiometric response (Figure 2.2). Figure 2.9 shows that the proposed model reproduces the ROMC multiple scattering BRDF quite accurately. The absolute differences are within 1% in both principal and perpendicular planes. This suggests that the model presented in this paper can estimate the multiple scattering field with high accuracy without adding the multiple bouncing scattering between the canopy and the ground for realistic NIR ground surface reflectance used in these ROMC reference models.

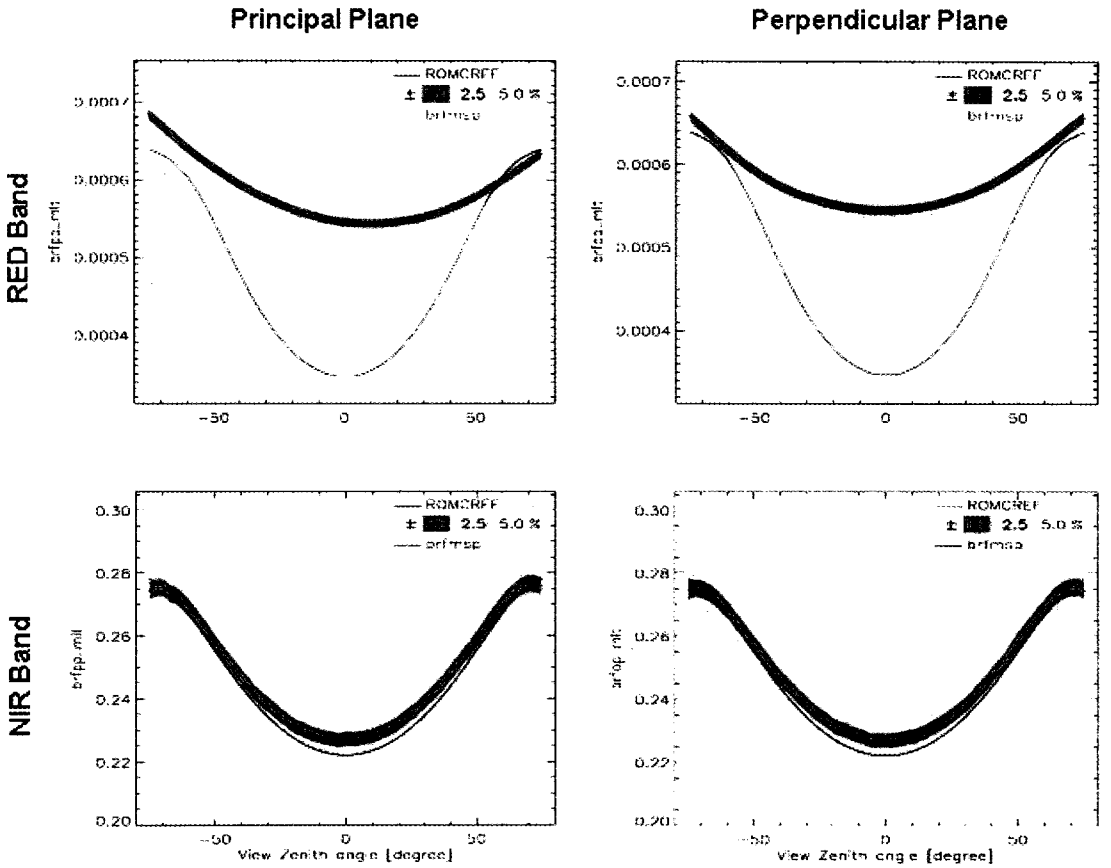

Figure 2.9: Comparison of BRDF of MS calculated using the proposed approximate model approach (solid line) (brfmsp) to RAMI reference (ROMCREF) in the red and near infrared bands. The simulations for the principal plane (brfpp_mlt) and perpendicular plane (brfop_mlt) were performed with an illumination angle of 20° and an LAI equal to 3. The three grey-colored envelopes correspond to 1, 2.5 and 5% of the multiple scattered BRF of the "surrogate truth" solution surrounding the reference solution.

2.5. Conclusion

The total upward scattering can be decomposed into three radiation fields. The zero scattering which can be calculated directly (gap fractions), the first scattering field which can be evaluated accurately using radiative transfer models and finally the multiple scattering field. Early canopy radiative transfer models have assumed an isotropic behaviour of the latter. Synthetic experiments have demonstrated that this assumption is incorrect and, thus, the anisotropic behaviour of multiple scattered radiation has to be addressed when simulating directional spectral remote sensing response over vegetation canopies. In this paper, a simple and effective approximation of the reflectance factor of multiple scattering is presented. The comparison to PARCINOPY Monte Carlo and ROMC data demonstrated the potential of this approach to approximate the reference data. Moreover, this scheme is fast when used for inversion purposes to extract canopy biophysical parameters from remote sensing data. There are two areas suggested that need future development. Firstly, the determination of reasonably accurate but simple parameterization of the relative escape probability needs to be established as a function of vegetation structure and illumination geometry. Secondly, the proposed approach should be further tested under bright soil conditions for heterogeneous canopies. Nevertheless, the radiative transfer theory based on the p theory has demonstrated once again its potential in describing photon interactions within the canopy.

Acknowledgements

The authors would like to gratefully acknowledge the support of the Canada Centre for Remote Sensing / Natural Resources Canada for the infrastructure access and the University

of Ottawa for financial support. We would also like to thank The ROMC system for the valuable standard references to assess our model.

References

Asrar, G, "Theory and Applications of Optical Remote Sensing", Wiley Series in Remote Sensing, John Wiley and Sons, Inc., 734 pages, 1989.

Bacour, C., Baret, F., Beal, D., Weiss., and Pavageau, K., "Neural network estimation of LAI, fAPAR, fCover and LAIxCab, froom top of canopy MERIS reflectance data: Principles and validation", Remote Sensing of Environment, 105: 313-325, 2006.

Chelle, M., and Andrieu, B., " PARCINOPY, un logiciel de simulation des échanges radiatifs dans les couverts végétaux par lance de rayons sur des maquettes informatiques tridimensionnelles", Rapport de recherches, INRA-bioclimatologie, 78850 Thiverval-Grignon, 1996.

Combal, B., Baret, F., Weiss, M., Trubuil, A., Macé, D., Pragnère, A., Myneni, R., Knyazikhin, Y., Wanget, L., "Retrieval of canopy biophysical variables from bi-directional reflectance using prior information to solve the ill-posed inverse problem", Remote Sensing of Environment, 84, 1–15, 2002.

Chen, J. M., Pavlic, G., Brown, L., Cihlar, J., Leblanc, S. G., White, H. P., Hall, R. J., Peddle, D. R., King, D. J., Trofymow, J. A., Swift, E., Van der Sanden, J., Pellikka, P. K. E., "Derivation and validation of Canada-wide coarse-resolution leaf area index maps using high-resolution satellite imagery and ground measurements", Remote Sensing of Environment, 80: 165–184, 2002.

Chen, J.M, and Leblanc, S. G., "Multiple-scattering scheme useful for geometric optical modeling", IEEE Transactions on Geoscience and Remote Sensing, 39(5): 1061–1071, 2001.

Chen, J.M, and Leblanc, S. G., "A Four-Scale bidirectional reflectance model based on canopy architecture", IEEE Transactions on Geoscience and Remote Sensing, 35(5): 1316–1337, 1997.

Chen, J. M., "Canopy architecture and remote sensing of the fraction of photosynthetically active radiation absorbed by boreal conifer forests", IEEE Transactions on Geoscience and Remote Sensing. 34(6): 1353-1368, 1996.

Chen, J. M. and Cihlar, J, "Retrieving leaf area index for boreal conifer forests using Landsat TM images", Remote Sensing of Environment, 55:153-162, 1996.

Disney, M., Lewis, P., Quaife, T., and Nichol, C., "A spectral invariant approach to modeling canopy and leaf scattering", Proceeding of the 9th International Symposium on Physical Measurements and Signatures in Remote Sensing (ISPMSRS), 17–19 October 2005, Beijing, China, Part 1(pp. 318-320), 2005.

Gobron, N., Pinty, B., Verstraete, M. M., and Govaerts, Y., "A semi-discrete model for the scattering of light by vegetation", Journal of Geophysical Research, 102: 9431–9446, 1997.

Huang, D., Knyazikhin, Y., Dickinson, R. E., Rautiainen, M., Stenberg, P., Disney, M., Lewis, P., Cescatti, A., Tian, Y., Verhoef, W., Martonchik, J. V., and Myneni, R.B., "Canopy spectral invariants for remote sensing and model applications", Remote Sensing of Environment, (106): 106-122, 2007.

Li, X, and Strahler, A. H., and Woodcock, C. E., "A hybrid geometric-optical radiative transfer approach for modeling albedo and directional reflectance of discontinuous canopies", IEEE Transactions on Geosciences and Remote Sensing, 33: 466-480, 1995.

Li, X, and Strahler, A. H., "Geometric-optical bidirectional reflectance modeling of the discrete crown vegetation canopy: effect of crown shape and mutual shadowing", IEEE Transactions on Geosciences and Remote Sensing, 30(2): 276-292, 1992.

Liang, S., "Quantitative Remote Sensing of Land Surfaces", John Wiley and Sons, Inc., 534 pages, 2004.

Liang, S. and Strahler, A. H., "The calculation of the radiance distribution of the coupled atmosphere and leaf canopy", IEEE Transactions on Geoscience and Remote Sensing, 31(2): 491-502, 1993.

Knyazikhin, Y., Martonchik, J. V., Myneni, R. B., Diner, D. J., and Running, S.W., "Synergistic algorithm for estimating vegetation canopy leaf area index and fraction of absorbed photosynthetically active radiation from MODIS and MISR data", Journal of Geophysical Research, 103(D24): 32257– 32276, 1998.

Kucharik, C. J., Norman, J. M., Murdock, L. M. and Gower, S., T., "Characterizing canopy nonradomness with a Multiband Vegetation Imager (MVI)", Journal of Geophysical Research, 102(D24): 29,445–29,473, 1997.

Kuusk, A., Andrieu, B., Chelle, M., and Aries, F., "Validation of a Markov chain canopy reflectance model", International Journal of Remote Sensing, 18(10): 2125-2146, 1997.

Mõttus, M., and Stenberg, P., "A simple parameterization of canopy reflectance using photon recollision probability", Remote Sensing of Environment, 112: 1545-1551, 2008.

Mõttus, M., "Photon recollision probability in discrete crown canopies", Remote Sensing of Environment, 110: 176–185, 2007.

Myneni, R. B., Marshak, A., Knyazikhin, Y., and Asrar, G., "Discrete ordinates method for photon transport in leaf canopies", Photon-Vegetation Interactions: Applications in optical Remote Sensing and Plant Ecology, edited by R. B. Myneni and J. Ross, 45-109, Springer, New York, 1991.

Myneni and Ross, 1991. Myneni, R.B., and Ross, J., Editors, "Photon-Vegetation Interactions", Springer Verlag, Berlin (1991).

Nilson, T., "A theoretical analysis of the frequency of gaps in plant stands.", Agricultural and Forest Meteorology, 8: 25-38, 1971.

Panferov, O., Knyazikhin, Y., Myneni, R.B., Szarzynski, J., Engwald, S., Schnitzler, K.G., and Gravenhorst, G., "The role of canopy structure in the spectral variation of transmission absorption of solar radiation in vegetation canopies", IEEE Transactions on Geoscience and Remote Sensing, 39: 241–253, 2001.

Pinty, B., Widlowski, J.-L., Taberner, N., Gobron, N., Verstraete, M. M., Disney, M., Gastellu-Etchegorry, J.-P., Jiang, L., Kuusk, A., Lewis, P., Li, X., Ni-Meister, W., Nilson, T., North, P. R. J., Qin, W., Su, L., Thomson, R., Verhoef, W., Wang, H., Wang, J., Yan, G., and Zhang, H., "Radiation Transfer Model Intercomparison (RAMI) exercise: Results from the second phase", Journal of Geophysical Research, 109(D06210), doi: 10.1029/2003JD004252, 2004.

Pinty, B., Widlowski, J. L., Gobron, N., Verstraete, M. M., and Diner, D. J., "Uniqueness of Multiangular Measurements Part 1: An Indicator of Subpixel Surface Heterogeneity from MISR", IEEE Transactions on Geoscience and Remote Sensing, 40(7): 1560-1573, 2002.

Pinty, B., Gobron, N., Widlowski, J.-L., Gerstl, S., Verstraete, M. M., Antuunes, M., Bacour, C., Gascon, F., Gastellu-Etchegorry, J.-P., Goel, N., Jacquemoud, S., North, P. R. J., Qin, W., and Thomson, R., "Radiation Transfer Model Intercomparison (RAMI)", Journal of Geophysical Research, 106(D11), 11937-11956, 2001.

Rautiainen, M., and Stenberg, P., "Application of photon recollision probability in coniferous canopy reflectance simulations", Remote Sensing of Environment, 96: 98–107, 2005.

Rochdi, N., Fernandes, R., and Chelle, M., "An assessment of needles clumping within shoots when modeling radiative transfer within homogenous canopies", Remote Sensing of Environment, 102:116-134, 2006.

Ross J., Marshak A., "Monte Carlo methods. - In: Photon-Vegetation Interactions. Applications in Optical Remote Sensing and Plant Ecology", Eds. R.B. Myneni, J. Ross. Springer Verlag, Berlin, 441-467, 1991.

Ross, J., "The radiation regime and architecture of plant stands, Netherlands: Junk, W., The Hague, 391 pages, 1981.

Sellers, P., "Canopy reflectance, photosynthesis and transpiration", International Journal of Remote Sensing, 6: 1335-1372, 1985.

Smolander, S., and Stenberg, P., "Simple parameterizations of the radiation budget of uniform broadleaved and coniferous canopies", Remote Sensing of Environment, 94: 355– 363, 2005.

Stenberg, P., "Simple analytical formula for calculating average photon recollision probability in vegetation canopies", Remote Sensing of Environment, 109): 221-224, 2007.

Verhoef, W., "Light scattering by leaf layers with application to canopy reflectance modeling: The SAIL model", Remote Sensing of Environment, 16: 125-141, 1984.

Wang, Y., Buermann,W., Stenberg, P., Smolander, H., Häme, T., Tian, Y., Hu, J., Knyazikhin, Y., and Myneni, R, B., "A new parameterization of canopy spectral response to incident solar radiation: Case study with hyperspectral data from pine dominant forest", Remote Sensing of Environment, 85: 304–315, 2003.

Weiss, M., Baret, F., Myneni, R. B., Pragnère, A., and Knyazikhin, Y, "Investigation of a model inversion technique to estimate canopy biophysical variables from spectral and directional reflectance data", Agronomie, 20: 3-22, 2000.

Widlowski, J.-L., Robustelli, M., Disney, M., Gastellu-Etchegorry, J.-P., Lavergne, T., Lewis, P., North, P. R. J., Pinty, B., Thomson, R., and Verstraete, M. M. "The RAMI On-line Model Checker (ROMC): A web benchmarking facility to canopy reflectance models", Remote Sensing of Envirement, 112:1067-1081, 2007.

White, H.P., Miller, J.R., and Chen, J.M, "Four-scale linear model for anisotropic reflectance (FLAIR) for plant canopies. I: Model description and partial validation", IEEE Transactions on Geoscience and Remote Sensing, 39(5), 1072-1083, 2001.

Chapter 3

Multiple scattering within the FLAIR model incorporating the photon re-collision probability approach

This chapter is based on

Omari, K., White, H. P., and Staenz, K. (2009), "An enhanced description of multiple scattering within the FLAIR model using the photon re-collision probability approach", IEEE Transactions on Geosciences and Remote Sensing, (in press).

Abstract:

In this paper, a combined approach based on the adding method is incorporated into the FLAIR canopy radiative transfer model to enhance the description of the spectrally dependent multiple scattered radiation field of a forest canopy. The proposed scheme is based on the decomposition of the multiple scattering radiation field into two parts. The first part deals with multiple scattering within the canopy considering a completely black soil and the second one deals with multiple scattering between the canopy and the background. Such advances to radiative transfer modelling are required to better exploit the potential of hyperspectral remote sensing for monitoring canopy biochemical indicators, such as chlorophyll concentration and equivalent water content. The validation was performed using the multi-angular data sets obtained by the airborne sensor POLarization and Directionality of the Earth's Reflectances (POLDER) during the BOReal Ecosystem-Atmosphere Study (BOREAS) campaign of 1994. The results indicate that this approach is well suited to the FLAIR model. It is also demonstrated that the multiple scattering problem can be parameterized by a limited number of architectural parameters and the leaf scattering coefficient.

2.1. Introduction

The optical response recorded by Earth Observation (EO) systems over vegetation canopies is strongly influenced by the structure and the spectral response of individual elements of these canopies. Several radiative transfer models have been developed during the last three decades to describe such behaviour (Chen and Leblanc, 1997; Pinty and Verstraete, 1991;

Nilson and Kuusk, 1989; Van de Hulst, 1980). These models mostly use either the two-stream approximation (Nilson and Peterson, 1991) or the numerical approaches using a Gauss-Seidel algorithm (Liang and Strahler, 1993) to describe the multiple scattering component. The two-stream approximation, despite its simplicity, is not appropriate to describe accurately the angular behaviour of the spectral reflectance in vegetation canopy media (Liang, 2004). The more complex four-stream approach of Liang and Strahler (1995) has been developed to improve the accuracy of the description of canopy radiative transfer while maintaining the efficiency of the two-stream approximation.

Many geometric optical models have opted for band specific factors to account for the multiple scattering effect (Chen and Leblanc, 1997; Li and Strahler, 1992; White et al., 2001a). Chen and Leblanc (2001) made an effort to increase the accuracy of the Four Scale model by introducing a more physically comprehensive angular dependence description to capture the angular distribution pattern of the radiance within the canopy. The scheme represents detailed interactions of photons with different scene components for orders of scattering higher than one. This approach is complex as the analytical determination of the view factors prove to be very difficult to derive. Therefore, many approximations have been made to keep the model simple and effective. Likewise, three dimensional (3D) radiative transfer models such as radiosity or Monte Carlo ray tracing models lead to a much more accurate representation of the radiance angular distribution (Disney et al., 2000). However, these models are not practically invertible and require large computing resources. Radiative transfer in stochastic media is an attempt to capture 3D effects by averaging 3D radiative transfer equations (Huang et al., 2007; Shabanov et al., 2005; Shabanov et al., 2000).

Based on the Four Scale radiative transfer theory, the Four Scale Linear Model for Anisotropic Reflectance (FLAIR) has been developed (White et al., 2001a). The initial version of the FLAIR model has demonstrated some limitations when characterizing the bidirectional reflectance behaviour of canopies. Approximations which were applied by the FLAIR Model developers were designed to improve the model's flexibility and tractability, particularly as applied to hyperspectral applications and model inversion as discussed in White et al. (2002a). These approximations, which employ Sellers' two-stream approach (Sellers, 1985), have been demonstrated to lack sufficient detail to truly quantify the spectral multiple scattering (MS) characteristics of a variety of canopies (White et al., 2002b). Therefore, incorporating a more physically based description of the multiple scattering contribution was pursued in order to better simulate the spectral behaviour of the bidirectional reflectance to promote the model's usefulness to quantitatively exploit the potential of deriving information products using non-nadir reflectance data.

The aim of this study is to investigate different approaches to simulate the angular and spectral multiple scattering within the FLAIR model. It is assumed that the vegetation canopies are comprised of a vegetation layer on top of a background and the method of adding the modelled scattered radiation between and within these canopy components is considered (Van de Hulst, 1980). The present examination consists of dividing the optical scattering and absorption into two basic sub-problems: (1) scattering considering a completely absorbing background and (2) scattering due to overstorey-background multiple interactions. The first sub-problem isolates the relationship between photon re-collision probability, Leaf Area Index (LAI) and both incident and viewing zenith angles for

simulating canopy reflectance. The second sub-problem introduces the scattering component between the canopy and the background. These enhancements are incorporated into the FLAIR model to describe the multiple scattered radiation field of the canopy. There are two basic reasons behind incorporating the new scheme:

1. To simulate bidirectional Hyperspectral Reflectances with a satisfactory accuracy and without increasing the model complexity. The proposed scheme attempts to use only the already defined parameters within the FLAIR model.
2. With the proposed approach, the FLAIR model is able to be linked to a leaf model such as PROSPECT or LIBERTY (Dawson et al., 1998; Jacquemoud and Baret, 1990) to retrieve canopy biophysics and biochemistry via inversion (Omari et al., 2009).

Model simulations will be used to demonstrate the impacts on the FLAIR extracted bidirectional reflectance factor (BRF) in wavelength regions where the scattering is significant. The simulated BRFs will be shown in comparison with the constant multiple scattering approach where the constants were derived by fitting the model to top of canopy airborne POLDER and PAROBOLA measurements. Therefore, this study will focus on how close the simulations produced by the new automated model are to those produced by the original FLAIR model.

2.2. Theory

The principal modifications to the FLAIR model compared to the four scale model (Chen and Leblanc, 1997) lie in the theory which defines the probabilities of viewing illuminated

background, directly illuminated crown foliage, shaded canopy and shaded background proportions. The FLAIR model expresses the canopy BRF as in White et al., (2001a):

$$BRF(\lambda) = r_T(\lambda)P_T + r_G(\lambda)P_G + r_{zt}(\lambda)(1 - P_{vg} - P_T) + r_{zg}(\lambda)(P_{vg} - P_G), \quad (3.1)$$

where r_T, r_G, r_{zt} and r_{zg} are the four mean scene component reflectivities as a function of the wavelength (λ); r_T, r_G point to the reflectivities of sunlit overstorey and background, while r_{zt} and r_{zg} refer to the reflectivities of shaded overstorey and background. P_T represents the probability of viewing illuminated crown foliage, P_G represents the probability of viewing illuminated background and P_{vg} represents the probability of directly viewing the background. P_T is approximated as:

$$P_T = F(1 - P_{ig}) + (1 - F)P_{Tf}(1 - P_{vg}), \quad (3.2)$$

where F represents the hot spot function parameterized as a function of LAI and the phase angle (φ) between the solar zenith and view zenith angles (θ_i and θ_v) (White et al., 2001a). P_{ig} corresponds to the probability of directly illuminating the background and P_{Tf} is the probability of viewing the foliage within the canopy defined here as:

$$P_{Tf} = \Omega.\Gamma(\xi)\left(\frac{G(\theta)}{\sin(\theta_i + 15^\circ) + \sin(\theta_v + 15^\circ)}\right), \quad (3.3)$$

where $\Gamma(\xi)$ is the phase function for leaf scattering depending on the phase scattering ξ. It is expressed by the empirically based relationship (Chen and Leblanc, 1997):

$$\Gamma(\xi)=\left(1-\frac{C_p\xi}{\pi}\right), \quad C_p=0.75, \tag{3.4}$$

where C_p is a coefficient empirically determined by the optical properties of foliage elements and the scattering angle ξ is defined as function of θi, θv and the phase angle φ as follows (Chen and Leblanc, 1997):

$$\xi=\cos^{-1}\left(\cos\theta_i\cos\theta_v+\sin\theta_i\sin\theta_v\cos\varphi\right). \tag{3.5}$$

P_G (in Eq. 3.1) can be written as follows:

$$P_G=P_{ig}\left[F\left(1-P_{vg}\right)+P_{vg}\right]. \tag{3.6}$$

The parameters P_{ig} and P_{vg} can be approximated as follows:

$$P_{ig}(\theta_i)=\exp\left(\frac{-G(\theta_i)LAI\,\Omega}{\cos(\theta_i)}\right)$$

and

$$P_{vg}(\theta_v)=\exp\left(\frac{-G(\theta_v)LAI\,\Omega}{\cos(\theta_v)}\right) \tag{3.7}$$

The azimuthally independent parameters $P_{ig}(\theta_i)$ and $P_{vg}(\theta_v)$ are the gap probabilities at angles θ_i and θ_v described by Beer's law as described in Li and Strahler (1988) where the canopy clumping index (Ω) is introduced to take into account the foliage grouping within the canopy (Kucharik et al., 1997; Chen, 1996; Nilson, 1971). LAI is the canopy overstorey leaf area index and $G(\theta)$ is the projection of a unit leaf area on a plane perpendicular to the direction θ.

The contributions of shaded overstorey and background to observed reflectance are very difficult to measure (Miller et al., 1997; White et al., 1995). Several models treat these components as negligible and/or to have no spectral dependence (White et al., 2001b), which introduces inaccuracies into the models. In the FLAIR model, constant multiple scattering factors (Eqs. 3.8 and 3.9) were used to approximate the contribution of the shaded components to the observed reflectance as follows:

$$\frac{r_{zt}}{r_T} = C_m F_{dt} \tag{3.8}$$

and

$$\frac{r_{zg}}{r_G} = C_m F_{dg} \ , \tag{3.9}$$

where C_m is the multiple scattering factor, F_{dt} and F_{dg} are the fractions of diffuse irradiance in the total incoming irradiance near the top (dt) and bottom (dg) of the canopy stand, respectively.

The multi-scattering factors are treated as angularly independent but spectrally dependent constants (White et al., 2002b). When simulating hyperspectral signatures, a more physically

based, wavelength-specific, multiple scattering description is required to understand and exploit the spectral bidirectional reflectance of a canopy. This is necessary as the magnitude of multiple scattering is a function of canopy structure as well as the wavelength. The radiative regime in vegetation canopies can be determined by three factors (Ross, 1981): the architecture of the canopy, which is wavelength independent, the optical properties of individual elements of the canopy (leaves, needles, shoots, stems, etc.) and the spectral and angular response of the understorey. Based on these factors and using the energy conservation law, the solar radiation transmitted and absorbed within a vegetation canopy can be described by relating the optical properties of the canopy elements (leaf reflectance and transmittance) and two canopy structural parameters (re-collision probability, interception) (Knyazikhin et al., 1998). In accordance with the same theory, the radiative transfer within the canopy can be split into two terms (Figure 3.1): (a) the interactions of radiation photons in the canopy with the assumption that the canopy underneath is a totally absorbing surface (known as the black soil (BS) problem) and (b) the remaining interactions between the vegetation canopy and its understorey (the "S" problem).

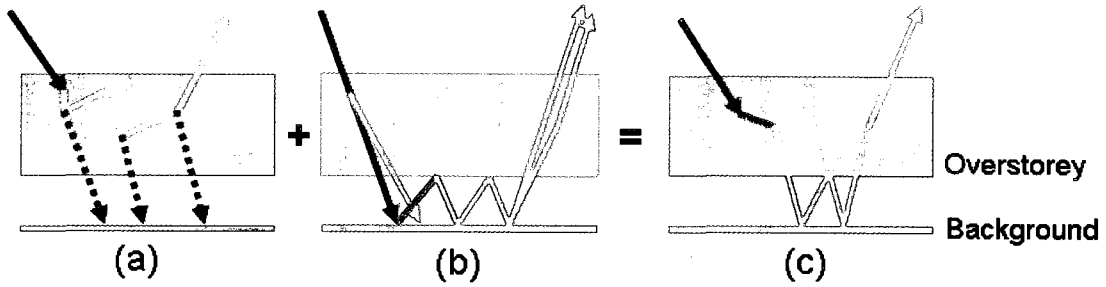

Figure 3.1: Representation of radiation transfer within the canopy based on the Black Soil (BS) approximation. In (a), the background is considered a completely absorbing media and the multiple scattering component is based on the result of multiple interaction within the canopy only. The scattering from (a) is proportional to $(1/(1-p\omega))$. In (b), the scattering due to the overstorey-background interactions of photons are directly transmitted through the canopy (the black descending arrow) and photons interacting only once before reaching the background (black changing to grey descending arrow) before they escape the canopy directly or interact only once toward the view angle after multiple ground-overstorey interactions. The scattering from (b) is proportional to $(1/(1-r_G r_T^*))$. The dark green color in (a) indicates a dense canopy. In this case, the contribution of the background is minimal and the multiple scattering is mainly coming from the canopy, while (b) indicates the opposite.

2.2.1. Non reflecting background case

After the first collision with foliage, photons will exit the canopy at an outgoing direction (θ_v) with the probability P_T as expressed in Eq.(3.1). This first interaction will also yield scattered photons that will interact again within the canopy with a probability p or will emerge from the canopy with a probability $(1-p)$. The parameter p is defined in Knyazikhin et al. (1998) and Smolander and Stenberg (2005) as the mean re-collision probability. They interpreted it as the probability of having two or more interactions of one photon within the

canopy. However, the re-collision probability is not purely structural and spectrally invariant as it can be demonstrated that multiple scattered radiation within the canopy is accompanied with a loss of energy. Thus, the probability of having an n^{th} interaction within the canopy can be quantified as $(p\omega)^n$, where $\omega(\lambda)$ represents the leaf scattering coefficient (or leaf albedo). Therefore, the p factor is used to provide a new efficient way to describe multiple scattered radiation within the canopy. The parameterization of the re-collision probability as a function of canopy LAI has been recently realised analytically (Mõttus and Stenberg, 2008; Mõttus, 2007; Stenberg, 2007) and using Monte Carlo simulations (Lewis and Disney, 2007; Smolander and Stenberg, 2005) as follows.

$$p = p_{\max}\left(1 - \exp\left(-kLAI^{b}\right)\right), \tag{3.10}$$

where the parameters p_{max}, k and b are computed numerically for a spherical leaf angle distribution in homogeneous canopy. This parameterization has been successfully demonstrated for calculating vegetation canopy albedo (Rautiainen and Stenberg, 2005). Huang et al. (2007) used the re-collision to compute the probability that a photon scattering m times will scatter again or will exit the canopy. They used this approach to estimate the radiation exiting the canopy; namely the canopy reflectance and transmittance. In Eq. (3.10), it is assumed that the leaf distribution is random within the canopy and that the photons interact only with the optically active elements inside the canopy. Therefore, for a value of n approaching infinity, the spherical canopy scattering coefficient, $S_{bs}(\lambda)$, can be expressed by the iterative formula as follows:

$$s_{bs}(\lambda) = i_0\omega(\lambda)^2 p(1-p) + i_0\omega(\lambda)^2 p^2\omega(\lambda)(1-p) + i_0\omega(\lambda)^2 p^3\omega^2(\lambda)(1-p) + \cdots$$
$$= \frac{i_0\omega(\lambda)^2 p(1-p)}{1-p\omega(\lambda)}, \tag{3.11}$$

where $\omega(\lambda) = r_L(\lambda) + \tau_L(\lambda)$, $r_L(\lambda)$ and $\tau_L(\lambda)$ are the leaf reflectance and transmittance, and i_o is the canopy interceptance which can be determined as $1 - P_{ig}(\theta_i)$. Eq. (3.11) is similar in form to the one proposed by Disney et al. (2003) where the structural parameter values were extracted using Monte Carlo simulations. Comparison of the $S_{bs}(\lambda)$ component to Monte Carlo simulations using the Ray Tracing Model, PARCINOPY, demonstrates the potential of the photon re-collision probability to parameterize the canopy multiple scattering (Omari et al., 2009).

At present, the relationship between p and top of canopy directional radiance is not well established even though some existing and proposed remote sensing platforms such as CHRIS/PROBA, EO1-Hyperion and EnMAP are designed to observe directional (non-nadir) reflected radiance. The canopy multiple scattering coefficient (Eq. 3.11) represents both the upward and the downward scattered fluxes emerging from the canopy. Huang et al. (2007) introduced the escape probability for partitioning the incoming radiation into canopy reflectance and transmittance. However, making an assumption that the amount of escaped radiation in the upward and downward directions are constants introduces errors since not only the first scattering, but also the multiple scattering are ($\theta i, \theta v$) dependent. To separate both quantities, the use of an approximation of the canopy scattering phase function is

generally used. The Henyey-Greenstein phase function is a good approximation to the real phase function (Liang and Strahler, 1995). Ross (1981) proposed a phase function relating leaf transmittance and albedo to the phase angle (ξ). However, these phase functions are not rotationally invariant (Liang, 2004). Results from a Ray Tracing model demonstrate that the multiple scattering is insensitive to variations in azimuth angle but depends on both incident and view zenith angles, particularly for dense canopies (Liang, 2004; Omari et al., 2009). The present function depends on the optical properties of the leaf and the scattering angle (ξ^*).

In this study, the Ross phase function (Eq. 3.12) is adopted with the exception of using ξ^* defined as $cos^{-1}[cos(\theta_i)cos(\theta_v)]$ instead of the phase angle (ξ) as defined in Eq.(3.5). This slight modification is due to the approximation that multiple scattering is independent of the azimuth angle (Liang, 2004). The phase function, $f(\xi^*)$, can be written as follows:

$$f(\xi^*)=\frac{1}{3\pi}(\sin\xi^*-\xi^*\cos\xi^*)+\frac{1}{3}\cos\xi^*\frac{\tau_L(\lambda)}{\omega(\lambda)}. \tag{3.12}$$

This phase function has to be defined so that it is unity for isotropic scattering and it can be normalized as follows:

$$\iint_{2\pi} f(\xi^*)S_{bs}(\lambda)\cos(\theta_v)\sin(\theta_v)d\theta_v d\varphi_v = \iint_{2\pi} S_{bs}(\lambda)\cos(\theta_v)\sin(\theta_v)d\theta_v d\varphi_v . \tag{3.13}$$

Since $S_{bs}(\lambda)$ does not depend on the view zenith angle θ_v and the view azimuth angle φ_v and the phase function is rotationally invariant ($f(\xi^*)$ does not depend on φ_v), the normalization condition is simplified to the integral as follows:

$$\int_0^{\pi/2} f(\xi^*)\cos(\theta_v)\sin(\theta_v)d\theta_v = \frac{1}{2}. \tag{3.14}$$

This integral is evaluated numerically using the trapezoidal method. A multiplicative constant (μ) is derived in each scenario based on Eq. (3.14) to generate a new value of $F(\xi^*)=\mu f(\xi^*)$ to evaluate the directionality of $S_{sb}(\lambda)$. $F(\xi^*)$ is the normalized phase function.

2.2.2. Reflecting background case

The approach used to describe the radiative transfer field between the canopy and its background ("s" problem) consists of modelling the fraction of downward fluxes ($f^{\downarrow}$) of photons that are transmitted directly to the background, $P_{ig}(\theta_i)$, and/or the photons that are subject to one interaction before reaching the background as sketched in Figure 3.1 (b). The downward flux can then be calculated as follows:

$$f^{\downarrow} = \left[P_{ig}(\theta_i) + f_d^{\downarrow}\right]. \tag{3.15}$$

Let us first quantify the downward diffuse radiation $f_d^{\downarrow}$ assuming that it is isotropically distributed and that the leaves are spherically oriented. The leaf inclination density function in this case is $\sin(\theta_l)$, where θ_l is the polar zenith angle of the leaf's upward normal. Under these assumptions, the diffuse downward flux can be approximated following Verhoef (1984) as:

$$\sigma(\theta_l) = \left(\frac{r_L + \tau_L}{2} - \frac{r_L - \tau_L}{2} \cos^2(\theta_l) \right), \tag{3.16}$$

where r_L and τ_L represent leaf reflectance and transmittance. Integrating $\sigma(\theta_l)$ over all directions yields:

$$\sigma = \frac{r_L + 2\tau_L}{3}. \tag{3.17}$$

By considering $l \in [0, LAI]$ as the vertical downward cumulative leaf area index, the probability that the incident radiation flux penetrates to the depth l without having any interaction with the canopy elements, $T_0^{\downarrow}(l)$, is given by Eq. (3.17). After being intercepted by an infinitesimal layer at the depth l, the fraction of reflected flux that is scattered downward without any further interaction, $T^{\downarrow}(l)$, is given by Verhoef (1984):

$$T_0^{\downarrow}(l) = e^{-\frac{G(\theta_l)\Omega}{\cos(\theta_l)} l} = e^{-K_l l} \tag{3.18}$$

and

$$T^{\downarrow}(l) = e^{-\Omega(LAI-l)}, \tag{3.19}$$

where K_i expresses the attenuation in illumination direction. Therefore, the downward diffuse radiation $f_d^{\downarrow}$ can be expressed as:

$$f_d^{\downarrow} = \int_0^{LAI} T_0^{\downarrow}(l)\sigma T^{\downarrow}(l)dl = \sigma \frac{e^{-\Omega LAI} - e^{-K_i LAI}}{K_i - \Omega}. \tag{3.20}$$

These photons will have multiple interactions between the background (r_G) and the bottom of the canopy (r_T^*). The upward fraction of these fluxes ($f^{\uparrow}$) that escape the canopy directly or after having one more interaction in the canopy ($f_d^{\uparrow}$) can be expressed as follows:

$$f^{\uparrow} = \left[P_{vg}(\theta_v) + f_d^{\uparrow}\right]. \tag{3.21}$$

Similarly to $f_d^{\downarrow}$, the upward diffuse radiation $f_d^{\uparrow}$ can be expressed as:

$$f_d^{\uparrow} = \int_0^{LAI} T^{\uparrow}(l^*)\sigma T_v^{\uparrow}(l^*)dl^* = \sigma \frac{e^{-\Omega LAI} - e^{-K_v LAI}}{K_v - \Omega}, \tag{3.22}$$

where $T^{\uparrow}(l^*)$ points to the fraction of reflected flux from the background that is scattered upward through the bottom of the canopy to the depth l^* without having any further

interaction with the canopy elements $\left(T^{\uparrow}(l^{*}) = e^{-\Omega(LAI-l^{*})}\right)$. After being intercepted by an infinitesimal layer at the depth l^{*}, the fraction of the reflected flux that exits the canopy in the view direction is $T_v^{\uparrow}(l^{*}) = e^{-K_v l^{*}}$ where $K_v = \frac{G(\theta_v)\Omega}{\cos(\theta_v)}$. Eqs. (3.15) and (3.20) are derived assuming an isotropic canopy where the leaf angle distribution is spherical. In this case, the surface-vegetation multiple interactions, $S_{sc}(\lambda)$, can be expressed as:

$$\begin{aligned} S_{sc}^{*}(\lambda) &= f^{\downarrow}\left[r_G(\lambda) + r_G^2(\lambda) r_t^{*}(\lambda) + r_G^3(\lambda) r_T^{*2}(\lambda) + \cdots\right] f^{\uparrow} \\ &= \frac{f^{\downarrow} f^{\uparrow} r_G(\lambda)}{1 - r_G(\lambda) r_T^{*}(\lambda)}. \end{aligned} \tag{3.23}$$

The reflectance (r_T^{*}) represents the downward spectral response generated by an isotropic source located at the bottom of the canopy (Knyazikhin et al., 1998; Van de Hulst, 1980; Zhang et al., 2002). Since the quantity $S_{sc}(\lambda)$ contains also the reflectance of illuminated background that is already taken into account (see Eqs. 3.1 and 3.6), the multiple scattering between the canopy and the background becomes:

$$S_{sc}(\lambda) = S_{sc}^{*}(\lambda) - P_{ig}(\theta_i) r_G(\lambda) P_{vg}(\theta_v). \tag{3.24}$$

In Eq. (3.24), it is assumed that the background surface reflects radiation isotropically and that the canopy is a homogenous medium containing gaps. For simplicity, the downward radiation field having more than one interaction before reaching the background is disregarded. The contribution of transmitted radiation in the downward direction due to multiple scattering between the overstorey and its background is shown to be particularly

significant in nadir view (Figure 3.2). This is caused in part by the increased presence of viewed background at nadir particularly with low LAI values. On the other hand, the upward field includes both scattered radiation through the gaps in the view direction and scattered radiation interacting once with a canopy element and then scattered in the view direction without further interaction. Figure 3.2 demonstrates that for moderate and high LAI values, the contribution of multiple scattering in the black soil case is more significant than the multiple scattering of the other case (reflecting background case). This supports the findings of Ni et al. (1997) who found that multiple bouncing between the canopy and the background has a small effect for snow free vegetated covers. It is considered that more than one interaction was sufficiently incorporated in the BS case.

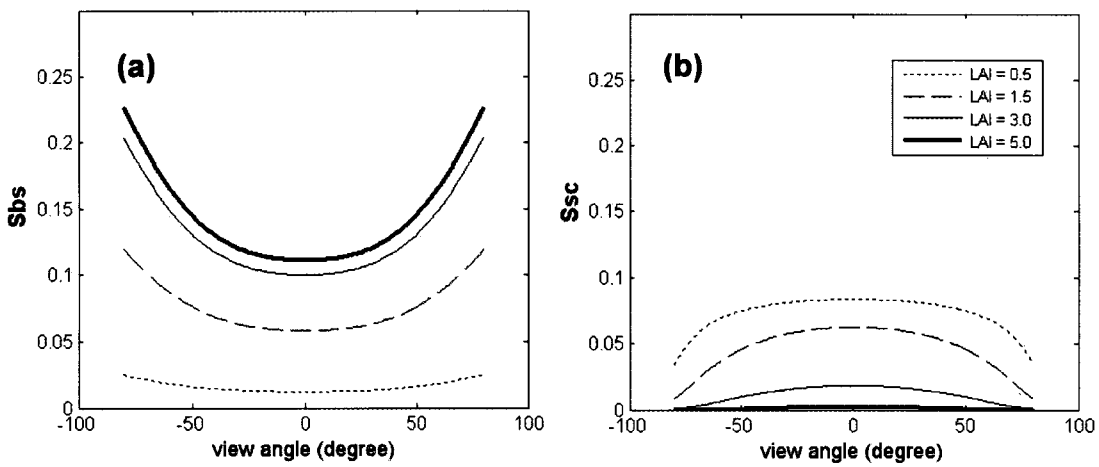

Figure 3.2: Comparison between the contribution of the canopy scattering with completely absorbing background following the scheme of the Figure 3.1. Case (a) uses Eqs. 11 and 12 and the contribution of the scattering due to the background-overstorey interactions, Case (b) which uses Eq. 15 for different LAI values. In both cases, $r_G = 0.3$, $r_T = 0.5$, τ_T=0.35 and the illumination angle is set to 40°.

3.2.3.Canopy BRF

Using the aforementioned descriptions, the canopy BRF can now be written as follows:

$$BRF(\lambda) = r_T(\lambda)P_T + r_G(\lambda)P_G + F(\xi^*)S_{sb}(\lambda) + S_{sc}(\lambda). \quad (3.25)$$

The first two terms of Eq. (3.25) represent the first order scattering with the upper canopy and the background using an optical-geometrical approach where the canopy structure controls the angular variation pattern and where the hot spot effect is considered in both scales within and between crowns, as described in the FLAIR Model (White et al., 2001a). The last two terms of Eq. (3.25) describe the multiple scattering based on the radiative transfer theory discussed in the previous sections. The contribution of these two terms to the total radiometric response changes as a function of LAI, angular geometry, and wavelength. For high values of LAI, model simulations demonstrate that $S_{sc}(\lambda)$ is generally weak compared to $S_{sb}(\lambda)$. However, simulations indicate the opposite for low LAI values. The contribution of both these components is relatively small compared to the first order scattering (first two terms) in the visible spectral region where the leaf/shoot absorption is strong. However, due to the high leaf albedo in the near infrared, the contribution of the multiple scattering within the canopy layer and between the background and the canopy is greater. It can exceed 50% of the upwelling canopy radiance (Liang and Strahler, 1993). Finally, Eq. (3.25) is a reformulation of the FLAIR model since now the last two terms of this equation replace the contribution of the shaded components of the background and the canopy. Figure 3.3 shows the sensitivity of the FLAIR model to LAI in the red and NIR

bands in the principal plane. Both the red and NIR reflectances increase with an increasing LAI in the hot spot region because of the increased probability of seeing the background. In the forward scatter direction, larger LAI induces more multi-scattering in the canopy. This is clearly observed in the NIR band in contrast to the red band (Figure 3.3). More sensitivity analyses of the FLAIR model is presented in (Omari et al., 2009).

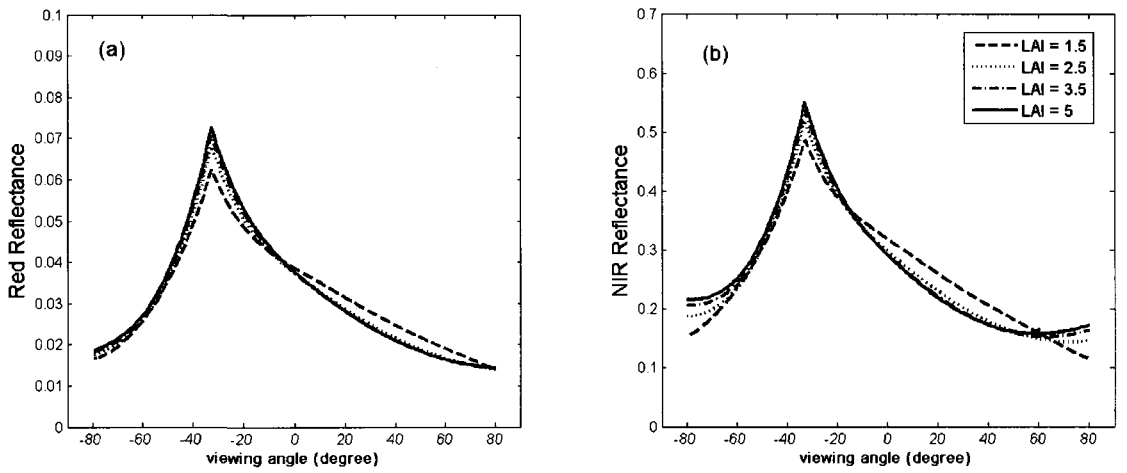

Figure 3.3: Effects of changing LAI on the simulated BRF in the solar principal plane in the red (a) and NIR bands (b). $\theta_i = 34°$, $r_G = 0.04$, $r_T = 0.08$, $\tau_T=0.05$ for the red band and $r_G = 0.3$, $r_T = 0.5$, $\tau_T=0.35$ for the NIR band.

3.3. Model validation: Comparison with airborne Polder data

3.3.1. Data Used for Model Validation

To demonstrate the impact of incorporating this multiple scattering approach, the BRF was simulated with the FLAIR model using both the original and the revised theories; referred to in this thesis as modelled with a spectrally dependant multiple scattering (AD-MS method) and with the previously published spectrally constant multiple scattering description (C-MS method). These simulations were then compared to measurements taken during the BOReal Ecosystem-Atmosphere Study (BOREAS) performed in the boreal forest regions of Canada in 1994 (Sellers et al., 1995). The comparison focuses on evaluating how the simulated BRFs, generated using both approaches, change as a function of the zenith and azimuth angles. It is known that most terrestrial vegetation canopies, such as boreal canopies, exhibit a bowl-shape anisotropic behaviour, which is most notable in the highly reflective NIR region. These canopies can be often be dense and the contribution of the background to the observed radiance is relatively low, especially when the viewing zenith angles are large. As a result, models predict an increase of the BRF values for large viewing zenith angles in the NIR region. This is mainly due to the effect of multiple scattering (Pinty et al., 2002).

The canopy BRF was acquired with the POLarization and Directionality of the Earth's Reflectances POLDER sensor which was mounted onboard the NASA C-130 airplane. This instrument is a radiometer designed to measure the directionality and polarization of the solar radiation scattered by the earth's surface with multi-view angles; ± 51° in the long-track

direction and ±43° in the across-track direction (Leblanc et al., 1999). Using a rotating filter wheel, measurements were acquired in five spectral bands centred at 443 nm, 550 nm, 670 nm, 864 nm and 910 nm with bandwidths ranging from 10 to 20 nm. In this report, only the red (670 nm) and near infrared (864 nm) bands are discussed. The ground pixel size which is proportional to the sensor altitude during this acquisition is 35 m x 35 m. The atmospheric correction algorithm (6S) was used to convert the POLDER measured radiance values to top of canopy bidirectional reflectance.

Table 3.1 summarizes the input parameters for the model as adapted from (Chen and Leblanc, 1997). The four sites investigated in this study were the Old Black Spruce (OBS), Old Jack Pine (OJP), Young Jack Pine (YJP) and Old Aspen (OA). OBS, YJP and OJP sites are located near Candle Lake, Saskatchewan, Canada. OBS has a density of around 4000 stems per hectare with an LAI ranging from 4 to 6. The understory is composed of young and small black spruce trees and Labrador tea while the background is covered by moss (Leblanc et al., 1999). YJP has a density approximating 4000 stems per hectare with an LAI of 2.6 to 3.1 with a ground cover composed of grasses, bearberry and lichens. The OJP site has a lower density compared to the YJP and OBS sites with 1850 stems per hectare and an LAI of 2.0 to 2.5 (Chen and Leblanc, 1997). The understory is covered by small young black spruce and the background is mainly composed of lichens. The OA site is located in the Prince Albert National Park, Saskatchewan, Canada. It has a lower stem density compared to the other three sites with approximatly 850 steems per hectare and a maximum LAI of around 2.4. The understory in this site is composed of hazelnut. More detailed descriptions for these sites are given in Leblanc et al. (1999). Table 3.2 and 3.3 report the coefficient of

determination (R^2) and RMSE calculated for all sites in the red and NIR regions between the POLDER data sets and the model simulations for the same observation geometries in both the solar principal and perpendicular planes. Note that the FLAIR Model with Constant multiple scattering (C-MS) has been previously evaluated with this data in White et al. (2001b) as part of a BOREAS investigation.

Table 3.1: Input parameters for the four canopies old black spruce (obs), young jack pine (yjp), old jack pine (ojp) and old aspen (oa).

Site	OBS	YJP	OJP	OA
Latitude N	53.985°	53.975°	53.916°	53.929°
Longitude W	-105.12°	-104.65°	-104.69°	-106.20°
Foliage Distribution				
$G(\theta)$	0.5	0.5	0.5	0.5
Ω	0.8	0.83	0.77	0.8
LAI	4.5	2.7	2.2	1.5
θ_i	33.5	37.2	35	39.3
Optical Properties				
r_G *(red)*	0.04	0.05	0.09	0.04
r_G *(nir)*	0.25	0.15	0.17	0.2
r_T *(red)*	0.11	0.05	0.07	0.07
τ *(red)*	0.05	0.03	0.05	0.07
r_T *(nir)*	0.5	0.53	0.53	0.5
τ *(nir)*	0.3	0.2	0.3	0.4
r_{ZT} *(red)*	0.003	0.005	0.003	0.01
r_{ZT} *(nir)*	0.11	0.19	0.13	0.2
r_{ZG} *(Red)*	0.002	0.004	0.003	0.02
r_{ZG} *(nir)*	0.11	0.08	0.09	0.15

Table 3.2: Comparison of coefficient of determination (R^2) and the root mean square error (RMSE) between the FLAIR model with the two Multiple Scattering methods for the four canopies OBS, YJP, OJP and OA in RED and NIR spectral regions for the solar principal plane. AD-MS refers to the Black Soil aproximation and C-MS means the constant multiple scattering approximation.

Principal Plane		OBS		OJP		YJP		OA	
		AD-MS	*C-MS*	*AD-MS*	*C-MS*	*AD-MS*	*C-MS*	*BS MS*	*C-MS*
R^2	NIR	0.98	0.98	0.98	0.97	0.90	0.75	0.87	0.73
	RED	0.98	0.98	0.98	0.98	0.99	0.97	0.87	0.86
RMSE	NIR	0.01	0.01	0.02	0.03	0.04	0.04	0.03	0.03
	RED	0.01	0.01	0.005	0.005	0.001	0.002	0.004	0.004

Table 3.3: Comparison of coefficient of determination (R^2) and the root mean square error (RMSE) between the flair model with the two multiple scattering methods for the four canopies OBS, YJP, OJP and OA in the RED and NIR spectral regions for the solar perpendicular plane. AD-MS refers to the black soil approximation and C-MS means the constant multiple scattering approximation.

Perpendicular Plane		OBS		OJP		YJP		OA	
		AD-MS	*C-MS*	*AD-MS*	*C-MS*	*AD-MS*	*C-MS*	*AD-MS*	*C-MS*
R^2	NIR	0.24	0.23	0.57	0.55	0.33	0.34	0.01	0.01
	RED	0.21	0.21	0.96	0.96	0.92	0.92	0.75	0.75
RMSE	NIR	0.02	0.02	0.02	0.03	0.04	0.03	0.04	0.04
	RED	0.008	0.009	0.007	0.007	0.002	0.002	0.004	0.004

3.3.2. Results and Discussion

The curves shown in Figures 3.4 to 3.7 were modelled using 1° view angle intervals in the solar principal plane and in the solar perpendicular plane using the nominal summer OBS, YJP, OJP architectural values (Table 3.1). The negative viewing angles refer to backscattering and positive ones to forward scattering. The dashed lines show the case where constant multiple scattering factors are used (C-MS) while the solid lines indicate the case where the newly implemented BS approximation is applied (AD-MS). The squares represent the acquired POLDER data.

a. Old Black Spruce Site: Figure 3.4 shows the simulated results from both multiple scattering approximations, C-MS and AD-MS, and the POLDER data over the OBS canopy. In the red region, both simulations exhibit precisely the same behaviour in both the solar principal and perpendicular planes. This is expected as multiple scattering in this spectral region has a very slight effect on the total radiometric response of dense vegetation canopies (with darker backgrounds) due to essentially large absorption and small scattering of the crown foliage. This figure indicates that the model slightly overestimates the measurements in the near-principal plane. Also note that the hotspot peak is not sharp. This is due to the fact that the POLDER data were acquired about 10° off the principal plane. Consequently, the FLAIR simulations were made at 10° off the principal plane. In the perpendicular plane, the variation of the BRFs computed with the model has an inverse bowl shape in contrast to the measured ones, which change slightly.

In the NIR, there is a slightly improved agreement between the measurements and the model using the AD-MS approximation compared to the C-MS method. R^2 values of 0.99 and 0.97 and an RMSE of 0.01 were found for AD-MS and C-MS approximations, respectively. Firstly, there is a difference in the width of the hotspot profile between the red and NIR bands. The hotspot signature in the NIR band is generally broader than in the red band. The difference between the two wavelength ranges results from a larger contribution of multiple scattering within the canopy in the NIR. Secondly, the shape of BRFs was reproduced particularly when the sun and the view angles are distant from each other (large scattering angles).

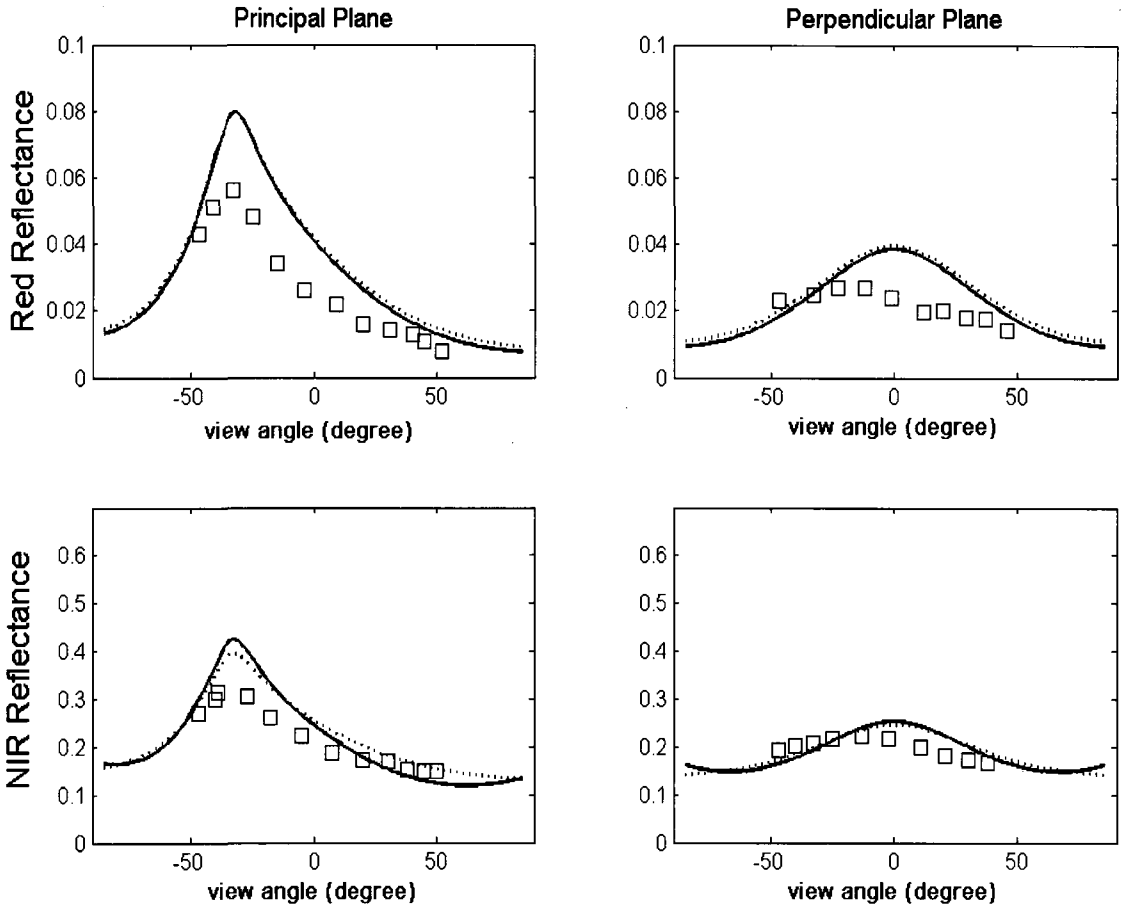

Figure 3.4: Comparison between solar principal plane and perpendicular-plane BRF values simulated with the FLAIR model using the AD-MS approximation (solid line) and constant multiple scattering (dashed line) and measurements acquired by POLDER (squares) over an Old Black Spruce site in the red and near-infrared regions.

In the vicinity of the hot spot region, the values of the BRF computed with the C-MS method are slightly lower than those calculated with the AD-MS approximation. This is mainly due to an improvement of the way the multiple scattering is computed. In the hot spot region, the probability of seeing shaded foliage is null and therefore the C-MS model doesn't account for the multiple scattering in this region since it is applied only as the

contribution of the shaded components. On the other hand, when the AD-MS scheme is incorporated into the model, multiple scattering contributions are computed from both sunlit and shaded background and foliage. However, both approximations appear to overestimate the BRF in the hot spot region observed for this site. Table 3.2 reports an R^2 of 0.98 and an RMSE of 0.01 for both NIR and red bands in near-principal plane simulations compared to the POLDER observed values. In the perpendicular plane (Table 3.3), the R^2 values decrease to 0.24 and 0.23 in the NIR for the AD-MS and C-MS cases, respectively and 0.21 for the red band. The RMSE is 0.02 for both approximations in the NIR and 0.008 and 0.009 in red band for AD-MS and C-MS cases, respectively.

b. Old Jack Pine Site: The general patterns of Figure 3.5 demonstrate a good agreement between both approximations and the measurements for this site in the red and NIR bands. In the red region, the calculated BRFs with both C-MS and AD-MS approximations mimic the shape and the magnitude of the measurements for the perpendicular plane and particularly the principal plane. In general, the BRFs computed with the models are slightly higher than the measurements in the hotspot direction for both principal and perpendicular planes. However, the variation of the simulated BRFs is very small in the perpendicular plane. This may be explained in part by the heterogeneity of the OJP site. A close inspection of both simulations revealed the effect of the relative enhancement of the multiple scattering with the AD-MS approximation over the C-MS model. Tables 3.2 and 3.3 show that for this stand the R^2 is 0.98 and the RMSE is 0.01 for both approximations in the red band. However, in the perpendicular plane, the R^2 is

0.96 and the RMSE is 0.007 for both the AD-MS and the C-MS approximations in the red band (Table 3.3).

In the NIR, it is found that the AD-MS simulation reproduces the POLDER measurements with an apparent bowl shaped forescatter region (Figure 3.5). The hotspot reflectance is slightly overestimated, and the general shape becomes relatively flat supporting the statements presented earlier on the shape of BRFs in the NIR bands. However, the width of the hotspot is generally larger compared to the OBS stand as identified by Nadal and Bréon (1999) who showed that this discrepancy can also be explained by the difference in the stand architecture. This demonstrates the usefulness of multiangle remote sensing to better characterize vegetated surfaces (Leblanc et al., 1999). Comparison between both approximations demonstrates a clear enhancement in the model with the AD-MS approximation in the principal plane and relative improvement in the perpendicular plane. For this stand the R^2 is of 0.98 for AD-MS and 0.97 for C-MS approximation in the principal plane (Table 3.2). The RMSE is 0.02 and 0.03 for AD-MS and C-MS approximations, respectively. However, in the perpendicular plane, the R^2 is 0.57 for AD-MS and 0.55 for C-MS and the RMSE is 0.02 and 0.03 for AD-MS and C-MS approximations, respectively (Table 3.3).

c. Young Jack Pine Site: As with the OJP stand, the models match the general shape and magnitude of the measurments in the red band for the YJP stand (Figure 3.6). The two approximations behave similarly, with the AD-MS simulations providing a closer agreement to the measurements than the C-MS simulations. In the principal plane, this is more apparent in the forward scatter direction. In the perpendicular plane, the

enhancement is evident when the view angle is away from the nadir position. The R^2 values in the red band for the principal plane are 0.99 and 0.97 with a RMSE of 0.001 and 0.002 for the AD-MS and C-MS simulations, respectively. In the perpendicular plane, both approximations have an R^2 equal to 0.92 and an RMSE equal to 0.002 in the red band.

In the NIR, the model simulations with AD-MS and C-MS approximations diverge when the view angle is away from the hotspot direction (Figure 3.6). The AD-MS simulation mimics the general shape of the measurements in the principal plane, with a bowl shape in the forscattering direction but not in backscattering direction where the model clearly diverge from the measurements. This may be explained by the relatively larger foliage density, which prevents a significant contribution of multiple scattering to the canopy BRF. In the perpendicular plane, the model doesn't reproduce the shape of measured BRF values; the measured and simulated values are close in the nadir viewing position but diverges for large viewing geometries. However, there is a noted improvement to the correlation between simulated and measured values when using the AD-MS approach instead of the C-MS approximation, with a R^2 of 0.90 and a RMSE of 0.04 for the AD-MS case compared to a R^2 of 0.75 and a RMSE of 0.04 for the C-MS simulations in the solar principal plane (Table 3.2). In the perpendicular plane, both approximations show low R^2 values; 0.33 with an RMSE of 0.04 for AD-MS and 0.34 with an RMSE of 0.03 for C-MS approximation in the NIR band (Table 3.3).

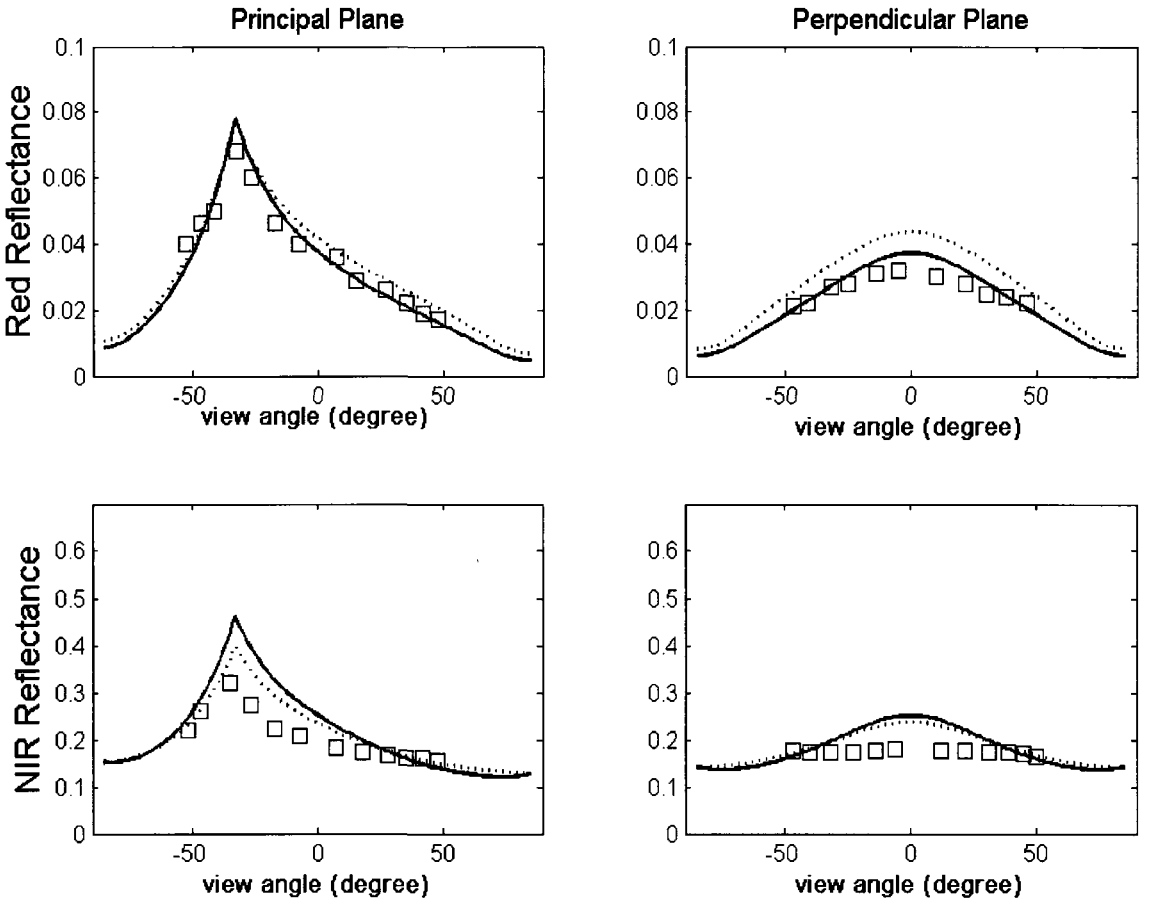

Figure 3.5: Comparison between solar principal plane and perpendicular-plane BRF values simulated with the FLAIR model using the AD-MS approximation (solid line) and constant multiple scattering (dots) and measurements acquired by POLDER (squares) over an Old Jack Pine site in the red and near-infrared regions.

d. Old Aspen Site: The multiple scattering in this site is of great importance as the scattering within the canopy is high, especially in the NIR spectral region. It is shown in Figure 3.7 that the shape and magnitude of observed BRFs are reproduced in the red band in both planes except in the hotspot region where some overestimation is found.

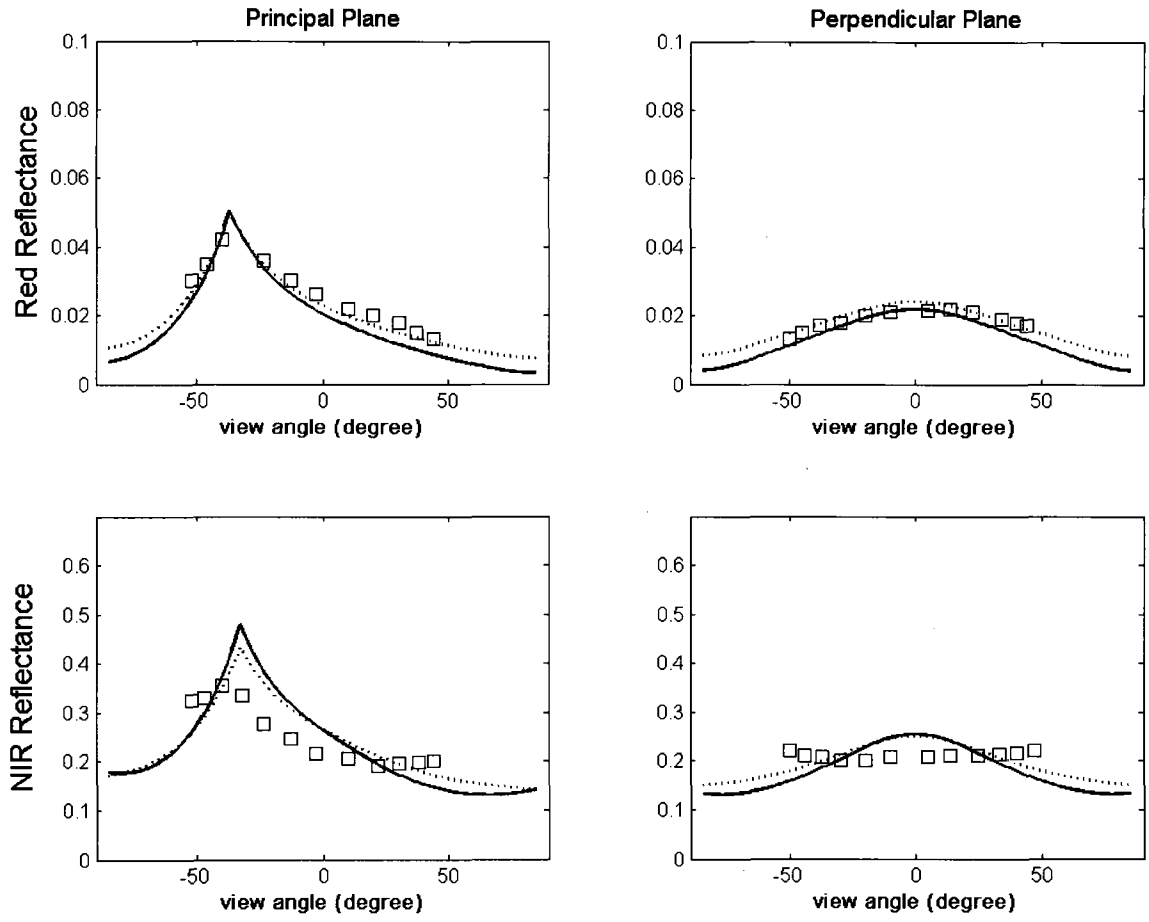

Figure 3.6: Comparison between solar principal plane and perpendicular-plane BRF values simulated with the FLAIR model using the AD-MS approximation (solid line) and constant multiple scattering (dashed line) and measurements acquired by POLDER (squares) over a Young Jack Pine site in the red and near-infrared regions.

The coefficient of determination between simulations and observation for the principal plane in the red band is around 0.87 and 0.86 and the RMSE is 0.004 (Table 3.2) for the AD-MS and C-MS simulations, respectively. In the NIR, it is demonstrated that the simulations with the FLAIR model using the AD-MS approximation can reproduce the general shape of the observed with both the AD-MS and C-MS simulations in the solar

principal plane. In this plane, a well defined bowl shape is present in the forward scattering region matching the shape of the measurements. However, the perpendicular plane, both approximations diverge from the measured data in view angles larger than 30°. The discrepancy is noticeable particularly in the backscatter region. More investigation is needed to understand this stand behaviour. The coefficient of determination in the solar principal plane is 0.87 and 0.86 for the AD-MS and C-MS simulations, respectively with an RMSE equal to 0.03 in the red band (Table 3.2). In the perpendicular plane, both approximations do not fit at all the measurements with an R^2 approaching zero but the RMSE is about the same as for the principal plane, i.e., 0.04 (Table 3.3).

Figure 3.8 illustrates a comparison of the two versions of the FLAIR model simulations to the POLDER observations for all the stands. In the red region, both approximations have similar behavior and reproduce the measurements with the exception of the OBS site where the simulations overestimate the measurements. This is potentially due to the approximations with respect to the FLAIR model in the characterization of the canopy architecture. In the NIR region, the shape of the BRF indicates that the FLAIR with AD-MS simulations generally provides a more realistic reproduction of the observations in comparison to the FLAIR with C-MS. The RMSE is equal to 0.0087 for FLAIR with C-MS compared to 0.0083 for FLAIR with AD-MS in the red band. In the NIR band, the RMSE is equal to 0.031 for FLAIR with C-MS compared to 0.022 for FLAIR with AD-MS. This is expected as the AD-MS approach is highlighted in spectral regions where scattering dominates over absorption.

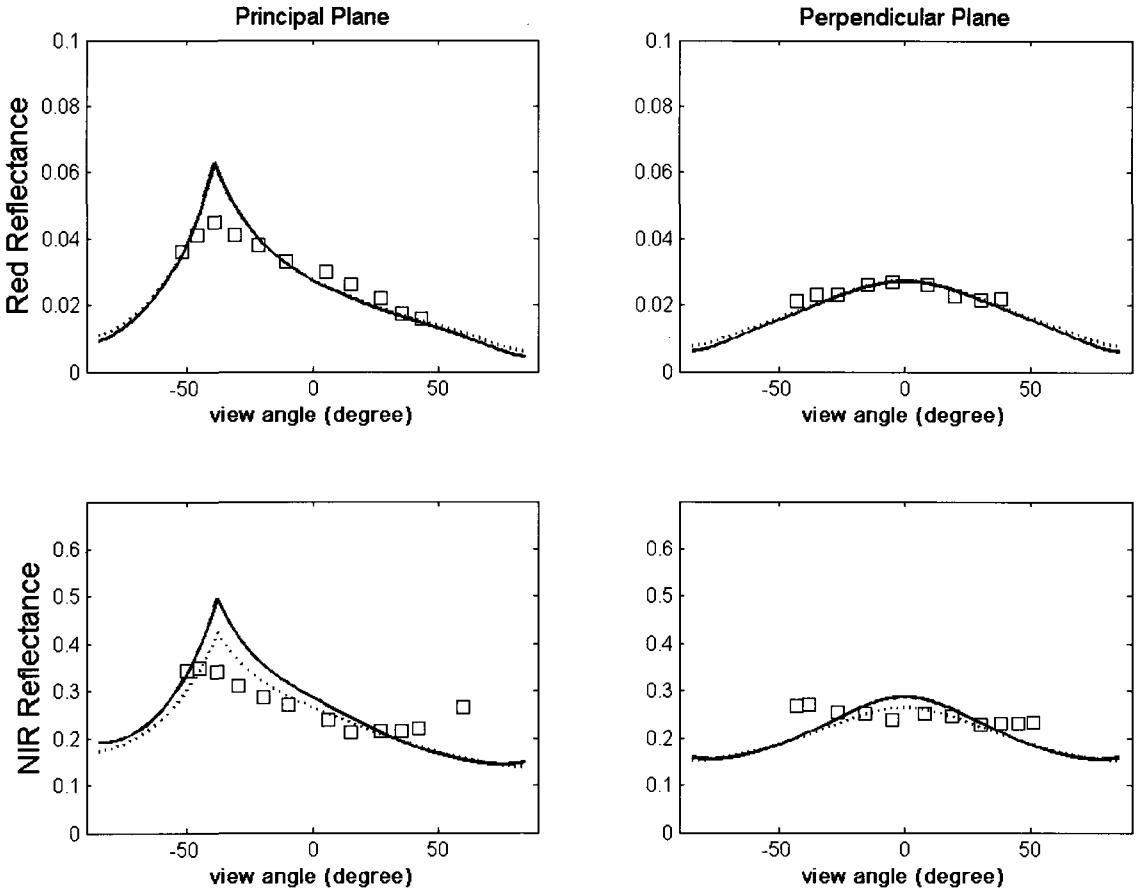

Figure 3.7: Comparison between solar principal plane and perpendicular-plane BRF values simulated with the FLAIR model using the AD-MS approximation (solid line) and constant multiple scattering (dots) and measurements made by POLDER (squares) over an Old Aspen site in the red and near-infrared regions.

Moreover, this Figure shows a significant difference between the two approximations. FLAIR with the AD-MS approach appears to more closely reproduce the Polder measurements than with the C-MS approach.

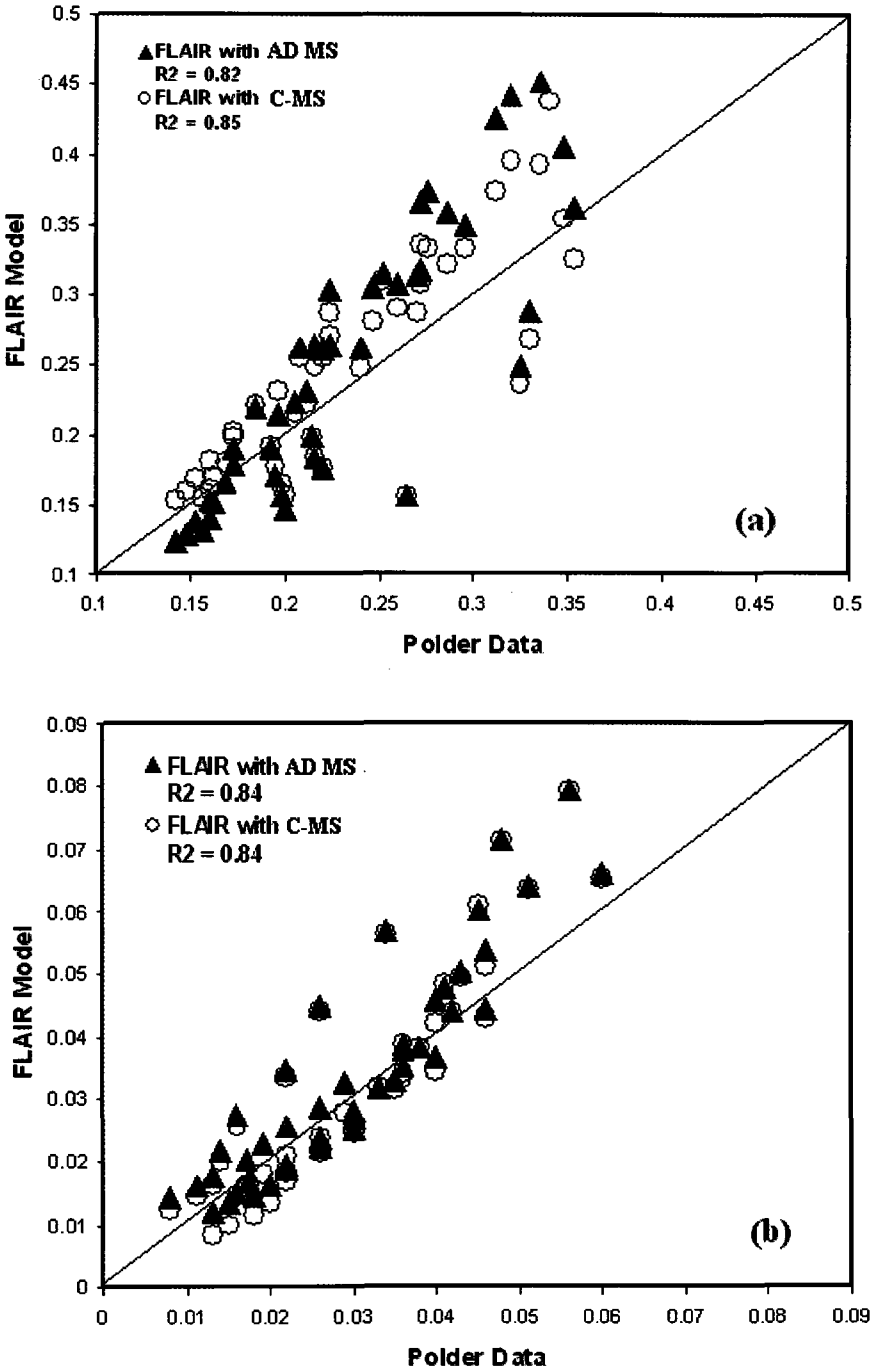

Figure 3.8: Comparison between POLDER measurements and the model for (a) NIR and (b) red bands.

The results illustrate the enhancements made by this newly implemented spectrally dependant multiple scattering scheme compared to the previous approximation using constant multiple scattering factors. There is a significant increase in the simulated hotspot NIR reflectance in all conifer and deciduous stands. The forward scattering is well modelled in the NIR spectral region within the solar principal plane; the bowl feature is well defined in all simulations, with a slight underestimation of the backscattered BRF in the case of the OJP and YJP stands. More investigations are recommended to evaluate the cause of this behavior. Furthermore, with this new scheme, the spectral components of the FLAIR model are calculated automatically at any given wavelength. Therefore, the potential to retrieve canopy biophysical parameters from multiangle high-spectral resolution imagery is enhanced.

3.4. Conclusions

The results presented in this study illustrate the impacts of incorporating the presented multiple scattering scheme into the FLAIR radiative transfer model to more accurately reproduce observed forest canopy BRF. The sensitivity to various physical and geometrical parameters is discussed in an upcoming paper. With this wavelength dependent approach, there is no longer a requirement to create a database of wavelength-specific multiple scattering factors. Therefore, it is more suitable to simulate hyperspectral signatures of vegetation canopies based only on the optical properties of the canopy elements and a limited number of structural parameters. At the leaf leaf/shoot level, Lewis and Disney (2007) have recently applied the concept of spectral invariant to approximate the PROSPECT model. This

new development may lead to the use of this theory to retrieve canopy biochemistry more accurately. The main consequence of introducing the spectral invariant approach into the FLAIR model is its ability now to reach the leaf/shoot level by applying the Lewis and Disney approach or by a linkage to a leaf reflectance model, such as PROSPECT or LIBERTY. This will allow leaf biochemical retrieval from hyperspectral data through model inversion techniques, such as a LUT-based method (Omari et al., 2009).

Acknowledgment

The authors would like to gratefully acknowledge the support of the Canada Centre for Remote Sensing / Natural Resources Canada for the infrastructure access and the University of Ottawa for financial support. We would also like to thank Nadia Rochdi and Richard Fernandes for their productive discussions and contributions, and the anonymous reviewers for their constructive comments and assistance in editing, resulting in completion of this paper.

References

Chen, J.M, and Leblanc, S. G., "Multiple-scattering scheme useful for geometric optical modeling", IEEE Transactions on Geoscience and Remote Sensing, 39(5): 1061–1071, 2001.

Chen, J.M, and Leblanc, S. G., "A Four-Scale bidirectional reflectance model based on canopy architecture", IEEE Transactions on Geoscience and Remote Sensing, 35(5): 1316–1337, 1997.

Chen, J. M., "Canopy architecture and remote sensing of the fraction of photosynthetically active radiation absorbed by boreal conifer forests", IEEE Transactions on Geoscience and Remote Sensing. 34(6): 1353-1368, 1996.

Dawson, T.P., Curran, P.J., and Plummer, S.E., "LIBERTY - Modelling the effects of leaf biochemical concentration on reflectance spectra", *Remote Sensing of Environment*, 65: 50-60, 1998.

Disney, M.I., Saich, P., Lewis, P., "Modelling the radiometric response of a dynamic 3D structural model of Scots pine in the optical and microwave domains", Proceedings of IEEE IGARSS'03 (Toulouse), Vol. 6, pp. 3537-3539, 2003.

Disney, M. I., Lewis, P., and North, P. R. J., "Monte Carlo ray tracing in optical canopy reflectance modeling", Remote Sensing Review, (18): 163-196, 2000.

Huang, D., Knyazikhin, Y., Wang, W., Deering, D. W., Stenberg, P., Shabanov, N., and Myneni, R.B., "Stochastic transport theory for investigating the three-dimensional canopy structure from space measurements," Remote Sensing of Environment, 112: 35-50, 2008.

Huang, D., Knyazikhin, Y., Dickinson, R. E., Rautiainen, M., Stenberg, P., Disney, M., Lewis, P., Cescatti, A., Tian, Y., Verhoef, W., Martonchik, J. V., and Myneni, R.B., "Canopy spectral invariants for remote sensing and model applications", Remote Sensing of Environment, (106): 106-122, 2007.

Jacquemoud, S., and Baret, F., "PROSPECT - a model of leaf optical-properties spectra", Remote Sensing of Environment, 34: 75–91, 1990.

Knyazikhin, Y., Martonchik, J. V., Myneni, R. B., Diner, D. J., and Running, S.W., "Synergistic algorithm for estimating vegetation canopy leaf area index and fraction of absorbed photosynthetically active radiation from MODIS and MISR data", Journal of Geophysical Research, 103(D24): 32257– 32276, 1998.

Kucharik, C. J., Norman, J. M., Murdock, L. M., and Gower, S., T., "Characterizing canopy nonradomness with a Multiband Vegetation Imager (MVI)", Journal of Geophysical Research, 102(D24): 29445–29473, 1997.

Leblanc, S. G., Bicheron, P., Chen, J., Leroy, M., and Cihlar, J., "Investigation of directional reflectance in boreal forests with an improved 4-scale model and Airborne POLDER data", IEEE Transactions on Geoscience and Remote Sensing, 37(3): 1396-1414, 1999.

Lewis, P., and Disney, M., "Spectral invariants and scattering across multiple scales from within-leaf to canopy", Remote Sensing of Environment, (109): 196-206, 2007.

Li, X, and Strahler, A. H., "Geometric-optical bidirectional reflectance modeling of the discrete crown vegetation canopy: effect of crown shape and mutual shadowing", IEEE Transactions on Geoscience and Remote Sensing, 30(2): 276-292, 1992.

Li, X, and Strahler, A. H., "Modeling the gap probability of a discontinuous vegetation canopy", IEEE Transactions on Geoscience and Remote Sensing, 26(2): 161-169, 1988.

Liang, S., "Quantitative Remote Sensing of Land Surfaces", John Wiley and Sons, Inc., 534 pages, 2004.

Liang, S., and Strahler, A. H., "An analytic radiative transfer model for a coupled atmosphere and leaf canopy, Journal of Geophysical Research, 100(D3): 5085–5094, 1995.

Liang, S., and Strahler, A. H., "The calculation of the radiance distribution of the coupled atmosphere and leaf canopy", IEEE Transactions on Geoscience and Remote Sensing, 31(2): 491-502, 1993.

Miller, J.R., White, H.P., Chen, J.M., Peddle, D.R., McDermid, G., Fournier, R.A., Shepherd, P., Rubinstein, I., Freemantle, J., Soffer, R., and LeDrew, E., "Seasonal change in understorey reflectance of boreal forests and influence on canopy vegetation indices", Journal of Geophysical Research, 102(24): 29475-29482, 1997.

Mõttus, M., and Stenberg, P., "A simple parameterization of canopy reflectance using photon recollision probability", Remote Sensing of Environment, 112: 1545-1551, 2008.

Mõttus, M., "Photon recollision probability in discrete crown canopies", Remote Sensing of Environment, 110: 176 -185, 2007.

Nadal, F., and Bréon, F.M., "Parameterization of surface polarized reflectance derived from POLDER spaceborne measurements", IEEE Transactions on Geoscience and Remote Sensing, 37(3): 1709 - 1718, 1999.

Ni, W., Li, X., Woodcock, C. E., Roujean, J. L., and Davis, R. E., "Transmission of solar radiation in boreal conifer forests: measurements and models", Journal of Geophysical Research, 102, 29555-29566, 1997.

Nilson, T., and Peterson, U., "A forest canopy reflectance model and a test case", Remote Sensing of Environment, 37: 131-142, 1991.

Nilson, T. and Kuusk, A., "A reflectance model for homogeneous plant canopy and its inversion", Remote Sensing of Environment, 27: 157-167, 1989.

Nilson, T., "A theoretical analysis of the frequency of gaps in plant stands", Agricultural and Forest Meteorology, 8: 25-38, 1971.

Omari, K., Fernandes, R., Staenz, K., Rochdi, N., and Chelle, M., "Parameterization of the angular distribution of the multiple scattering radiation using photon re-collision probability", Remote Sensing of Environment, (in review), 2009.

Omari, K., Staenz, K., King, D.J., and White, H, P., "Retrieval of canopy biophysical parameters inverting PROFLAIR leaf-canopy reflectance model using the LUT approach", Canadian Journal of Remote Sensing, (in review), 2009.

Pinty, B., Widlowski, J. L., Gobron, N., Verstraete, M. M., and Diner, D. J., "Uniqueness of Multiangular Measurements Part 1: An Indicator of Subpixel Surface Heterogeneity from MISR", IEEE Transactions on Geoscience and Remote Sensing, 40(7): 1560-1573, 2002.

Pinty, B., and Verstraete, M. M., "Extracting information on surface properties from bidirectional reflectance measurements", Journal of Geophysical Research, 96(D2): 2865-2874, 1991.

Rautiainen, M, and Stenberg, P., "Application of photon recollision probability in coniferous canopy reflectance simulations", Remote Sensing of Environment, 96: 98–107, 2005.

Ross, J., "The radiation regime and architecture of plant stands, Netherlands: Junk, W., The Hague, 391 pages, 1981.

Sellers, P., Hall, F., Margolis, H., Kelly, B., Baldocchi, D., Hartogden, G., Cihlar, J., Ryan, M.G., Goodison, B., Crill, P., Ranson, K.J., Lettenmaier, D., and Wickland, D.E., "The Boreal Ecosystem-Atmosphere Study (BOREAS): An overview and early results from the 1994 field year", Bulletin of American Meteorological Society, 76(9): 1549-1577, 1995.

Sellers, P., "Canopy reflectance, photosynthesis and transpiration", International Journal of Remote Sensing, 6: 1335-1372, 1985.

Shabanov, N.V., Kotchenova, S., Huang, D., Yang, W., Tan, B., Knyazikhin Y., Myneni, R. B., Ahl, D. E., Gower, S. T., Huete, A. R., Aragao, L. E. O. C., and Shimabukuro, Y. E., "Analysis and optimization of the MODIS leaf area index algorithm retrievals over broadleaf forests", IEEE Transactions on Geoscience and Remote Sensing, 43(8): 1855–1865, 2005.

Shabanov, N. V., Knyazikhin, Y., Baret, F., and Myneni, R. B., "Stochastic modeling of radiation regime in discontinuous vegetation canopies," Remote Sensing of Environment, 74: 125–144, 2000.

Smolander, S., and Stenberg, P., "Simple parameterizations of the radiation budget of uniform broadleaved and coniferous canopies", Remote Sensing of Environment, 94: 355– 363, 2005.

Stenberg, P., "Simple analytical formula for calculating average photon recollision probability in vegetation canopies", Remote Sensing of Environment, 109): 221-224, 2007.

Van de Hulst, H. C., "Multiple light scattering. Tables, formulas and applications", New York: Academic Press, 1980.

Verhoef, W., "Light scattering by leaf layers with application to canopy reflectance modeling: The SAIL model", Remote Sensing of Environment, 16: 125-141, 1984.

White, H.P., Sun, L., Staenz. K., Fernandes, R., and Champagne, C.M., "Determining the contribution of shaded elements of a canopy to remotely sensed hyperspectral signatures", Proceedings of the 1st International Symposium on Recent Advances in Quantitative Remote Sensing, Valencia, Spain, pp. 159-166, 2002a.

White, H.P., Deguise, J.C., Schwarz. J., Hitchcock, J. R. and Staenz, K., "Defining shaded spectra by model inversion for spectral unmixing of hyperspectral datasets - theory and preliminary application", Proceeding of Joint 24th Canadian Symposium of Remote Sensing and IGARSS, Toronto, Ontario, Canada, pp. 989-991, 2002b.

White, H.P., Miller, J.R., and Chen, J.M, "Four-scale linear model for anisotropic reflectance (FLAIR) for plant canopies. I: Model description and partial validation", IEEE Transactions on Geoscience and Remote Sensing, 39(5): 1072-1083, 2001a.

White, H.P., Miller, J.R., and Chen, J.M., "Four-scale linear model for anisotropic reflectance (FLAIR) for plant canopies. II: Validation and Inversion with CASI, POLDER, and PARABOLA data at BOREAS", IEEE Transactions on Geoscience and Remote Sensing, 40(5): 1038-1046, 2001b.

White, H.P., Miller, J.R., Chen, J. and Peddle, D.R., "Seasonal change in mean understorey reflectance for Boreas sites, Preliminary results", Proceedings of the 17th Canadian Symposium on Remote Sensing, Saskatoon, Saskatchewan, pp. 189-194, 1995.

Zhang, Y., Shabanov, N., Knyazikhin, Y., and Myneni, R.B., "Assessing the information content of multiangle satellite data for mapping biomes", Remote Sensing of Environment, 80: 435– 446, 2002.

Chapter 4

Study site description, data acquisition and processing

4.1. Study Site

A detailed understanding of the canopy composition (architectural and optical properties) is a prerequisite for successful data collection and, subsequently, acquisition of reliable data. This chapter outlines the methodology for acquisition of field and laboratory data used in testing the algorithms described in chapter 5. A description of the study site is given in the next section followed by an overview of the protocol used in acquiring field data and hyperspectral remote sensing data processing.

4.1.1. Topography and Hydrology

The abandoned Kamkotia mine (48° 35' N, 81° 41' W) is situated about 20 km north-west of the city of Timmins in the Kamiskotia region, Ontario, Canada. The region of Kamiskotia is an overlap area of the Canadian Shield and the Boreal forest. It covers a distance of 3800 km from east Newfoundland to Northern Alberta. Due to glacial activities, the topography of the region is generally flat due to the glacial lake deposits. Sporadic bedrock outcrops such as Mount Jamison (416 m ASL) provide occasional reliefs. The test site selected within the Kamiskotia region is a flat area with low local relief. The drainage in the area is sluggish, which is the result of typical land slopes of 0.7 to 1% of clay soils. The poor drainage in the region has created wetland areas around the mine site. The landscape of the Kamiskotia region is generally dominated by forests, lakes, rivers and marshes. The surface water bodies include the Kamiskotia Lake south-west of the study site and the Kamiskotia River which

flows from the north-east portion of the study site to the north to ultimately discharge into the James Bay.

4.1.2. Weather and vegetation

The climate of the Kamiskotia region is continental with long and cold winters and relatively short summers. The cold wind streams coming from Hudson Bay cause a large variation of the amount of annual rainfall between the east and the west sides of Kamiskotia region (around 1000 mm in the west compared to approximately 400 mm in the east). The average temperature varies from -15°C in January to 17°C in July. These climate factors, plus the exposed rocks, the frequent forest fires and the soil acidity affect considerably the ecosystem of this region. In general, conifers are well adapted to these conditions, including species such as black spruce (Picea mariana), white spruce (Picea glauca) and balsam fir (Abies balsamea). Aspen (Populus tremuloides), white birches (Betula papyrifera), jack pine (Pinus banksiana) and balsam poplar (Populus balsamifera) are also present, although a mixture of different conifers and deciduous trees are frequently in less humid areas (Berry, 1944; Wiken, 1986).

4.1.3. Geology

The Kamiskotia deposit is part of the Volcanic Complex of the Kamiskotia assemblage. This supracrustal assemblage is within the 2.75-2.69 billion year old Abitibi Greenstone Belt which comprises a portion of the Abitibi Sub-province, about 300 km by 800 km in size,

within the Superior Province of the Canadian Shield. The Abitibi Greenstone Belt is considered the largest greenstone belt in the world. It is dominated by supracrustal and granitoid rocks and its abundance of minerals in various deposits (Thurston et al., 1991; Jackson and Fyon, 1991). Within the Kamiskotia deposit, the greenschist facies Kamiskotia Assemblage is composed of the Kamiskotia Volcanic Complex (2707±2 mA; mA means million years) and is underlain by the synvolcanic, tholeiitic Kamiskotia Gabbroic Complex (2705 ±2 mA) (Barrie and Davis, 1990). This assemblage is bounded in the north by a metavolcanic assemblage, the Mattagami Fault to the east and the Carscallen Assemblage to the south and west sides. The primary bedrock geological formations in the Kamkotia area are metavolcanics, mafic flows, intermediate and mafic metavolcanics and felsic metavolcanics (Figure 4.1). The principal ore minerals include pyrite, pyrrhotite, chalcopyrite, sphalerite and traces of magnetite and galena (Thurston et al., 1991). The Kamkotia mine site and tailings areas are covered with glaciofluvial and glaciolacustrine derived materials of silt, clay and sand fractions. Overburden deposits range in depth over 60 meters (Ferguson et al., 1994).

4.1.4. History of the Kamkotia mine

The Kamkotia mine was exploited first by Hollinger Mines Ltd. from 1942 to 1950 to fill the needs of the war in zinc and copper. Afterwards, Kamkotia Mine Ltd. took over the mine and operated it from 1950 to 1970. In the mid seventies it was recognized as a source of environmental contamination. Drainage from the site has impaired the quality of the Kamiskotia Lake and Little Kamiskotia River and shown high levels of dissolved metals,

sulphates and depressed pH (Levesque, 2001). Local groundwater on the site showed similar impairments. Acid generating tailings are the source of contamination of the ground and surface water on the site. Approximately 6 million tonnes of acid generating tailings were deposited in the area surrounding the site (Levesque, 2001). The high acidity of drainage from the tailings has killed large areas of vegetation, in particular where the northeast-unimpounded tailings (NUT) were deposited (Figure 4.2). Theses tailings contain large amounts of pyrite, pyrrhotite, chlorites, micas, quartz, and Cu and Zn sulphides. The problems of acid drainage are present despite the construction of a 7-m high dam to impound the tailings from the north. The tailings continued to leak in the north-east from the dam, which caused the drainage to spread and enlarged the tailings areas to the north-east through two creeks into the forest (Levesque, 2001).

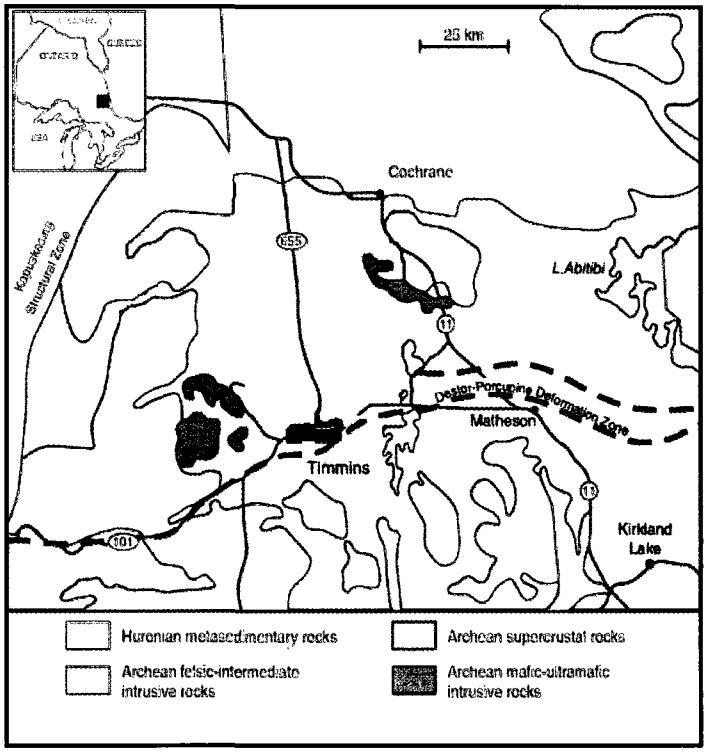

Figure 4.1: Geological map of the Kamiskotia region. (http://gsc.nrcan.gc.ca/geochem/timmins/geology).

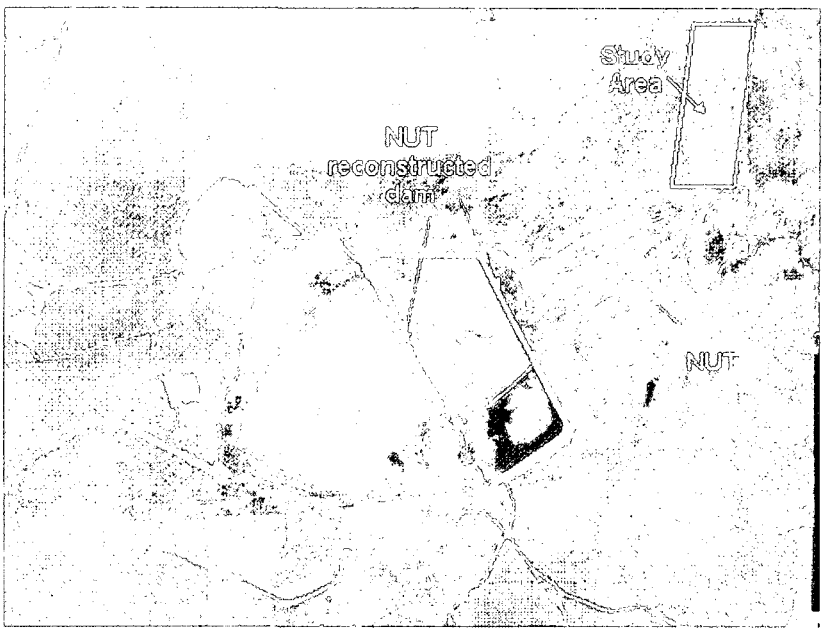

Figure 4.2: Kamkotia mine site shwon on mosaic of 2004 air-photos. NUT refers to northeast-unimpounded tailings and NIT to north impounded tailings.

4.1.5. Acid mine drainage problem

During the mining operations at the Kamkotia site, tailings and waste rocks have been disposed of in an adjacent space-bounded dyke. Theses tailings are composed of fine grainy incoherent dust that contains very large amounts of pyrite and other sulphide minerals. The sulphide minerals in the tailings undergo chemical reactions when exposed to oxygen and water to produce Acid Mine Drainage (AMD) characterized by a high degree of acidity and

abundance of metals. The acidity is defined as the availability of hydrogen ions to neutralize bases. Given their high solubility in acidic solutions, metals such as copper, zinc, cadmium are often found with very high concentrations in acidic waters which make them highly toxic (Kelly, 1988). Subsequently, these metals can cause environmental damage to the fauna and flora. The degree of toxicity varies from metal to another and from one organism to another.

The oxidation of sulphide minerals, especially pyrite, is commonly considered as a major source of acid generation from tailings and waste rocks. The geochemical aspect of the process of oxidation of pyrite can be summarized in the following paragraphs (Richer, 2004; Lévesque, 2001).

Firstly, the oxidation of pyrite (equation 4.1) releases hydrogen ions, ferrous (Fe^{2+}) iron and sulphate as follows (Nordstorm et al., 1999):

$$2FeS_2 + 7O_2 + 2H_2O \rightarrow 2Fe^{2+} + 4SO_4^{2-} + 4H^+. \qquad [4.1]$$

Following that, the ferrous iron is oxidized with oxygen to produce ferric iron (Fe^{3+}) in an acidic setting (pH is less than 4.3) following the reaction of equation 4.2. This reaction is described as the "rate-determining step"; it is significantly slower than the first reaction (equation 4.1). Secondary microorganisms catalyze this reaction leading to an increase of the oxidation rate by a factor of 10^6 over the abiotic rate (Singer et al., 1970):

$$4Fe^{2+} + O_2 + 4H^+ \rightarrow 4Fe^{3+} + 2H_2O \quad [4.2]$$

Subsequently, the ferric iron is hydrolyzed to form solid ferric hydroxide (ferrihydrite) and hydrogen ion following the reaction of equation 4.3 if the setting is less acidic (pH is greater than 3.5):

$$Fe^{3+} + 3H_2O \rightarrow Fe(OH)_3 + 3H^+. \quad [4.3]$$

However, if the pH remains less than 3.5, the oxidation of pyrite will continue with the ferric iron produced in the first two reactions (equations 4.1 and 4.2) until the supply of pyrite and the production of ferric iron is exhausted (Nordstorm et al., 1999).

During this geochemical process, a wide variety of secondary minerals is formed. Their type and composition depend on factors such as primary mineral type, the acidity, the temperature and the moisture content. For example, the ferric hydroxide can be converted to hematite (Fe_2O_3) if the pH is maintained between 5 and 9. The hydrolysis of the hematite produces goethite (FeO(OH)) (Alpers et al., 1994; Nordstorm et al., 1999). However, if the pH is outside the range [5 - 9], the ferric hydroxide dissolves and re-precipitates directly as goethite following the reaction:

$$Fe_2O_3 + H_2O \rightarrow 2FeO(OH) \quad [4.4]$$

Note that oxidation processes of other sulphide minerals such as pyrrhotite (iron sulphide), sphalerite (zinc iron sulphide) and chalcopyrite (copper iron sulphide) are similar to the oxidation of pyrite (Levesque, 2001).

Following this processes, the AMD charged with metals dissipates in the surrounding ecosystem through groundwater, rivers and lakes. This causes a visibly marked damage to the landscape (Figure 4.2). For instance, ADM can increase the soil acidity, salinity and toxicity in the organic matter (Nordstorm et al., 1999).

4.1.6. Effects of mine tailings on vegetation

The spread of metals in soil depends on its soil physical properties. The uptake of theses metals by the tree roots is constrained primarily by the state of soil acidity. An increase of soil acidity increases the solubility of metals and, subsequently, increases the probability of absorption into the roots of trees. The tree roots form a system that absorbs nutrient elements from soil, carrying them to all tree elements and accumulating part of them as reserves. All plants have the ability to accumulate heavy metals that are essential for their growth and development such as magnesium, zinc, copper, iron, etc. (Verburg et al., 2001). However, excessive accumulation of these heavy metals can make them potentially harmful to most plants. Accordingly, the effects of these biogeochemical agents on the health of the plants depend on their concentrations. They can restrain their growth, leading to a gradual decline, which is usually noticed after a period of more than one season. The immediate symptoms of

this decline can be shown by discoloration or loss of foliage in the case of a severe stress. Before one can observe a loss of foliage, the tree may show some signs of stress as a loss of vigour and deterioration of the root system. These signs may also be manifested by leaf size shrinking and an increase of crown transparency, thereby reducing the volume of the tree leading to changes in the architecture of the entire canopy (Olthof, 1999). Although, it is very difficult to distinguish between these structural changes and those due to the natural cycle of tree growth, a spatial-temporal analysis of these changes can be useful.

4.1.7. Previous environmental studies at the Kamkotia mine site

At the Kamkotia mine site, environmental studies have been initiated to investigate the effect of the acid drainage problem on the adjacent forest since 1992. Fieldwork studies have been carried out to investigate the relationship between the soil chemistry, forest structure, and leaf spectra with distance from the tailings edge (Walsworth and King, 1999; Lévesque and King, 1999 and 2003; Olthof and King, 2000). Airborne digital camera imagery was used at the Kamkotia site to develop a forest health index (Olthof and King, 2000), analyze temporal forest structural condition (Cosmopoulos and King, 2004; Seed and King, 2003) and estimate forest stand Leaf Area Index (LAI) (Olthof et al., 1999). Furthermore, semivariogram analysis showed a significant relationship between the semivariogram range and some forest canopy parameters such as crown size, tree height and crown closure (Lévesque and King, 1999).

The next section attempts to analyze the effects of biogeochemical agents on forest biochemistry and biophysics by taking advantage of hyperspectral remote sensing data using the relationship between several narrow spectral bands (absorption features) and leaf biochemistry. For this purpose, the radiative transfer modelling theory described in the chapter 5 is used. The FLAIR model with its new multiple scattering component is linked to the PROSPECT leaf model to quantify the leaf biochemistry and the canopy biophysics from hyperspectral data. To achieve this objective, a fieldwork study was carried out along with Hyperion data acquisition in August 2005. The next section is a description of field and remote sensing data acquired during this campaign.

4.2. Field and remote sensing data acquisition

The study site is a forested area located in the northeast of the NUT tailings (Figure 4.2). This forest is a typical mixed boreal forest bounded by two creeks from the east, north and west whereas the tailings are in the south. The forest cover is composed of mature trembling aspen, a few pockets of co-dominant balsam poplar, jack pine and an understorey of young black spruce, white spruce and balsam fir. The major stress factors at the Kamkotia site were identified as high acidity drainage from the tailings in the study area direction wind deposition of tailings dust on the forest and forest floor and mechanical wind effects causing observed structural damage in the canopy near the tailings (Olthof and King, 2000, Levesque and King, 1999).

4.2.1. Field data collection

Adequate ground reference data are necessary for using remote sensing techniques to produce accurate results. The aim of the fieldwork campaign carried out in August 2005 in the Kamkotia region was to see whether leaf chlorophyll content and canopy LAI could be predicted through radiative transfer modelling using hyperspectral data. The objective of the fieldwork was to acquire sufficient data to link leaf reflectance and leaf biochemical contents through a leaf model (PROSPECT) and, subsequently, leaf level to canopy level reflectance through radiative transfer modeling (FLAIR).

The plot design was planned before the fieldwork taking into account the land cover type of the study area. Previous environmental studies (Lévesque and King, 1999) and air-photos were used to select the plots. This section summarizes details of the field campaign and the procedures used to measure the parameters for this study.

a. Sampling plots

It was decided to select the plots along a transect within the canopy in order to have proper gradient of damage in trees since the area is a contamination site (Figure 4.3). In this case, a gradual increase/decrease of vegetation stress indicators along this transect would be explained by the contamination from the tailings. This will also exclude the other vegetation stress sources such as natural stress, or disease and insect damages. The selection of the transect was based on the direction of the drainage (Levesque and King, 1999). Due to time constraints, the measurements were limited to deciduous species only; Aspen and Poplar

trees were identified as dominants trees. The selected plots are very close to the ones previously set up and studied by Levesque and King, (1999). They cover an area of 60 x 60 m^2, which represents approximately four Hyperion image pixels as shown in Figure 4.4. Within each subplot of 30 m by 30 m, four dominant trees were identified for analysis, which was based on tree height and crown volumes.

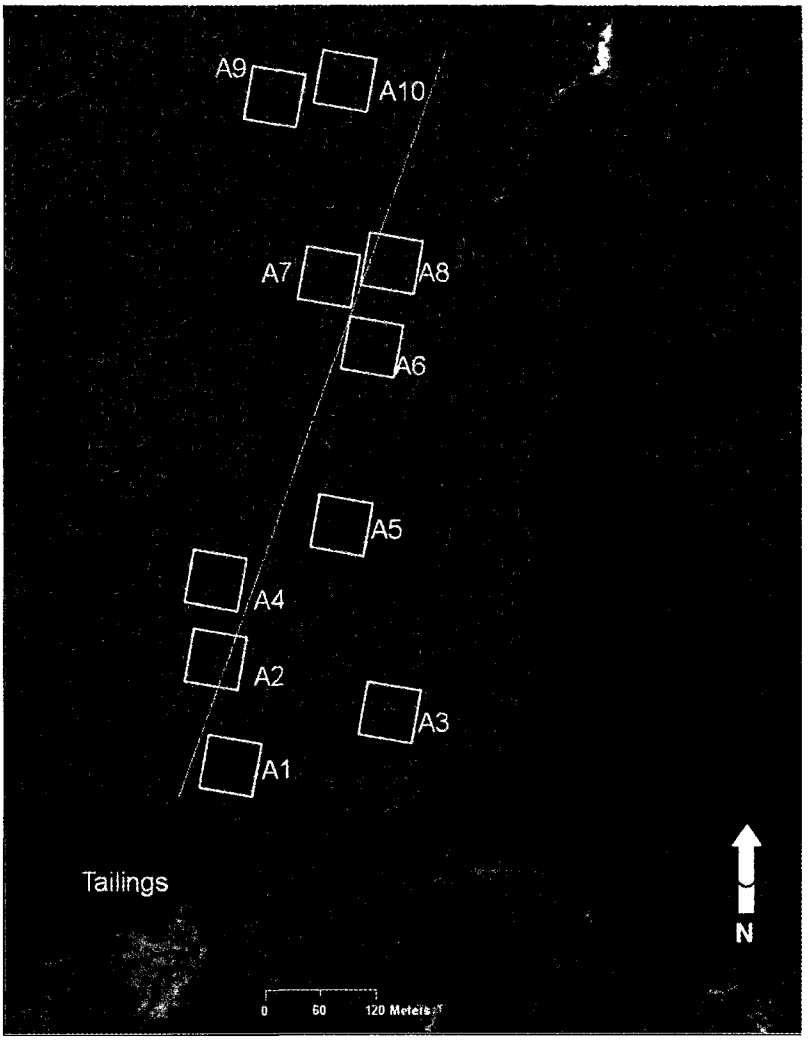

Figure 4.3: The study site plots shown on a 2004 air-photo. White squares indicate the location of the plots. The drainage direction is in a north-northeast direction from the tailings source (yellow line).

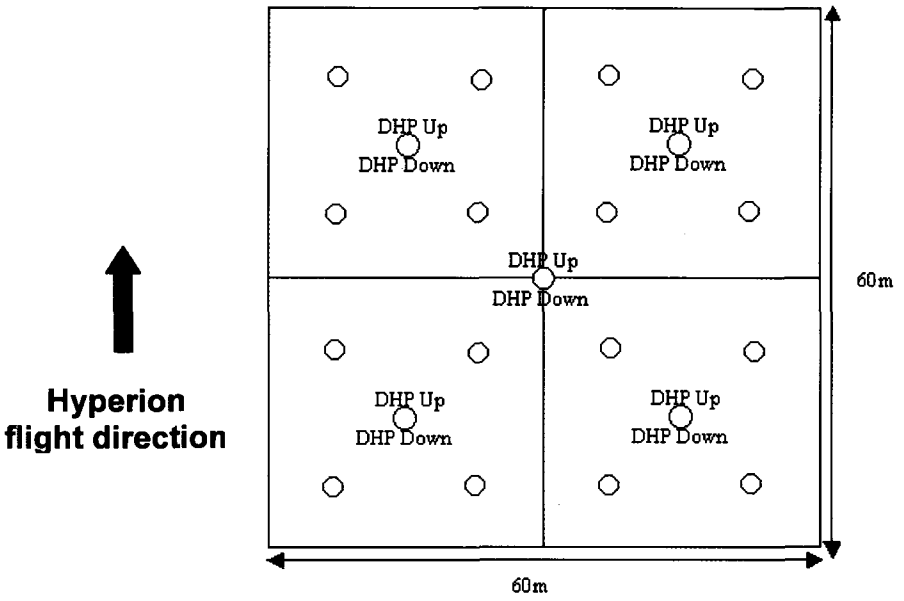

Figure 4.4: A schematic presentation of the sampling plot. The 60 x 60 m^2 was divided into four square quadrants each representing a Hyperion pixel. Four dominant trees per quadrant were identified for analysis.

b. Sampled parameters

In addition to characterisation of the ground cover types and Global Positioning System (GPS) data acquired at the centre of each plot, the following parameters were measured.

Canopy Structural parameters: The structural measurements were performed within four days from 16 to 19 of August 2005. The structural measurements include:

- Tree density: number of dominant trees per quadrant (per 30 m by 30 m),
- Tree height using Hypsometer
- Trunk diameter at breast height (dbh).
- Digital Hemispherical Photos (DHP) for LAI estimation.

    - The approach is based on taking DHPs with a fish-eye lens attached to a digital camera in upward and downward looking directions. The DHPs data is then processed using the Can-Eye freeware package to extract effective and true LAI values from the gap fraction measure (Weiss, 2002). The gap fraction is derived from the measured transmitted light using a Poisson model.

Spectral and biochemical measurements: Both leaf reflectance and transmittance measures were performed within a 12-hour time frame from the sampling (August 23, 2005). The measurements included:

- ***Understorey measurements:*** Spectral measurements of three leaf samples from the understorey cover were collected from each plot. These measurements were acquired using a Li-COR Integrating Sphere Spectroradiometer. A circular area of approximately 2.5 cm in diameter was marked on each leaf (avoiding the mid-vein if possible) for leaf reflectance measurements. The spectral reflectance measurements were carried out on all leaf samples using a LI-COR 1800 Integrating sphere coupled by a 200-μm diameter single mode fiber to an ASD field spectrometer with a 1-nm sampling interval between

350 and 2500 nm. The protocol used for leaf reflectance corrections was based on the methodology described in Harron (2000).

- ***Overstorey measurements:*** One branch of each sampled tree was shot down from the top of the tree crown and immediately tagged (named and numbered) and placed into a plastic bag for analysis purposes. These samples were then stored in a cooler (cold not frozen) and sent to the lab for spectral measurements using similar method as for the understorey leaf samples.

  After reflectance measurements, leaf samples were stored immediately into a plastic bag and transported in a frozen condition with dry ice to the laboratory for biochemical analysis at the Ontario Forest Research Institute in Sault Ste. Marie, Ontario. The measured parameters were the concentration of total chlorophyll within the leaf and water content (fresh weight measurement of leaf sample - dry weight measurement of leaf sample).

4.2.2. Hyperspectral data acquisition and pre-processing

A Hyperion image was acquired over the Kamkotia study site on August, 14, 2005. The demonstrator technology Hyperion sensor, carried by the National Aeronautics and Space Administration (NASA) Earth Observing 1 (EO-1) satellite is the first spaceborne Hyperspectral instrument to acquire both visible/near-infrared (VNIR; 360 – 1000 nm) and shortwave infrared (SWIR; 1000 – 2500 nm) spectral data. This pushbroom sensor nominally

provides 242 spectral bands with a 30-m ground sampling distance over a 7.65 km swath. Some of the bands, particularly those at the lower and upper ends of the wavelength range, exhibit a poor signal-to-noise ratio. As a result, just about 192 of the 242 bands are exploitable. Hyperion consists of two distinct spectrometers, one with about 70 bands covering the VNIR region with an average full-width at half maximum (FWHM) of 10.90 nm and the other one with 172 bands in the SWIR with an average FWHM of 10.14 nm.

The processing of post-level 1B1 Hyperion data acquired over the Kamkotia study site was carried out using the Imaging Spectrometer Data Analysis System (ISDAS), a software package developed at the Canada Centre for Remote Sensing (Staenz et al., 1998). The flowchart in Figure 4.5 presents an overview of the different preprocessing steps applied to the Hyperion data. The following steps summarize the major type of corrections performed on Hyperion imagery in order to extract reflectances at the canopy level (Khurshid et al., 2006).

1) A spatial shift in the form of a vertical offset exists between pixels 128 and 129 of the right half versus the left half of the SWIR image. A correction of this problem is achieved by simply shifting up the right half of the image by one pixel.
2) A destriping technique, the spectral moment approach, is applied to the data to remove systematic noise (stripes) (Sun et al., 2008). This is done by replacing the affected columns and pixels using the spatial and spectral information of adjacent pixels of the at-sensor radiance data.

3) In order to improve the quality of the at-sensor radiance Hyperion data, the noise is reduced using an average smoothing procedure (Khurshid et al., 2006).

4) An angular shift due to a spatial misregistration between the VNIR and the SWIR data exists. Adjusting this effect is achieved by rotating the VNIR data by an angle of 0.22^{o} in counterclockwise direction.

5) The smile/frown refers to an across-track wavelength shift of the centre wavelength on a column-by-column basis in a particular band. This effect exists in Hyperion data, particularly in the VNIR bands where the shift can reach 2.6 to 3.5 nm. Such a shift is less severe in the SWIR bands, usually smaller than 1 nm. The detection of the band centre wavelength and its bandwidth in ISDAS is based on using atmospheric spectral absorption features of at-sensor radiance spectra (Neville et al., 2008). Correlation between Hyperion at-sensor radiance in given spectral absorption features and its equivalent at-sensor radiance modeled with the radiative transfer code MODTRAN 4.2 permits the estimation and, subsequently, the correction of wavelength shifts due to smile/frown. This leads to a new set of wavelength centres and bandwidths for each column along the track (White et al., 2004). Recalibrated gain and offset values are incorporated in the smile detection procedure (Khurshid et al., 2006). The recalibration of gain/offset values is performed within an atmospheric feature matching approach to enhance the at-sensor radiance.

6) Atmospheric correction is performed on the data using the radiative transfer model, MODTRAN 4.2, to retrieve at-surface reflectance from at-sensor radiance using atmospheric absorption features via a LUT approach (Staenz and Williams, 1997).

7) Correction of smile/frown.

8) In a final step, a post-processing procedure is applied to the data in order to remove remaining band-to-band errors which are due to atmospheric correction and the other pre-processing procedures applied. This final procedure consists of applying a technique based on the calculation of correction gains and offsets using a spectrally flat target pixel approach (Staenz et al., 1999).

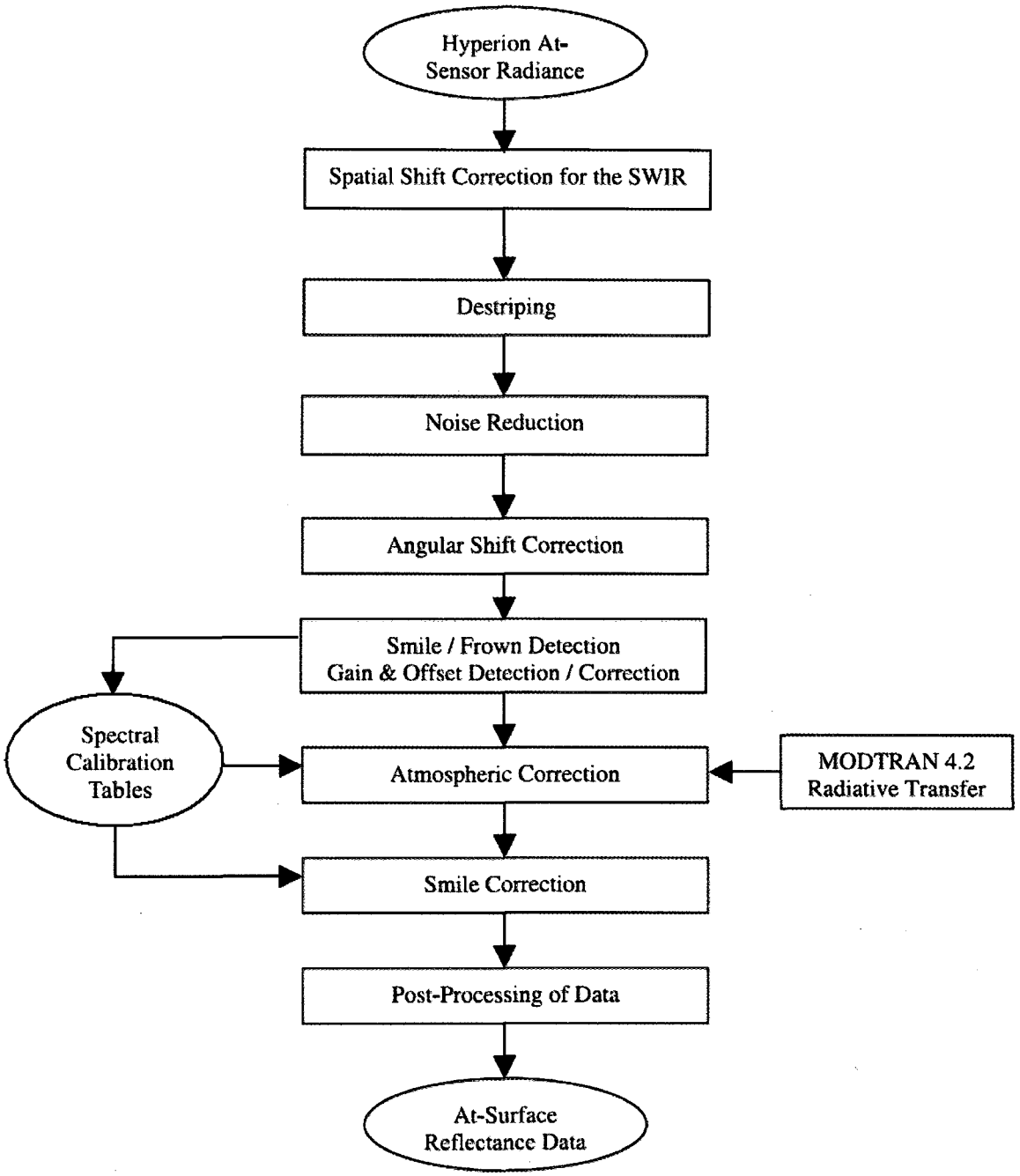

Figure 4.5: At-sensor radiance to at-surface reflectance processing steps of Hyperion imagery acquired at the Kamkotia study site

Chapter 5

Retrieval of forest canopy parameters by inversion of the PROFLAIR leaf-canopy reflectance model using the LUT approach

This chapter is based on

Omari, K., Staenz, K., King, D.J., and White, H, P., (2009) "Retrieval of forest canopy parameters by inversion of the PROFLAIR leaf-canopy reflectance model using the LUT approach", Canadian Journal of Remote Sensing, (in review).

Abstract:

The potential of simulating broad leaf forest canopy spectral reflectance using a canopy-leaf PROFLAIR (PROSPECT + FLAIR) model was investigated in this study. The model was inverted with hyperspectral Hyperion data using a look up table (LUT) approach to retrieve canopy leaf area index (LAI), leaf chlorophyll content (C_{a+b}) and canopy integrated chlorophyll content (LAI x C_{a+b}). The LUT was populated by simulating the model in forward mode using a space of realization generated based on the specific distribution of the input parameters and based on *a priori* information from the field. The estimated variables were then compared to ground measurements collected in the field. The results showed the ability of the PROFLAIR model to realistically simulate canopy spectral reflectance. When compared to ground measurements, the model showed a satisfactory performance to retrieve canopy LAI with an RMSE of 0.47 and leaf chlorophyll content with an RMSE of 4.46 $\mu g/cm^2$. These are similar to accuracies of other well-known models.

5.1. Introduction

As hyperspectral technologies continue to develop towards operational Earth Observation missions, there exists significant interest in developing models which can extract quantitative estimation of canopy biophysical properties such as leaf area index (LAI), fraction of absorbed photosynthetically active radiation (fAPAR), albedo and canopy biochemical properties. These vegetation parameters are primary inputs to models of land surface processes (Sellers, 1985). The accuracy and precision of their estimation is critical to

successful quantification of the energy exchange between the atmosphere and terrestrial vegetation (Knyazikhin et al., 1998). Fortunately, the increased availability of a variety of remote sensing satellite data types contributes effectively in deriving such parameters on a regular basis. Moreover, the spatial, spectral and directional dimensions of such data help in improving the accuracy of the estimated variables.

The goal of this study is to evaluate the potential of the leaf-canopy model PROFLAIR, which includes the leaf model PROSPECT (Jacquemoud and Baret, 1990) and the Four-Scale Linear Model for AnIsotropic Reflectance model (FLAIR) (Omari et al., 2008a; White et al., 2001) for the interpretation of hyperspectral data and the estimation of surface biophysical and biochemical properties. The following questions are addressed:

- Can the coupled model PROFLAIR reproduce realistically measured canopy spectra using a set of input parameters measured in the field?
- How well does the PROFLAIR model perform in retrieving biophysical and biochemical characteristics of broad leaf forest canopies using the LUT inversion approach?

PROFLAIR was tested using Hyperion data acquired over a forested area in the vicinity of a heavy metal acid tailings site. The LUT inversion approach was then used to retrieve LAI and canopy chlorophyll content. The extracted parameters were evaluated against in-situ measurements acquired in the field. Assuming a reasonable performance of the modelling approach, PROFLAIR was used to verify the hypothesis that there is a gradient in canopy

structural and chemical damage in the study site related to its adjacency to the abandoned mine tailings site. Section 5.3 describes the adopted inversion approach and discusses the results of leaf chlorophyll content, canopy integrated chlorophyll content and LAI retrievals.

5.2. Data sets and methods

5.2.1. Data sets

(See Field and remote sensing data acquisition section in Chapter 4)

5.2.2. PROFLAIR model: forward mode

In this study, the combined leaf-canopy model PROFLAIR is used to derive chlorophyll content at the canopy level from hyperspectral data. PROSPECT is one of the most common leaf radiative transfer models used to investigate the effects of leaf biochemical and structural properties on leaf hemispherical reflectance and transmittance spectra (Jacquemoud and Baret, 1990). It has been validated frequently and shown to achieve good accuracy in the VNIR and SWIR wavelengths (400 - 2500 nm). The output spectrum is a function of four input parameters: leaf chlorophyll content (C_{a+b}), leaf water content (Cw), dry matter content (Cm), leaf carotenoid content (Car) and the structure parameter (N) representing leaf anatomy. An improved (1nm resolution) and recalibrated version of PROSPECT was combined with various canopy models in numerous studies to extract canopy and leaf biophysical and biochemical properties (Jacquemoud et al., 2000). FLAIR was initially intended to describe the angular behaviour of canopy reflectance (Omari et al., 2008a; White

et al., 2001). It uses the physical description of canopy structure previously reported in the Four-Scale model (Chen and Leblanc, 1997). To fully exploit all spectral information from hyperspectral data, a multiple scattering scheme was introduced recently into the FLAIR model (Omari et al., 2009a and b). This scheme is based on the decomposition of the multiple scattering radiation field into two parts. The first part deals with multiple scattering within the canopy considering a black background and the second part deals with multiple scattering between the canopy and the background. The bidirectional behaviour of the new model has been tested against multi-angular airborne data (Omari et al., 2009a) acquired during the BOReal Ecosystem-Atmosphere Study (BOREAS) campaign of 1994 (Sellers et al., 1995). Figure 5.1 is a schematic representation of the coupled model. As it can be seen, leaf spectral properties generated by PROSPECT using a set of leaf biochemical constituents are used, in part, as FLAIR input parameters to generate canopy spectral reflectance. Figure 5.2 shows the effects of leaf biochemical constituents on the canopy spectral reflectance simulated with the PROFLAIR model. From this figure, the effect of each constituent is observable in specific wavelength ranges. For example, in Figure 5.2a, reflectance in the wavelength range between 500-720 nm responds to pigments in foliage and is lower for healthier leaves and higher for stressed ones. Moreover, the wavelengths at 550 nm and between 700 to 710 nm are the most adequate for foliage pigment monitoring (Gitelson et al., 2003). These simulations may also help to pinpoint appropriate wavelengths for retrieval of other canopy parameters when inverting the model as described in section 5.2.3.

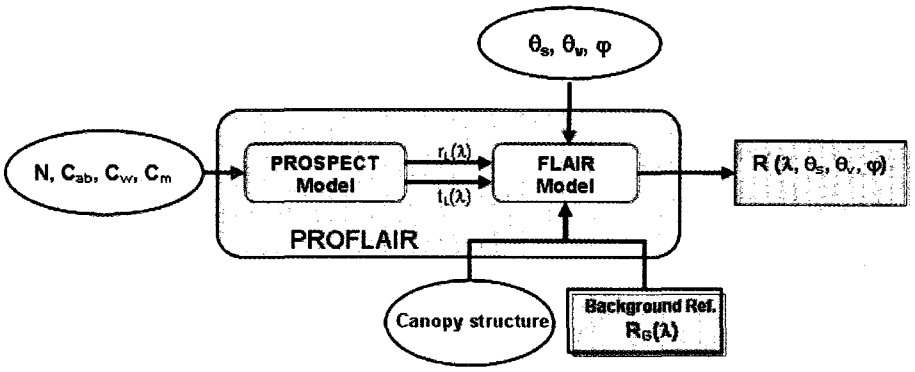

Figure 5.1: Outline of the PROFLAIR model.

The validation of PROFLAIR in forward mode was performed by running the model on a set of chlorophyll, water content, ground background spectral reflectance, structural canopy parameters, and illumination/view geometry data collected in the field. The derived spectral canopy bidirectional reflectance factors (BRFs) were then compared to Hyperion data acquired over the study site. To evaluate the performance of the coupled model, a set of data collected in the field was used. Figure 5.3 presents the simulated spectral canopy reflectance produced with the PROFLAIR model and the corresponding Hyperion data. In this figure, the Hyperion spectral reflectance is an average of 3-by-3 pixels (~90 m by 90 m) to reduce any uncertainties caused when image registration is performed. Also, a 3-by-3 average smoothing window was applied to Hyperion spectra to reduce residual radiometric noise. On the other hand, as previously mentioned, the collected ground measurement data were an average of 16 samples collected in a 60 m by 60 m area. This figure shows generally a good agreement between simulated and measured canopy spectral reflectances over the range of

500-1300 nm. It also demonstrates the benefit of incorporating the multiple scattering scheme of Omari et al. (2009a and b) for this spectral region (comparison between the PROFLAIR with and without the incorporation of multiple scattering component). The contribution of the multiple scattering component can exceed 50% of the total reflected radiation in the near infrared region. Figure 5.3 also shows that estimated canopy-level reflectance is lower than the mean reflectance of plot leaf samples and the background reflectivity. This is expected as canopy-level reflectance includes shadows as well as vegetation.

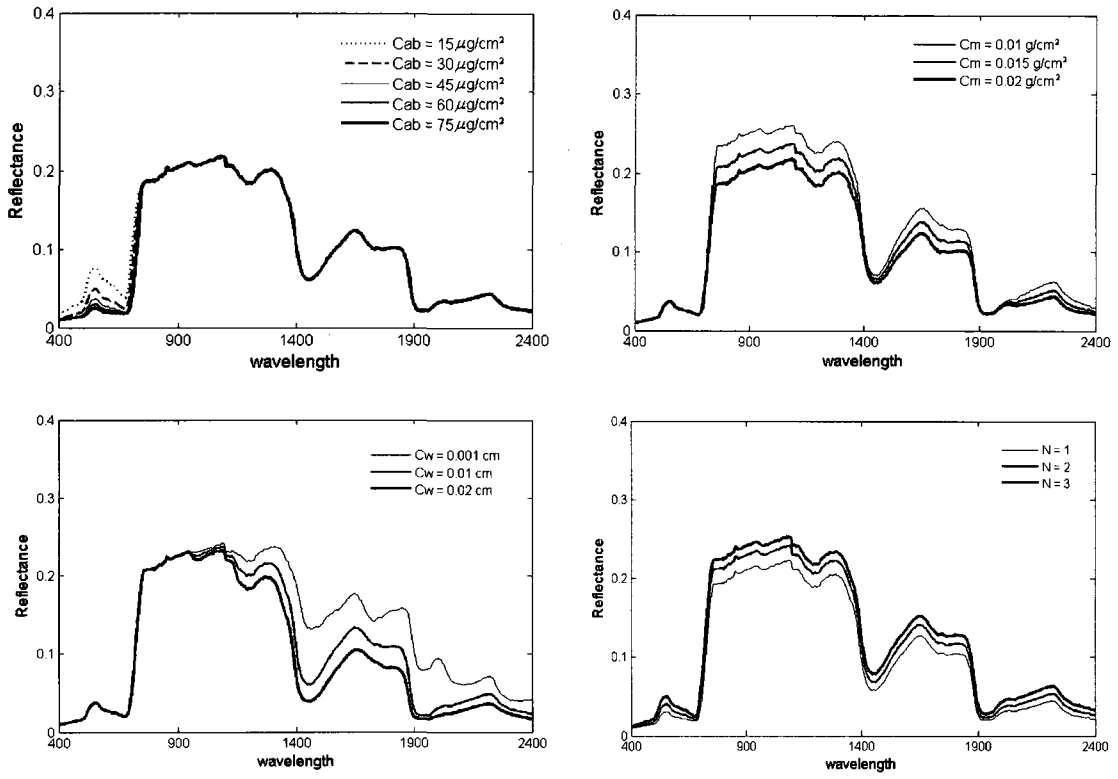

Figure 5.2: Effects of leaf biochemical properties on canopy spectral reflectance simulated by the PROFLAIR model: (a) chlorophyll content (C_{a+b}) using C_w = 0.01 *cm*, N = 1.75 and C_m = 0.01 *g/cm²*, (b) dry matter (C_m) using C_{a+b}= 45 *μm/cm²*, C_w = 0.01 *cm* and N = 1.75, (c) equivalent water thickness (C_w) using C_{a+b}= 45 *μm*/cm², C_m = 0.01 *g/cm²* and N = 1.75 and (d) leaf structure (N) using C_{a+b}= 45 *μm*/cm², C_m = 0.01 *g/cm²* and C_w = 0.01 *cm*. In all simulations LAI is set to 3 and view, illumination and phase angles are set to 5°, 40° and 0°, respectively.

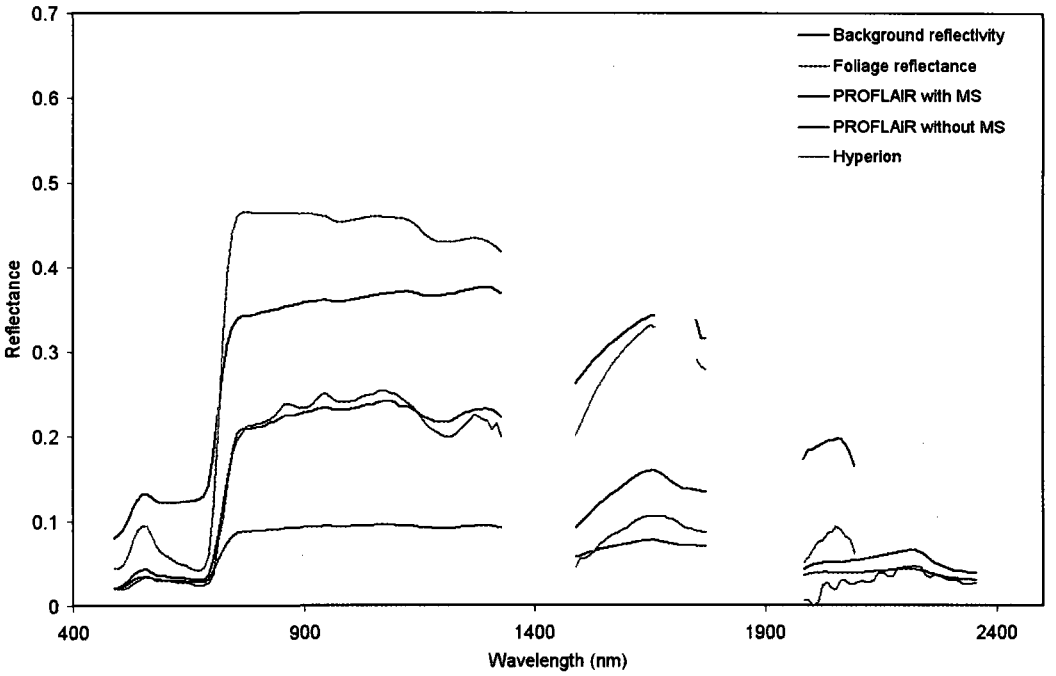

Figure 5.3: Example of simultated spectra generated using the PROFLAIR model with (with MS) and without (without MS) incorporating the multiple scattering scheme compared to Hyperion data. Background reflectivity was measured as a composite of 40% of black soil reflectance and 60% mean understorey reflectance. The foliage reflectance is considered as the mean of leaf sample reflectance of the same plot.

5.2.3. Inversion strategy

The LUT was generated by simulating the top of canopy (TOC) reflectance using the view/illumination geometry of the Hyperion acquisition from a wide range of PROFLAIR input parameters using the protocol of Figure 5.4. Some prior information on the range of variation of all the canopy variables and the type of soil is incorporated in order to obtain reliable and stable solutions (Combal et al., 2002).

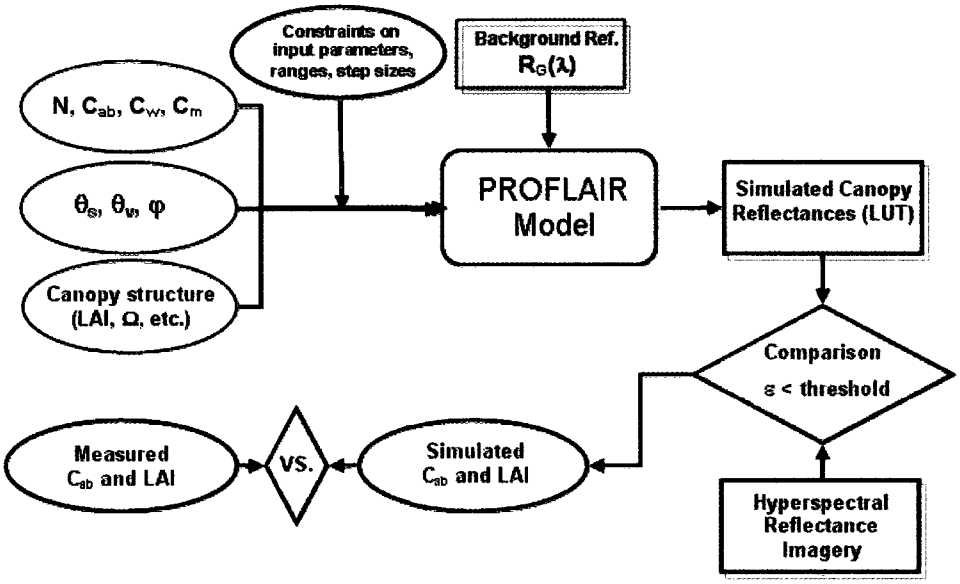

Figure 5.4: Flow-chart representing the inversion strategy.

In a first step, sampling the space of canopy realization was achieved by generating each model input parameter within a specific range with the assumption that these variables follow

normal distributions (Table 5.1). A software routine was designed and used to draw each variable values by providing its mean and standard deviation and the desired number of samples with the normal distribution assumption. Visual inspection of measurement data allowed estimation of the probable mean and range (based on the standard deviation) of chlorophyll content and LAI. These two parameters are the focus of this study since they are key variables to assess the physiological health of vegetation (Carter, 1994). The other input parameters were generated based on previous studies. The PROFLAIR model was then used to generate the corresponding reflectance and transmittance LUT. The generated 1-nm PROSPECT leaf reflectances and transmittances were convolved to the Hyperion spectral characteristics assuming that the Spectral Response Function (SRF) of Hyperion follows a Gaussian distribution. Previous studies highlighted the effect of the background spectral properties on biophysical parameter retrieval (e.g., Meroni et al., 2004). A proper background spectral reflectance measured in the field will enhance the retrieval. Moreover, it is difficult to know the exact spectral contribution of the background within each pixel when mapping these parameters. Meroni et al. (2004) suggest that the accuracy of the retrieval is not dramatically compromised if standard background spectra are used in the inversion process. To limit the impact of the background on retrieval, three understorey vegetation samples that occur most frequently in each plot were collected, and the reflectance of these samples was averaged. The background reflectance was generated by combining a standard black soil reflectance ($R_{blacksoil}(\lambda)$) and the average of the vegetation understorey reflectance ($R_{veg}(\lambda)$). The selection of the type of bare soil was based on observation of the most typical one of the forest area under investigation,. The fraction of each component is considered by measuring the understorey f-cover (f_{under_cover}) from digital hemispherical photos taken in downward

direction. Therefore, the background reflectance can be expressed as follows (Bacour et al., 2006):

$$R_g(\lambda) = f_{under\_cover} \times R_{veg}(\lambda) + (1 - f_{under\_cover}) \times R_{blacksoil}(\lambda). \quad (1)$$

The illumination and view angles were derived from Hyperion acquisition characteristics as well as the date, time and location of the image acquisition. Only selected spectral bands were used according to Weiss et al., (2000). In the case of Hyperion, optimal spectral sampling is crucial to biophysical and biochemical parameter estimation. Using the complete Hyperion spectrum increases the noise and decreases retrieval performance. An approach similar to Weiss et al. (2000) was followed by testing different band combinations with the root mean square error (RMSE) computed as the distance between measured and estimated canopy integrated chlorophyll content ($LAI*C_{a+b}$). The best combination corresponding to the minimum RMSE included bands, which are centered at 498.87, 630.32, 691.37, 711.72, 793.13, 844.00, and 915.23nm. The inversion approach is then a process of finding the "closest" simulated reflectance to the measured ones. In this case, the corresponding set of input variables represents the solution of the problem. The cost function, χ, can be written as follows (Weiss et al., 2000):

$$\chi = \sqrt{\frac{1}{n_b} \sum_{i=1}^{nb} \left(\frac{\rho_i^{mes} - \rho_i^{LUT}}{\rho_i^{mes}} \right)^2}, \quad (2)$$

where ρ_i^{mes} and ρ_i^{LUT} are the canopy reflectances acquired by Hyperion and simulated using PROFLAIR (found in the LUT), respectively. The cost function is weighted by the number

of selected wavelengths (n_b). The possible solutions considered were those corresponding to the median of the 10 lowest χ (as suggested in Combal et al., 2002). It was found that using a second cost function to remove small perturbations in the data as suggested by Combal et al. (2002) was not necessary. In Combal et al. (2002), a second cost function that include additional constraints on the χ based on radiometric and priori information about each parameter to be retrieved is suggested. Instead, this information was used to optimize the LUT size in this study.

Table 5.1: Distribution of the PROFLAIR input variables used to simulate the space canopy realization used to populate the look up table (LUT). Here, it is assumed that input parameters follow normal distributions. Mean and standard deviation values are based on priori information extracted from measurements. The parameters are leaf area index (LAI), leaf chlorophyll content (C_{a+b}), leaf water content (C_w), dry matter (C_m), leaf carotenoids (Car) and the leaf structural parameter (N)

Parameters	Mean	Standard deviation	Number of samples
LAI	2.5	1.5	20
$C_{a+b}(\mu g/cm^2)$	45	15	20
$Car(\mu g/cm^2)$	5	4.5	5
$C_m\ (g/cm^2)$	0.015	0.005	10
$C_w(g/cm^2)$	0.008	0.007	10
N	1.75	0.5	5

5.3. Results and discussion

Comparison between leaf chlorophyll content measured in the field and chlorophyll content estimated from the model is presented in Figure 5.5. The horizontal errors bars represent +/- one standard deviation for measured chlorophyll of all samples and the vertical bars represent the confidence range of 10%. The selection of this value was based on the agreement to the standard deviation of measurements. The results show that the LUT enables retrieval of chlorophyll content with an RMSE of 4.46$\mu g/cm^2$ for the ten plots. This figure also shows that there is no trend in under or overestimation of chlorophyll as most of the points are approximately equally distributed above and under the 1:1 line. A linear regression represented by a dashed line yielded a poor coefficient of determination of $R^2 = 0.25$. These results might become worse if the plot represented with measured $C_{a+b} = 39$ $\mu g/cm^2$ is considered as an outlier. Pigment estimate uncertainties can be caused in part by the heterogeneity within the site. As mentioned previously, the sampled trees were limited to trembling aspen. This species is dominant in the study site with 50 to 80% of the cover. Other species including poplar and jack pine trees were not sampled and the understorey is composed mostly of alder (*Alnus*), raspberry (*Rubus*) and jack pine trees 2 to 5 m in height. The degree of heterogeneity changes between plots as in most natural boreal forests. The impact of plot heterogeneity increases when taking into account that the estimated chlorophyll is an average over 90 m by 90 m compared to the sampled plot of 60 m by 60 m. Other sources of uncertainties include errors propagated during the pre-processing steps of Hyperion data. The sampling scheme may also contribute to these estimate uncertainties. As

an example, a high standard deviation in chlorophyll measurement is shown within each plot and even between samples taken from the same tree. The temporal shift of 9 days between the date of acquisition of the Hyperion data and the date of field measurements has a small effect since both dates were during the peak LAI period several weeks before senescence. It also has been reported that inverting PROSPECT to retrieve the biochemical parameters with good accuracy is not always achievable (Le Maire et al., 2004).

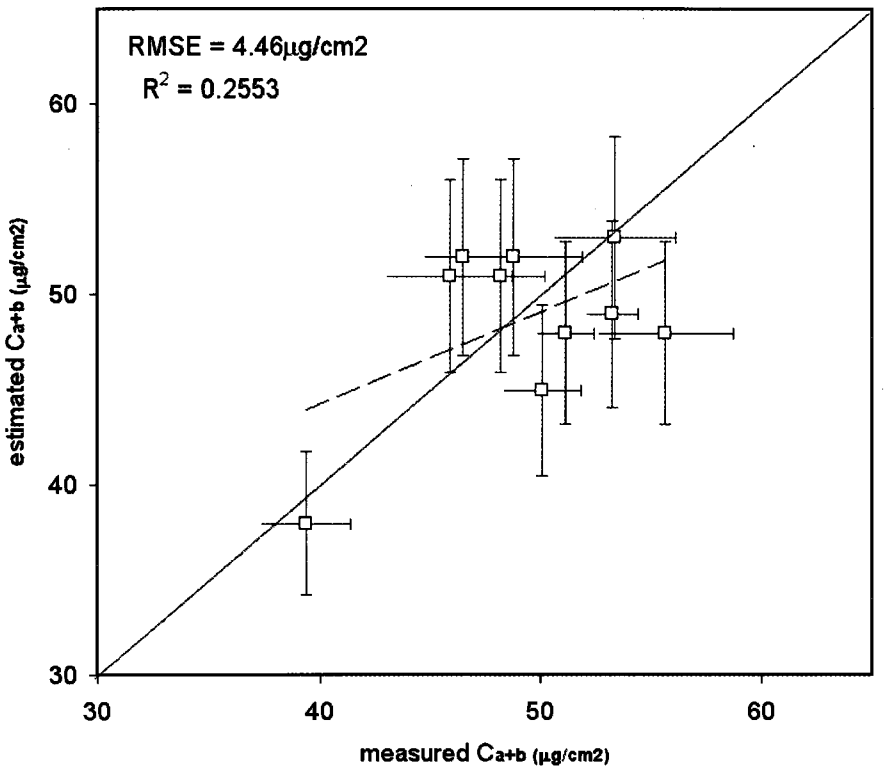

Figure 5.5: Comparison between measured and estimated chlorophyll content (C_{a+b}). Each measured value is an average of 16 samples taken from the top of the trees in a 60 by 60 m^2 plot. The estimated values are the output of inverting the PROFLAIR model using Hyperion data. Each Hyperion spectrum is an average of 3 by 3 pixels.

To evaluate the performance of LAI retrieval, modelled LAI values were compared to those measured in the field as illustrated in Figure 5.6. This Figure shows a satisfactory agreement, with an RMSE of 0.47 and an $R^2 = 0.58$. Figure 5.6 also shows a slight overestimation of LAI values. The uncertainties may be explained by the underestimation of LAI because of foliage clumping and/or the possibility that the model is taking the understorey into account as well. Field measurements, such as acquiring and processing digital hemispherical photos, may also have contributed to these errors, even though comprehensive procedures to optimize acquiring and processing the data were followed. Canopy integrated chlorophyll content can be estimated as $LAI*C_{a+b}$. Figure 5.7 illustrates the comparison between measured and simulated canopy integrated chlorophyll content showing an RMSE of 24.44 $\mu g/cm^2$ and an R^2 of 0.60. In general, these results show the potential of using the PROFLAIR model in estimating broad leaf forest canopy biophysical and biochemical characteristics. The accuracies of the chlorophyll and LAI estimates fall within the validation range of other physically based models tested on broadband multispectral and hyperspectral data (Bacour et al., 2006; Koetz et al., 2005; Meroni et al., 2004; Zarco-Tejada et al., 2001).

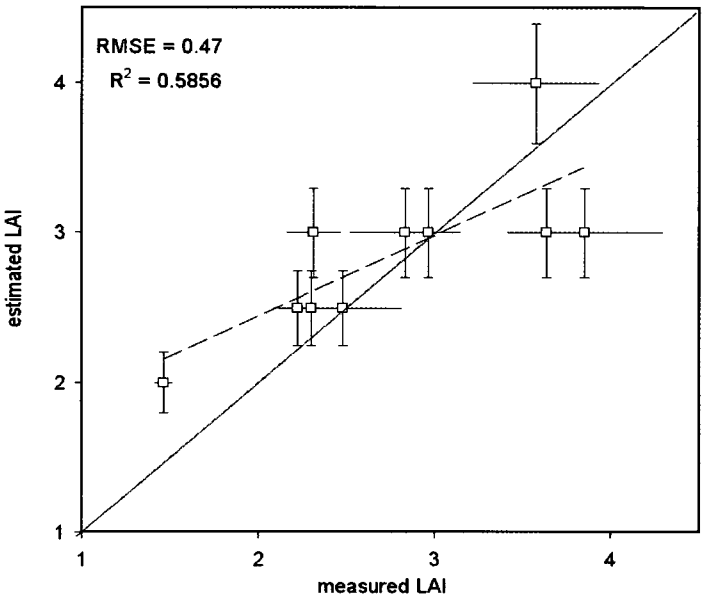

Figure 5.6: Comparison between measured and estimated leaf area index (LAI). Each measured value was extracted from digital hemispherical photos of a 60 by 60 m^2 plot. The estimated values are the output of inverting the PROFLAIR model using Hyperion data. Each Hyperion spectrum is an average of 3 by 3 pixels.

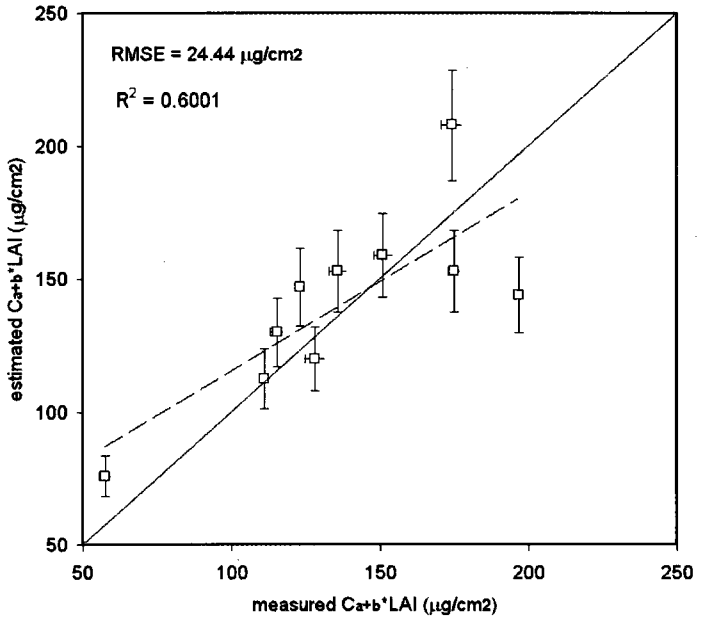

Figure 5.7: Comparison between measured and estimated canopy integrated chlorophyll content ($LAI*C_{a+b}$) by inverting PROFLAIR with the LUT approach.

The ten plots (Figure 4.3) were established along a transect within the forest with an increasing distance from the tailings and following the drainage direction (Levesque and King, 2003). Figure 5.8 is an attempt to sense a potential gradient of damage along the transect by estimating the canopy integrated chlorophyll content in the field plots. This Figure shows a slight increase of canopy integrated chlorophyll as distance from the tailings increases. The lack of change of leaf chlorophyll content along the transect suggest that the trend shown in Figure 5.8 is mainly due to a structural change (LAI) and that the leaf chlorophyll content information contributed very little to this trend. The leaf chlorophyll results suggest generally that the physiological status of the plots varied from healthy to very healthy. This confirms previous results in the same site using high spatial resolution multispectral imagery (Levesque and King, 1998 and 2003; Cosmopoulos and King, 2004), suggesting that the damage is structural rather than physiological. Their finding implies that the leaf reflectance varied too much within and between crowns to see a subtle gradient. They also found that aspen trees are resistant to metal and pH stress, even though the soil analyses showed low pH and high concentration of Al, Mg and Mn. This is confirmed with the result of the leaf chlorophyll analysis, which indicates that the aspen trees in this site vary from a healthy to a very healthy range. Most of these studies demonstrated that within and between crown shadows and texture can provide valuable indications of the stress at this site. High stress means more open canopy near the tailings, and the forest floor becomes covered with understory vegetation such as alders and raspberry. These produce a reflectance signal that mixes heavily with the overstorey and falsely gives the impression in quantitative analysis that the forest is healthier than in reality.

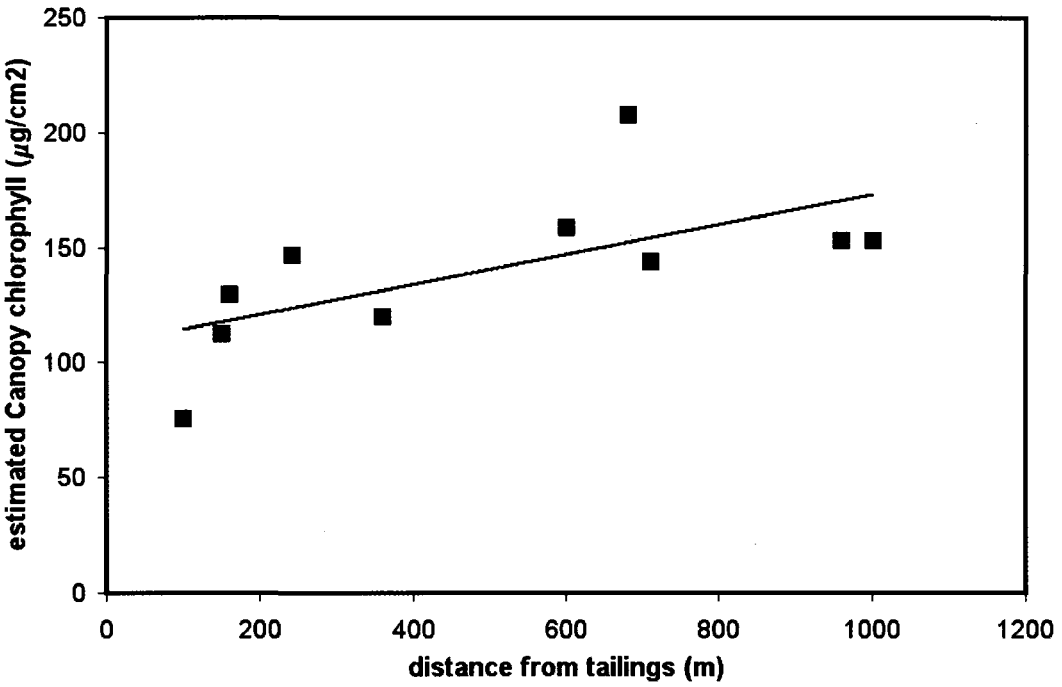

Figure 5.8: Estimated canopy integrated chlorophyll versus the distance from the tailings content alongside the defined transect.

5.4. Conclusion

In this study, the potential of the PROFLAIR model was investigated to retrieve biochemical and biophysical characteristics of broadleaf forest canopy from hyperspectral Hyperion imagery. This linked model showed its ability to simulate realistic forest canopy spectra if properly parameterized. The simulated spectra by the PROFLAIR model were quite comparable to those extracted from Hyperion in the VNIR and portions of the SWIR regions. The look up table (LUT) approach was employed to invert the model; it was found that this approach is flexible and easy to implement. The LUT was populated by running the model

for a space of canopy realization generated by randomly involving each input model variable. Some *a priori* information about the data and the canopy structure were used to optimize the size of the LUT, and a cost function was used to retrieve leaf area index (LAI) and chlorophyll content (C_{a+b}). The canopy integrated chlorophyll content was then deduced for selected wavelengths. The results showed a satisfactory agreement between estimated and measured LAI with a RMSE of 0.47 and a R^2 of 0.58. This is an acceptable agreement when compared to other model performances. The results also indicate a RMSE of 4.46 $\mu g/cm^2$ and a R^2 of 0.25 between estimated and measured chlorophyll content. These uncertainties may be due to the model used in the estimates, the hyperspectral image processing, the uncertainties associated with the field data, or a combination all these error sources. In spite of that, further improvement of the PROFLAIR model, such as enhancing the hot spot function and the anisotropy of the background, is needed. An effort has also to be made in improving field data collection, particularly the design of the sampling scheme, number of plots and number of sampled trees per plot. In addition, enhancing the performance of hyperspectral sensor data is critical to produce high quality data for better retrievals. The growing interest placed in developing hyperspectral technologies and initiating hyperspectral missions in several organizations will make high quality and fully exploitable data available in the future. This will certainly enhance the quantitative estimation of vegetation biochemistry and biophysics.

Acknowledgements:

The authors gratefully acknowledge the support of the Canada Centre for Remote Sensing / Natural Resources Canada for the infrastructure access and the University of Ottawa for financial support. We would also like to thank Richard Fernandes, Marie Weiss and Nadia

Rochdi for their productive discussions and contributions, and the anonymous reviewers for their constructive comments and assistance in editing resulting in completion of this paper.

References:

Bacour, C., Baret, F., Béal, D., Weiss, M., and Pavageau, K., "Neural network estimation of LAI, fAPAR, fCover and LAI×C_{ab}, from top of canopy MERIS reflectance data: Principles and validation", Remote Sensing of Environment, 105: 313-325, 2006.

Baret, F., Clevers, J., and Steven, M., "The robustness of canopy gap fraction estimates from red and near infrared reflectances: a comparison of approaches", Remote Sensing of Environment, 54, 141– 151, 1995.

Carter, G. A., "Ratios of leaf reflectances in narrow wavebands as indicators of plant stress", International Journal of Remote Sensing, 15: 697-703, 1994.

Combal, B., Baret, F., Weiss, M., Trubuil, A., Macé D., Pragnère A., Myneni, R., Knyazikhin, Y., and Wang, L., "Retrieval of canopy biophysical variables from bidirectional reflectance using prior information to solve the ill-posed inverse problem", Remote Sensing of Environment, 84: 1-15, 2002.

Cosmopoulos, P., and King, D.J., "Temporal analysis of forest structural condition at an acid mine site using multispectral digital camera imagery", International Journal of Remote Sensing, 25: 2259-2275, 2004.

Gitelson, A. A., Gritz, U., Merzlyak, M. N., "Relationships between leaf chlorophyll content and spectral reflectance and algorithms for non-destructive chlorophyll assessment in higher plant leaves", Journal of Plant Physiology, 160: 271-282, 2003.

Hitchcock, R., White, H. P., "Processing EO-1 Hyperion data using ISDAS", Canada Centre for Remote Sensing, Technical Note 2, 30 pages, 2007.

Jacquemoud, S., Bacour, C., Poilve, H., and Frangi, J. P., "Comparison of four radiative transfer models to simulate plant canopies reflectance direct and inverse mode", Remote Sensing of Environment, 74: 471–481, 2000.

Jacquemoud, S., F. and Baret, F., "PROSPECT: A model of leaf optical properties spectra", Remote Sensing of Environment, 34: 75–91, 1990.

Knyazikhin, Y., Martonchik, J. V., Myneni, R. B., Diner, D. J., and Running, S.W., "Synergistic algorithm for estimating vegetation canopy leaf area index and fraction of absorbed photosynthetically active radiation from MODIS and MISR data", Journal of Geophysical Research, 103: 32257-32276, 1998.

Koetz, B., Baret, F., Poilvé, H., and Hill, J., "Use of coupled canopy structure dynamic and radiative transfer models to estimate biophysical canopy characteristics", Remote Sensing of Environment, 95: 115-124, 2005.

Khurshid, S., Staenz, K., Sun, L., Neville, R.A., White, H. P., Bannari, A., Champagne, C.M., and Hitchcock, R., "Preprocessing of EO-1 Hyperion Data", Canadian Journal of Remote Sensing, 32: 84-97, 2006.

Le Maire, G., Francois, C., and Dufrene, E., "Towards universal broad leaf chlorophyll indices using PROSPECT simulated database and Hyperspectral reflectance measurements", Remote Sensing of Environment, 89: 1-28, 2004.

Lévesque, J., and King, D.J., "Spatial analysis of radiometric fractions from high-resolution multispectral imagery for modeling individual tree crown and forest canopy structure and health", Remote Sensing of Environment, 84: 589-602, 2003.

Lévesque, J., and King, D. J., "Airborne digital camera image semivariance for evaluation of forest structural damage at an acid mine site", Remote Sensing of Environment, 68, 112– 124, 1999.

Meroni, M., Colombo R., and Panigada, C., "Inversion of a radiative transfer model with hyperspectral observations for LAI mapping in poplar plantations", Remote Sensing of Environment, 92: 195-206, 2004.

Neville, R.A., Sun, L., and Staenz, K., "Spectral Calibration of Imaging Spectrometers by Atmosphere Absorption Matching", Canadian Journal of Remote Sensing, 34, Suppl. 1: S29-S42, 2008.

Omari, K., White, H. P., and Staenz, K., "An enhanced description of multiple scattering within the FLAIR model using the photon re-collision probability approach", IEEE Transactions on Geoscience and Remote Sensing, in press, 2009.

Omari, K., Fernandes, R., Staenz, K., Rochdi, N., and Chelle, M., "A simple parameterization of the angular distribution of the multiple scattered radiation", Remote Sensing of Environment, in review, 2009b.

Sellers, P., Hall, F., Margolis, H., Kelly, B., Baldocchi, D., Hartogden, G., Cihlar, J., Ryan, M.G., Goodison, B., Crill, P., Ranson, K.J., Lettenmaier, D., and Wickland, D.E., "The Boreal Ecosystem-Atmosphere Study (BOREAS): An overview and early results from the 1994 field year", Bulletin of American Meteorological Society, 76(9): 1549-1577, 1995.

Sellers, P.J., "Canopy reflectance, photosynthesis and transpiration", International Journal of Remote Sensing, 6: 1335-1372, 1985.

Staenz, K., Szeredi, T., and Schwarz, J., "ISDAS-A system for processing/analyzing hyperspectral data", Canadian Journal of Remote Sensing, 42: 99-113, 1998.

Staenz, K., and Williams, D., "Retrieval of surface reflectance from hyperspectral data using a look-up table approach", Canadian Journal of Remote Sensing, 23(4): 354-368, 1997.

Sun, L., Neville, R.A., Staenz, K., and White, H.P., "Automatic Destriping of Hyperion Imagery Based on Spectral Moment Matching", Canadian Journal of Remote Sensing, 34(Supplement 1): S68-S81, 2008

Weiss, M., "EYE-CAN User Guide", NOV-3075-NT-1260, NOVELTIS, Toulouse, France, 2002.

Weiss, M., Baret, F., Myneni, R. B., Pragnere, A., and Knyazikhin, Y., "Investigation of a model inversion technique to estimate canopy biophysical variables from spectral and directional reflectance data", Agronomie, 20: 3-22, 2000.

Weiss, M., and Baret, F., "Evaluation of canopy biophysical variable retrieval performances from the accumulation of large swath satellite data", Remote Sensing of Environment, 70: 293−306, 1999.

White, H.P., Dickinson, H., Trebble, A., Alfoÿdi, T., " Presenting a Web Based Evaluation Tool to Interactively Explore the Relationship Between Observed Bi-directional Reflectance and Canopy Characteristics", Proceedings of the 26th Canadian Symposium of Remote Sensing, pp. 451-455, 14-17 June 2005, Wolfville, Nova Scotia.

White, H.P., Sun, L., Staenz. K., Fernandes, R., and Champagne, C.M., "Determining the contribution of shaded elements of a canopy to remotely sensed hyperspectral signatures", Proceedings of the 1st International Symposium on Recent Advances in Quantitative Remote Sensing, Valencia, Spain, 159-166, 2002a.

White, H.P., Miller, J.R., and Chen, J.M., "Four-scale linear model for anisotropic reflectance (FLAIR) for plant canopies. I: Model description and partial validation", IEEE Transactions on Geoscience and Remote Sensing, 39(5): 1072-1083, 2001.

Zarco-Tejada, P.J., Miller, J.R., Noland, T.L., Mohammed, G.H., and Sampson, P.H., "Scaling-up and model inversion methods with narrowband optical indices for chlorophyll content estimation in closed forest canopies with hyperspectral data", IEEE Transactions on Geoscience and Remote Sensing, 39(7): 1491–1506, 2001.

Chapter 6

Conclusions, Recommendations and Outlook

6.1. Conclusions

The inversion of physically based models are the next step in providing quantitative capabilities to directly extract biophysical and biochemical variables of vegetation canopies from remote sensing data. Such variables are key parameters for revealing vegetation condition and tracking its phenological development. The advantage of using the physically based approaches is their ability to offer synthesized physical and chemical information governing the interactions between the electromagnetic radiation and vegetation canopy elements. In previous studies, the FLAIR model has demonstrated its limitations when characterizing the bidirectional reflectance behaviour of canopies, particularly when applied to hyperspectral applications and model inversion. The major weakness of this model is its lack of ability to quantify the angular and spectral distribution of its multiple scattering component. In fact, the previous version of this model requires a database of wavelength-specific multiple scattering factors to characterize this component. In this thesis, the four hypotheses made in the introduction were tested.

The first step of the thesis was dedicated to test the first hypothesis. The focus was on the development of a simple and effective approximation of the reflectance factor of multiple scattering using radiative transfer theory. The presented scheme, which assumes that the background is a completely absorbing medium, is based essentially on combining the following two aspects:

- The contribution of multiple scattered radiation to the bi-hemispherical reflectance using the p theory where the spectral properties of canopy elements and canopy spectral invariants related to the re-collision probability (p) are taken into account; and
- A simple and effective approximation of the phase function for multiple scattering based on few structural and viewing geometry variables.

The proposed scheme was tested against synthetic data generated with the PARCINOPY Monte Carlo model and against RAMI On-line Checker reference data sets (ROMC) in the red and near-infrared spectral regions. In general, the results demonstrated the potential of this approach to approximate the reference data in simulated homogenous canopies. In particular, the results showed that the model's performance is best in both the solar principal and perpendicular planes at low and mid LAI levels for all solar zenith angles. Accordingly, the first hypothesis is true. The comparison to the On-line Checker data sets shows also that the model is a suitable approach to describe the multiple scattering components of physically based models. The results show that the absolute differences are within 1% in both principal and perpendicular planes in the near-infrared band. In the red band, however, there is a significant underestimation of multiple scattering reflectances by the model when the view angle is approaching nadir view. This discrepancy can be explained by the effect of the soil brightness as the ROMC considers a relatively bright ground underneath the canopy compared to the completely absorbing ground considered in the proposed model.

In the second step, which was intended to verify the second hypothesis, a combined approach based on the adding method was incorporated into the FLAIR model to describe the distribution of spectral and angular distribution of the multiple scattered radiation field of a forest canopy. The proposed scheme is based on the decomposition of the multiple scattering radiation field into two parts. The first part deals with multiple scattering within the canopy using the approach developed in the first step of the thesis. The second part deals with multiple scattering between the canopy and the background. The performance of the new version of the FLAIR model was compared simultaneously to the previous version of FLAIR and to the multi-angular data sets acquired by the airborne POLDER during the BOREAS campaign of 1994. The results indicate a relative enhancement of the FLAIR model. Indeed, the new version of FLAIR simulates closely the BRFs produced by the original version that uses a constant multiple scattering, derived previously by fitting the model to the top of canopy airborne POLDER and PARABOLA measurements in the red and near-infrared regions. The R^2 and RMSE values showed slight differences between the two versions in comparison to the airborne POLDER reflectance data. Thus, this multiple scattering approach is well suited to the FLAIR model, particularly as applied to hyperspectral data. Therefore, the second hypothesis was confirmed. It also demonstrated that the multiple scattering problem can be parameterized by the optical properties of the canopy elements and a limited number of structural parameters. Such advances to radiative transfer modelling are required to better exploit the potential of hyperspectral data for monitoring canopy biochemical indicators, such as chlorophyll and equivalent water content.

The next step was set to verify the third and fourth hypotheses. The main objective was to explore an effective tool for extracting vegetation biochemical and biophysical information from hyperspectral data using radiative transfer theory and inverse modelling techniques. The FLAIR model with the enhancements made in the first two steps of the thesis was linked to the PROSPECT leaf model. The objectives of coupling the two models was to simulate broadleaf forest canopy spectral reflectance using canopy biophysical parameters and leaf biochemical properties and then investigate the retrieval of canopy biophysical and biochemistry variables from hyperspectral data using the look-up-table (LUT) inversion technique. To fulfill theses objectives, a field campaign was conducted in August 2005 over a forest area near the Kamkotia mine site in Timmins, Ontario. Foliage samples were collected for laboratory spectral measurements and extraction of chlorophyll content and hemispherical photographs were collected to retrieve LAI. The sampled leaves were harvested from sample trees within each of the ten preselected plots. The information obtained from field data was used to test the PROFLAIR model. The results showed that the proposed model was able to simulate realistic forest canopy spectra. The PROFLAIR simulated spectra were quite comparable to those extracted from Hyperion data in the VNIR and portions of the SWIR regions. Accordingly, the third hypothesis was validated. Following that, the model was inverted with Hyperion data using a LUT approach to retrieve canopy leaf area index (LAI), leaf chlorophyll content (C_{a+b}) and canopy integrated chlorophyll content (LAI x C_{a+b}). The LUT was populated by simulating the model in forward mode using a space of realization generated based on the specific distribution of the input parameters and based on *a priori* information from the field. The estimated variables were then compared to the ground measurements. The results showed that the PROFLAIR

model can be used with a reasonable performance to retrieve canopy LAI with an RMSE of 0.47 and leaf chlorophyll content with an RMSE of 5.98 $\mu g/cm^2$. These are similar to accuracies achieved with other well-known models. Therefore, the fourth hypothesis is true.

Theses results were also used to assess the hypothesis that there is a gradient in canopy structural and chemical damage in the study site related to its adjacency to the abandoned mine tailings site. The outcome of this assessment confirmed previous study findings at the same site. Theses findings suggest that the occurring stress is mainly structural rather than physiological.

6.2. Recommendations

Throughout the proposed methodology and in light of the obtained results, further improvements are required. Thus, the following recommendations for future research are made:

- Modelling perspective: The presented approach to parameterize the angular distribution of multiple-scattered radiation still needs more research and development. In particular, the relative escape probability as a function of vegetation structure and illumination geometry needs to be improved. Further investigations are also needed to test the implemented approach using heterogeneous canopies and different soil conditions. Other areas in the PROFLAIR model which need further enhancements include the parameterization of the hot spot function and the

anisotropy of the background and the mathematical description of the sub-pixel variability of model input parameters (such as chlorophyll content).

- Data acquisition perspectives: As mentioned earlier, adequate ground reference data are necessary for using remote sensing techniques to produce accurate results. Improving field data collection, particularly the design of the sampling scheme, number of plots and number of sampled trees per plot are crucially needed. In addition, enhancing the pre-processing techniques of hyperspectral data is also critical for better retrievals. Hyperion was the first spaceborne sensor to acquire hyperspectral data. The advantages and limitations in the quality of these data are definitely a valuable insight for developing new generations of hyperspectral sensor systems. This will make high quality and fully exploitable data available.

6.3. Outlook

The enhancements to the PROFLAIR model, mentioned in the thesis recommendations, will improve the model to simulate realistically vegetation canopy spectra. However, these advancements will increase the complexity of the model by introducing new parameters to describe canopy architecture. Moreover, knowledge of prior distribution of these additional parameters will constitute a limitation. Therefore, model inversion will not necessarily yield better retrieval performances, since the model will require additional input parameters. In this case, linking some of the PROFLAIR input variables to other sources of remote sensing information, such as LiDAR, SAR and high spatial resolution data, should definitely improve model performance in providing more realistic range coverage of structural parameters for

particular vegetation canopies. Another perspective to enhance the retrieval of canopy variables is to take advantage of the spatial contextual information as observed in the imagery. This spatial structure such as inter-pixel surface characteristic dependency or inter-pixel correlation can be seen particularly at high spatial resolution. These patterns can be exploited to additionally constrain the retrieval of biophysical and biochemical parameters. The object-retrieval approach proposed by Atzberger (2004), which is based on the use of the covariance between canopy parameters as observed over a limited cluster of pixels representing the same class of object, may significantly enhance the model's retrieval performance. In addition, temporal constrains provided by the information about the dynamics of the canopies (e.g., crop growth models) over time will also improve the model's retrieval performance. One of the promising and flexible approaches is to couple the PROFLAIR with an atmospheric model (e.g., data assimilation). This would certainly enhance the retrieval accuracy of canopy biophysical and biochemical parameters. With all these improvements, the PROFLAIR model is better suited to be used in an operational environment. For this purpose, the model should be extensively validated on different forest canopy cover types. Moreover, with further improvements it can be adapted to other vegetation canopy types such as crops.

References

7. References:

Alpers, C. N., Blowes, D. W., Nordstorm, K. D., and Jambor, J. L., "Secondary minerals and acid mine-water chemistry", dans "Jambor, J. L. et Blowes, D. W. (Editors)" Short course handbook on environmental geochemistry of sulfide mine-wastes, Mineralogical Association of Canada, Nepean, ON, Canada, 22, pp. 247-270, 1994.

Asner, G.P., "Biophysical and biochemical sources of variability in canopy reflectance", Remote Sensing of Environment, 64: 234–253, 1998.

Asrar, G., "Theory and Applications of Optical Remote Sensing", Wiley Series in Remote Sensing, John Wiley and Sons Inc., 734 pages, 1989.

Atzberger, C., "Object-based retrieval of biophysical canopy variablesusing artificial neural nets and radiative transfer models", Remote Sensing of Environment, 93: 53-67, 2004.

Bacour, C., Baret, F., Béal, D., Weiss, M., and Pavageau, K., "Neural network estimation of LAI, fAPAR, fCover and LAI×C_{ab}, from top of canopy MERIS reflectance data: Principles and validation", Remote Sensing of Environment, 105(4), 313-325, 2006.

Baret, F., Clevers, J., and Steven, M., "The robustness of canopy gap fraction estimates from red and near infrared reflectances: a comparison of approaches", Remote Sensing of Environment, 54: 141-151, 1995.

Barrie, C.T. and Davis, D. W., "Timing and magmatism and deformation in the Kamiskotia-Kidd Creek area, western Abitibi Subprovince, Canada", Precarnbrian Research, 46(3): 217-240, 1990.

Berry, L. G., "Geology of the Robb-Jamieson area", dans le 53ème rapport annuel du département des mines de l'Ontario, Bowman, T.E., Toronto, ON, Canada, 53 (4):1-16, 1944.

Carter, G. A., "Ratios of leaf reflectances in narrow wavebands as indicators of plant stress", International Journal of Remote Sensing, 15: 697-703, 1994.

Chelle, M., and Andrieu, B., " PARCINOPY, un logiciel de simulation des échanges radiatifs dans les couverts végétaux par lance de rayons sur des maquettes informatiques tridimensionnelles", Rapport de recherches, INRA-bioclimatologie, 78850 Thiverval-Grignon, 1996.

Chen, J. M., Pavlic, G., Brown, L., Cihlar, J., Leblanc, S. G., White, H. P., Hall, R. J., Peddle, D. R., King, D. J., Trofymow, J. A., Swift, E., Van der Sanden, J., Pellikka, P. K. E., "Derivation and validation of Canada-wide coarse-resolution leaf area index maps using high-resolution satellite imagery and ground measurements", Remote Sensing of Environment, 80: 165–184, 2002.

Chen, J.M., and Leblanc, S. G., "Multiple-scattering scheme useful for geometric optical modeling", IEEE Transactions on Geoscience and Remote Sensing, 39(5): 1061-1071, 2001.

Chen, J.M., and Leblanc, S. G., "A Four-Scale bidirectional reflectance model based on canopy architecture", IEEE Transactions on Geoscience and Remote Sensing, 35(5): 1316–1337, 1997.

Chen, J. M., "Canopy architecture and remote sensing of the fraction of photosynthetically active radiation absorbed by boreal conifer forests", IEEE Transactions on Geoscience and Remote Sensing, 34(6): 1353-1368, 1996.

Chen, J. M. and Cihlar, J., "Retrieving leaf area index for boreal conifer forests using Landsat TM images", Remote Sensing of Environment, 55:153-162, 1996.

Combal, B., Baret, F., Weiss, M., Trubuil, A., Macé D., Pragnère A., Myneni, R., Knyazikhin, Y., and Wang, L., "Retrieval of canopy biophysical variables from bidirectional reflectance using prior information to solve the ill-posed inverse problem", Remote Sensing of Environment, 84: 1-15, 2002.

Coops, N.C., Smith, M.L., Martin, M.E., and Ollinger, S., "Prediction of Eucalypt Foliage Nitrogen Content From Satellite-Derived Hyperspectral Data", IEEE Transactions on Geoscience and Remote Sensing, 41(6): 1338-1346, 2003.

Cosmopoulos, P., and King, D.J., "Temporal analysis of forest structural condition at an acid mine site using multispectral digital camera imagery", International Journal of Remote Sensing, 25(12): 2259-2275, 2004.

Curran, P.J., Kupiec, J.A., and Smith, G.M., "Remote Sensing the Biochemical Composition of Slash Pine Canopy", IEEE Transactions on Geoscience and Remote Sensing, 35(2): 415-420, 1997.

Dawson, T.P. and Curran, P.J., "A new technique for interpolating red edge position", International Journal of Remote Sensing, 19(11): 2133-2139, 1998.

Dawson, T.P., Curran, P.J., and Plummer, S.E., "LIBERTY - Modelling the effects of leaf biochemical concentration on reflectance spectra", Remote Sensing of Environment, 65: 50-60, 1998.

Disney, M., Lewis, P., Quaife, T., and Nichol, C., "A spectral invariant approach to modeling canopy and leaf scattering", Proceeding of the 9th International Symposium on Physical Measurements and Signatures in Remote Sensing (ISPMSRS), 17–19 October 2005, Beijing, China, Part 1, pp. 318-320, 2005.

Disney, M.I., Saich, P., and Lewis, P., "Modelling the radiometric response of a dynamic, 3D structural model of Scots pine in the optical and microwave domains", Proceedings of the IEEE IGARSS'03 (Toulouse), Vol. 6, pp. 3537-3539, 2003.

Disney, M. I., Lewis, P., and North, P. R. J., "Monte Carlo ray tracing in optical canopy reflectance modeling", Remote Sensing Review, 18: 163-196, 2000.

Gagnon, J.Y., Bruce, B.D., and Crowder, N., "The use of remote sensing for describing and evaluating the regeneration potential of an abandoned mining waste site, Western Quebec, Canada", Proceedings of Symposium on Surface Mining, Hydrology, sedimentology and Reclamation, December 9- 1 3, (University of Kentucky Colleges of Engineering and of Agriculture, and Institute for Mining and Minerals Research) Lexington, Kentucky, pp. 273-277, 1985.

Gitelson, A. A., Gritz, U., and Merzlyak, M. N., "Relationships between leaf chlorophyll content and spectral reflectance and algorithms for non-destructive chlorophyll assessment in higher plant leaves", Journal of Plant Physiology, 160, 271-282, 2003.

Gobron, N., Pinty, B., Verstraete, M. M., and Govaerts, Y., "A semi-discrete model for the scattering of light by vegetation", Journal of Geophysical Research, 102: 9431-9446, 1997.

Goel, N.S., "Models of vegetation canopy reflectance and their use in estimation of biophysical parameters from reflectance data", Remote Sensing Reviews, 4: 1-212, 1988.

Gong, P., Pu, R., Biging, G.S., and Larrieu, M.R., "Estimation of Forest Leaf Area Index Using Vegetation Indices Derived From Hyperion Hyperspectral Data", IEEE Transactions on Geoscience and Remote Sensing, 41(6): 1355-1362, 2003.

GTC: Geological Testing Consultants Ltd. "Kam-Kotia Tailings reclamation project-detailed hydrological investigation program", Ontario Ministry of the Environment and Ontario Ministry of Natural Resources, Ottawa, ON, Canada, 1984.

Harron, J.W., "Optical properties of phytoelements in conifers", M. Sc. Thesis, Graduate Program in Earth and Space Science, p. 193, York University, Toronto, 2000.

Huang, D., Knyazikhin, Y., Wang, W., Deering, D. W., Stenberg, P., Shabanov, N., and Myneni, R.B., "Stochastic transport theory for investigating the three-dimensional canopy structure from space measurements," Remote Sensing of Environment, 112: 35-50, 2008.

Huang, D., Knyazikhin, Y., Dickinson, R. E., Rautiainen, M., Stenberg, P., Disney, M., Lewis, P., Cescatti, A., Tian, Y., Verhoef, W., Martonchik, J. V., and Myneni, R.B., "Canopy spectral invariants for remote sensing and model applications", Remote Sensing of Environment, 106: 106-122, 2007.

Jacquemoud, S., Bacour, C., Poilve, H., and Frangi, J. P., "Comparison of four radiative transfer models to simulate plant canopies reflectance direct and inverse mode", Remote Sensing of Environment, 74: 471-481, 2000.

Jacquemoud, S., F. and Baret, F., "PROSPECT: A model of leaf optical properties spectra", Remote Sensing of Environment, 34: 75-91, 1990.

Kelly, M., "Mining and the freshwater environment", Elsevier Applied Science in association with British Petroleum Company, London, New York, 231 p, 1988.

Khurshid, S., Staenz, K., Sun, L., Neville, R.A., White, H.P., Bannari, A., Champagne, C.M., and Hitchcock, R., "Preprocessing of EO-1 Hyperion Data", Canadian Journal of Remote Sensing, 32(3): 84-97, 2006.

Kimes, D., Knyazikhin, Y., Privette, J.L., Abuelgasim, A. A., and Gao, F., "Inversion methods for physically-based models", Remote Sensing review, 18: 381-439, 2000.

Knyazikhin, Y., Martonchik, J. V., Myneni, R. B., Diner, D. J., and Running, S.W., "Synergistic algorithm for estimating vegetation canopy leaf area index and fraction of absorbed photosynthetically active radiation from MODIS and MISR data", Journal of Geophysical Research, 103(D24): 32257-32276, 1998.

Koetz, B., Baret, F., Poilvé, H., and Hill, J., "Use of coupled canopy structure dynamic and radiative transfer models to estimate biophysical canopy characteristics", Remote Sensing of Environment, 95: 115-124, 2005.

Kucharik, C. J., Norman, J. M., Murdock, L. M., and Gower, S., T., "Characterizing canopy nonradomness with a Multiband Vegetation Imager (MVI)", Journal of Geophysical Research, 102(D24): 29445-29473, 1997.

Kuusk, A., Andrieu, B., Chelle, M., and Aries, F., "Validation of a Markov chain canopy reflectance model", International Journal of Remote Sensing, 18(10): 2125-2146, 1997.

Leblanc, S. G., Bicheron, P., Chen, J. M., Leroy, M., and Cihlar, J., "Investigation of directional reflectance in boreal forests with an improved 4-scale model and Airborne POLDER data", IEEE Transactions on Geoscience and Remote Sensing, 37(3): 1396-1414, 1999.

Le Maire, G., Francois, C., and Dufrene, E., "Towards universal broad leaf chlorophyll indices using PROSPECT simulated database and Hyperspectral reflectance measurements", Remote Sensing of Environment, 89: 1-28, 2004.

Lévesque, J., and King, D.J., "Spatial analysis of radiometric fractions from high-resolution multispectral imagery for modeling individual tree crown and forest canopy structure and health", Remote Sensing of Environment, 84: 589-602, 2003.

Lévesque, J., "Modelling forest structure and health using high-resolution airborne imagery: investigation of spectral unmixing and spatial analysis of radiometric fractions", Ph D thesis, Carleton University, Ottawa, ON, Canada, 258 p, 2001.

Lévesque, J., and King, D. J., "Airborne digital camera image semivariance for evaluation of forest structural damage at an acid mine site", Remote Sensing of Environment, 68: 112-124, 1999.

Lewis, P., and Disney, M., "Spectral invariants and scattering across multiple scales from within-leaf to canopy", Remote Sensing of Environment, 109: 196-206, 2007.

Li, X., and Strahler, A. H., and Woodcock, C. E., "A hybrid geometric-optical radiative transfer approach for modeling albedo and directional reflectance of discontinuous canopies", IEEE Transactions on Geoscience and Remote Sensing, 33: 466-480, 1995.

Li, X., and Strahler, A. H., "Geometric-optical bidirectional reflectance modeling of the discrete crown vegetation canopy: effect of crown shape and mutual shadowing", IEEE Transactions on Geoscience and Remote Sensing, 30(2): 276-292, 1992.

Li, X., and Strahler, A. H., "Modeling the gap probability of a discontinuous vegetation canopy", IEEE Transactions on Geoscience and Remote Sensing, 26(2): 161-169, 1988.

Liang, S., "Quantitative Remote Sensing of Land Surfaces", John Wiley and Sons, Inc., 534 pages, 2004.

Liang, S., and Strahler, A. H., "An analytic radiative transfer model for a coupled atmosphere and leaf canopy, Journal of Geophysical Research, 100(D3): 5085–5094, 1995.

Liang, S., and Strahler, A. H., "The calculation of the radiance distribution of the coupled atmosphere and leaf canopy", IEEE Transactions on Geoscience and Remote Sensing, 31(2): 491-502, 1993.

Martin, M.E., and Aber, J.D., "High spectral resolution remote sensing of forest canopy lignin, nitrogen, and ecosystem processes", Ecological Applications, 7(2): 431-443, 1997.

Meroni, M., Colombo R., and Panigada, C., "Inversion of a radiative transfer model with hyperspectral observations for LAI mapping in poplar plantations", Remote Sensing of Environment, 92: 195-206, 2004.

Miller, J.R., White, H.P., Chen, J.M., Peddle, D.R., and McDermid, G., Fournier, R.A., Shepherd, P., Rubinstein, I., Freemantle, J., Soffer, R., and LeDrew, E., "Seasonal change in understorey reflectance of boreal forests and influence on canopy vegetation indices", Journal of Geophysical Research, 102(24): 29475-29482, 1997.

Mõttus, M., and Stenberg, P., "A simple parameterization of canopy reflectance using photon recollision probability", Remote Sensing of Environment, 112: 1545-1551, 2008.

Mõttus, M., "Photon recollision probability in discrete crown canopies", Remote Sensing of Environment, 110: 176-185, 2007.

Myneni, R. B., Marshak, A., Knyazikhin, Y., and Asrar, G., "Discrete ordinates method for photon transport in leaf canopies", Photon-Vegetation Interactions: Applications in optical Remote Sensing and Plant Ecology, edited by Myneni, R. B., and Ross, J., 45-109, Springer, New York, 1991.

Myneni, R.B., and Ross, J., Editors. "Photon-Vegetation Interactions", Springer-Verlag, Berlin, 1991.

Nadal, F., and Bréon, F.M., "Parameterization of surface polarized reflectance derived from POLDER spaceborne measurements", IEEE Transactions on Geoscience and Remote Sensing, 37(3): 1709 - 1718, 1999.

Natural Resources Canada, http://gsc.nrcan.gc.ca/geochem/timmins/geology_f.php.

Neville, R.A., Sun, L., and Staenz, K., "Spectral Calibration of Imaging Spectrometers by Atmosphere Absorption Matching", Canadian Journal of Remote Sensing, 34, Suppl. 1: S29-S42, 2008.

Ni, W., Li, X., Woodcock, C. E., Roujean, J. L., and Davis, R. E., "Transmission of solar radiation in boreal conifer forests: measurements and models", Journal of Geophysical Research, 102: 29555-29566, 1997.

Nilson, T., and Peterson, U., "A forest canopy reflectance model and a test case", Remote Sensing of Environment, 37: 131-142, 1991.

Nilson, T., and Kuusk, A., "A reflectance model for homogeneous plant canopy and its inversion", Remote Sensing of Environment, 27: 157-167, 1989.

Nilson, T, "A theoretical analysis of the frequency of gaps in plant stands", Agricultural and Forest Meteorology, 8: 25-38, 1971.

Nordstorm, K. D., and Alpers, C. N., "Geochemistry of acid mine waters", in Plumlee, G. S., and Logsdon, M. J. (Editors): "The environmental geochemistry of mineral deposits. Part A: Processes, techniques and health issues", Reviews in Economic Geology, Society of Economic Geologists, Littleton, CO, USA, 6, pp. 133-160, 1999.

Olthof, I., and. King, D.J., "Development of a forest health index using multispectral airborne digital camera imagery", Canadian Journal of Remote Sensing, 26: 166-176, 2000.

Olthof, I., "Development of a forest health index using high-resolution remotely-sensed multispectral digital imagery", MA Thesis, Department of Geography and Environmental Studies, Carleton University, Ottawa, Canada, 184 pages, 1999.

Omari, K., Fernandes, R., Staenz, K., Rochdi, N., and Chelle, M., "Parameterization of the angular distribution of the multiple scattering radiation using photon re-collision probability", Remote Sensing of Environment, in review, 2009.

Omari, K., Staenz, K., King, D.J., and White, H, P., "Retrieval of forest canopy parameters by inversion of the PROFLAIR leaf-canopy reflectance model using the LUT approach", Canadian journal of Remote Sensing, in review, 2009.

Omari, K., White, H. P., and Staenz, K., "An enhanced description of multiple scattering within the FLAIR model using the photon re-collision probability approach", IEEE Transactions on Geoscience and Remote Sensing, in press, 2009.

Panferov, O., Knyazikhin, Y., Myneni, R.B., Szarzynski, J., Engwald, S., Schnitzler, K.G., and Gravenhorst, G., "The role of canopy structure in the spectral variation of transmission absorption of solar radiation in vegetation canopies", IEEE Transactions on Geoscience and Remote Sensing, 39: 241-253, 2001.

Pinty, B., Widlowski, J.-L., Taberner, N., Gobron, N., Verstraete, M. M., Disney, M., Gastellu-Etchegorry, J.-P., Jiang, L., Kuusk, A., Lewis, P., Li, X., Ni-Meister, W., Nilson, T., North, P. R. J., Qin, W., Su, L., Thomson, R., Verhoef, W., Wang, H., Wang, J., Yan, G., and Zhang, H., "Radiation Transfer Model Intercomparison (RAMI) exercise: Results from the second phase", Journal of Geophysical Research, 109(D06210), doi: 10.1029/2003JD004252, 2004.

Pinty, B., Widlowski, J. L., Gobron, N., Verstraete, M. M., and Diner, D. J., "Uniqueness of Multiangular Measurements Part 1: An Indicator of Subpixel Surface Heterogeneity from MISR", IEEE Transactions on Geoscience and Remote Sensing, 40(7): 1560-1573, 2002.

Pinty, B., Gobron, N., Widlowski, J. -L., Gerstl, S., Verstraete, M. M., Antuunes, M., Bacour, C., Gascon, F., Gastellu-Etchegorry, J. -P., Goel, N., Jacquemoud, S., North, P. R. J., Qin, W., and Thomson, R., "Radiation Transfer Model Intercomparison (RAMI)", Journal of Geophysical Research, 106(D11): 11937-11956, 2001.

Pinty, B., and Verstraete, M. M., "Extracting information on surface properties from bidirectional reflectance measurements", Journal of Geophysical Research, 96(D2): 2865-2874, 1991.

Rautiainen, M., and Stenberg, P., "Application of photon recollision probability in coniferous canopy reflectance simulations", Remote Sensing of Environment, 96: 98-107, 2005.

Richter, N., "Delineation of the Kam-Kotia Mine Tailings Areas (Ontario, Canada) Using Hyperspectral TRWIS III Data", Ph. D thesis, University of Potsdam, Suisse, 99 pages, 2004.

Robert, G., "A review of the application of BRDF models to infer land cover parameters at regional and global scales", Progress in Physical Geography, 25(4): 483-511, 2001.

Rochdi, N., Fernandes, R., and Chelle, M., "An assessment of needles clumping within shoots when modeling radiative transfer within homogenous canopies", Remote Sensing of Environment, 102: 116-134, 2006.

Ross J., Marshak A., "Monte Carlo methods. - In: Photon-Vegetation Interactions. Applications in Optical Remote Sensing and Plant Ecology", Eds. R.B. Myneni, J. Ross. Berlin: Springer Verlag, pp. 441-467, 1991.

Ross, J., "The radiation regime and architecture of plant stands, Netherlands: Junk. W, The Hague, 391 pages, 1981.

Sellers, P., Hall, F., Margolis, H., Kelly, B., Baldocchi, D., Hartog den, G., Cihlar, J., Ryan, M.G., Goodison, B., Crill, P., Ranson, K.J., Lettenmaier, D., and Wickland, D.E., "The Boreal Ecosystem-Atmosphere Study (BOREAS): An overview and early results from the 1994 field year", Bulletin of American Meteorological Society, 76(9): 1549-1577, 1995.

Sellers, P.J., "Canopy reflectance, photosynthesis and transpiration", International Journal of Remote Sensing, 6(8): 1335-1372, 1985.

Shabanov, N.V., Kotchenova, S., Huang, D., Yang, W., Tan,B., Knyazikhin Y., Myneni, R. B., Ahl, D. E., Gower, S. T., Huete, A. R., Aragao, L. E. O. C., and Shimabukuro, Y. E., (2005), "Analysis and optimization of the MODIS leaf area index algorithm retrievals over broadleaf forests", IEEE Transactions on Geoscience and Remote Sensing, 43(8): 1855-1865.

Shabanov, N. V., Knyazikhin, Y., Baret, F., and Myneni, R. B., "Stochastic modeling of radiation regime in discontinuous vegetation canopies," Remote Sensing of Environment., 74(1): 125-144, 2000.

Smith, M.L., Martin, M.E., Plourde, L., and Ollinger, S.V., "Analysis of hyperspectral data forest canopy nitrogen concentration: Comparison between an airborne (AVIRIS) and a spaceborne (Hyperion) sensor", IEEE Transactions on Geoscience and Remote Sensing, 41(6): 1332-1337, 2003.

Smolander, S., and Stenberg, P., "Simple parameterizations of the radiation budget of uniform broadleaved and coniferous canopies", Remote Sensing of Environment, 94: 355– 363, 2005.

Staenz, K., Neville, R.A., Levesque, J., Szeredi, T., Singhroy, V., Borstad, G.A., and Hauff, P., "Evaluation of casi and SFSI Hyperspectral data for environmental and geological applications — two case studies", Canadian Journal of Remote Sensing, 25: 311-322, 1999.

Staenz, K., Szeredi, T., and Schwarz, J., "ISDAS-A system for processing/analyzing hyperspectral data", Canadian Journal of Remote Sensing, 42(2), 99-113, 1998.

Staenz, K., and Williams, D., "Retrieval of surface reflectance from hyperspectral data using a look-up table approach", Canadian Journal of Remote Sensing, 23(4): 354-368, 1997.

Stenberg, P., "Simple analytical formula for calculating average photon recollision probability in vegetation canopies", Remote Sensing of Environment, 109: 221-224, 2007.

Sun, L., Neville, R.A., Staenz, K., and White, H.P., "Automatic Destriping of Hyperion Imagery Based on Spectral Moment Matching", Canadian Journal of Remote Sensing, 34(Supplement 1): S68-S81, 2008.

Thurston, P.C., Williams, H.R., Sutcliffe, R.H., et Scott, C.M., "Geology of Ontario", Ontario Geological Survey, Ministry of Northern Development and Mines, Toronto, Ontario, Special Volume 4, Part I and 2, 1991.

Van de Hulst, H. C., "Multiple light scattering. Tables, formulas and applications", New York: Academic Press, 1980.

Verburg, P.S.J., Johnson, D.W., and Harrison, R, "Long-term nutrient cycling patterns in Douglas-fir and red alder stands: a simulation study", Forest Ecology and Management, 145(3): 203-217, 2001.

Verhoef, W., "Light scattering by leaf layers with application to canopy reflectance modeling: The SAIL model", Remote Sensing of Environment, 16: 125-141, 1984.

Walsworth, N., and King. D.J., "Image modelling of forest changes associated with acid mine drainage", Computers and Geosciences, 25: 567-580, 1999.

Wang, Y., Buermann,W., Stenberg, P., Smolander, H., Häme, T., Tian, Y., Hu, J., Knyazikhin, Y., and Myneni, R, B., "A new parameterization of canopy spectral response to incident solar radiation: Case study with hyperspectral data from pine dominant forest", Remote Sensing of Environment, 85: 304-315, 2003.

Weiss, M., Baret, F., Myneni, R. B., Pragnere, A., and Knyazikhin, Y., "Investigation of a model inversion technique to estimate canopy biophysical variables from spectral and directional reflectance data", Agronomie, 20: 3-22, 2000.

Weiss, M., and Baret, F., "Evaluation of canopy biophysical variable retrieval performances from the accumulation of large swath satellite data", Remote Sensing of Environment, 70: 293–306, 1999.

White, H.P., Sun, L., Staenz. K., Fernandes, R., and Champagne, C.M., "Determining the contribution of shaded elements of a canopy to remotely sensed hyperspectral signatures", Proceedings of the 1st International Symposium on Recent Advances in Quantitative Remote Sensing, Valencia, Spain, 159-166, 2002a.

White, H.P., Deguise, J.C., Schwarz. J., Hitchcock, J. R. and Staenz, K., "Defining shaded spectra by model inversion for spectral unmixing of hyperspectral datasets - theory and preliminary application", Proceedings of the Joint 24th Canadian Symposium of Remote Sensing and IGARSS, Toronto, Ontario, Canada, 989-991, 2002b.

White, H.P., Miller, J.R., and Chen, J.M, "Four-scale linear model for anisotropic reflectance (FLAIR) for plant canopies. I: Model description and partial validation", IEEE Transactions on Geoscience and Remote Sensing, 39(5), 1072-1083, 2001a.

White, H.P., Miller, J.R., and Chen, J.M., "Four-scale linear model for anisotropic reflectance (FLAIR) for plant canopies. II: Validation and Inversion with CASI, POLDER, and PARABOLA data at BOREAS", IEEE Transactions on Geoscience and Remote Sensing, 40(5): 1038-1046, 2001b.

White, H.P., Miller, J.R., Chen, J., and Peddle, D.R., "Seasonal change in mean understorey reflectance for Boreas sites: Preliminary results", 17th Canadian Symposium on Remote Sensing, Saskatoon, Saskatchewan, 189-194, 1995.

Widlowski, J. -L., Robustelli, M., Disney, M., Gastellu-Etchegorry, J. -P., Lavergne, T., Lewis, P., North, P. R. J., Pinty, B., Thomson, R., and Verstraete, M. M., "The RAMI On-line Model Checker (ROMC): A web benchmarking facility to canopy reflectance models", Remote Sensing of Environment, 112: 1144-1150, 2008.

Wiken, E. B., "Terrestrial ecozones of Canada", Ecological land classification series No. 19, Environment Canada, Hull, QC, Canada, 26 pages, 1986.

Zarco-Tejada, P.J., Miller, J. R., Morales, A., Berjón, A., and Agüera, J., "Hyperspectral indices and model simulation for chlorophyll estimation in open-canopy tree crops", Remote Sensing of Environment, 90: 463-476, 2004.

Zarco-Tejada, P.J., Miller, J.R., Noland, T.L., Mohammed, G.H., and Sampson, P.H., "Scaling-up and model inversion methods with narrowband optical indices for chlorophyll content estimation in closed forest canopies with hyperspectral data", IEEE Transactions on Geoscience and Remote Sensing, 39(7): 1491–1506, 2001.

Zhang, Y., Shabanov, N., Knyazikhin, Y. and Myneni, R.B., "Assessing the information content of multiangle satellite data for mapping biomes", Remote Sensing of Environment, 80: 435- 446, 2002.